Study of the function of PGC-1β in white adipose tissue and its contribution to the development of insulin resistance

Natalia Enguix Elena

Phd Thesis
Barcelona, 2014

Laboratory of Metabolism and Obesity
Unit of Diabetes and Metabolism
Vall d'Hebron Research Institute

Department of Biochemistry and Molecular Biology
Autonomous University of Barcelona

Study of the function of PGC-1β in white adipose tissue and its contribution to the development of insulin resistance

Natàlia Enguix Elena

Thesis submitted for the Degree of Doctor in Biochemistry, Molecular Biology and Biomedicine

Barcelona, 2014

Josep A. Villena Delgado
Thesis Director

Anna Meseguer Navarro
Tutor

Natàlia Enguix Elena

ABBREVIATIONS

A

ACC	acetyl-CoA carboxylase
a.u.	Arbitrary units
ABHD5	adipose triglyceride lipase co-activator
AC	adenylate cylcase
Acaa2	acetyl-Coenzyme A acyltransferase 2
Acadm	acyl-Coenzyme A dehydrogenase, medium chain
acetyl CoA	acetyl coenzyme A
Aco2	aconitase 2
ACOD	acyl-CoA oxidase
ACS	acyl-CoA synthetase
Acss1	acyl-CoA synthetase short-chain family member 1
ADD-1	adipocyte determination and differentiation-dependent factor 1
Adipoq	adiponectin, C1Q and collagen domain containing
AEBSF	4-(2-Aminoethyl) benzenesulfonyl fluoride hydrochloride (serine protease inhibitor)
AGPAT	lysophosphatide acyltransferase
AJ-9677	β3-agonist
AKT	protein kinase B
AMPK	AMP-dependent kinase
ANOVA	analysis of the variance
aP2	adipocyte fatty acid-binding protein 4
AQP7	aquaporin 7
AS160	160-kDa substrate of Akt
ATF2	Activating Transcription Factor 2
ATF6	activating transcription factor-6
Atgl/Pnpla2	adipose trigliceride lipase, also known as patatin-like phospholipase domain containing 2
Atp5a1	ATP synthase, H+ transporting, mitochondrial F1 complex, alpha subunit 1
Atp5b	ATP synthase, H+ transporting mitochondrial F1 complex, beta subunit
Atp5o	ATP synthase, H+ transporting, mitochondrial F1 complex, O subunit

B

BAC	Bacterial Artificial Chromosome
BAT	brown adipose tissue
BCA	Bicinchoninic Acid
BLAST	Basic Local Alignment Search Tool
BMI	Body mass index
Bp	Bases pairs
BP	Biological proces
Brite	brown in white
BSA	Bovine serum albumin

C

C/EBPα	CCAAT/enhancer binding protein α
C/EBPβ	CCAAT/enhancer binding protein β

C/EBPδ	CCAAT/enhancer binding protein δ
C57BL/6	Common inbred strain of laboratory mouse
cAMP	Cyclic adenosine monophosphate
Carboxy-H2DCFDA	6-carboxy-2',7'-dichlorodihydrofluorescein diacetate (general oxidative stress indicator)
Cat	catalase
CC	Cellular component
CCCP	Carbonyl cyanide m-chlorophenyl hydrazone
CD36/FAT	fatty acid translocase
Cdk4/6	cyclin dependent kinases
cDNA	complementary DNA
Ci	curie
Cidea	cell death-inducing DNA fragmentation factor, alpha subunit-like effector A
Cideb	cell death-inducing DNA fragmentation factor, alpha subunit-like effector B
CL-316,243	β3-agonist
CoA-SH	thiol group
COD	cholesterol oxidase
COE	cholesterol esterase
Complex I	NADH-ubiquinone oxidoreductase
Complex II	succinate dehydrogenase
Complex III	Ubiquinol-cytochrome c reductase
Complex IV	Cytochrome c oxidase
Cox4i1	cytochrome c oxidase subunit IV isoform 1
Cox5a	cytochrome c oxidase subunit Va
Cox5b	cytochrome c oxidase subunit Vb
Cox7a1	cytochrome c oxidase subunit VIIa 1
Cox8b	cytochrome c oxidase subunit VIIIb
Cpt1b	carnitine palmitoyltransferase 1b, muscle
Cre	recombinase
CREB	cAMP Responsive Element Binding Protein
Cs	citrate synthase
CT	computed tomography
CtBP	C-terminal-binding protein
Cyc1	cytochrome c-1
Cycs	cytochrome c, somatic
Cypa/Ppia	cyclophilin A, also known as peptidylprolyl isomerase A

D

DAG	diacylglycerol
DAVID	Database for Annotation, Visualization and Integrated Discovery
db/db mice	mice with mutation in the leptin receptor gene
DCIP	2,6-Dichlorophenolindophenol
Decyl-Q	Decylubiquinone

DEPC	Diethyl pyrocarbonate
DGATs	diacylglycerol acyltransferases
DharmaFECT 4	cationic lipid-based reagent (Thermo Fisher Scientific)
Dio2	deiodinase, iodothyronine, type II
Dlk1	preadipocyte factor 1
DMEM	Dubelcos's Eagle Modified Medium
DMSO	Dimethyl sulfoxide
dpm	disintegrations per minute
dsRNA	Double-stranded RNA
DTNB	5,5'-dithiobis-(2-nitrobenzoic acid)
DTT	Dithiothreitol
dUTP	deoxyuridine-triphosphate

E

EASE score	a modified Fisher Exact P-Value
ECL	Enhanced chemiluminescence
EDTA	Ethylenediaminetetraacetic acid
EGTA	ethylene glycol tetraacetic acid
Elovl6	ELOVL family member 6, elongation of long chain fatty acids (yeast)
ER	Endoplasmic reticulum
ERK	Mitogen-activated protein kinases
ERREs	ERR response elements
ERs	estrogen receptors
ESPT	ethyl-sulphopropyl-toluidine
Esrra	estrogen related receptor, alpha
Esrrg	estrogen-related receptor gamma

F

Fabp3	fatty acid binding protein 3, muscle and heart
Fabp4	fatty acid binding protein 4, adipocyte
FABPm	Fatty acid binding protein plasma membrane
FADH2	Flavin Adenine Dinucleotide Reduced
FASN	fatty acid synthase
FATP	fatty acid transporter protein
FBS	Fetal Bovine Serum
FDG-PET	fluorodeoxyglucose-positron emission tomography
FFA	free fatty acid
Flox	Floxed LoxP
FLP	flippase (recombinase)
FOXO1	Forkhead box protein O1
FRT	short flippase recognition target sites

G

G-6-Pase	glucose-6-phosphatase
G1 phase	Growth phase

GABP	GA-binding protein
Gapdh	glyceraldehyde-3-phosphate dehydrogenase
Gastroc.	gastrocnemius muscle
GDP	guanosine diphosphate
Gi	inhibitory regulatory protein
GK	glycerol kinase
GLUT4	glucose transporter 4
GO	gene ontology
Gon. WAT	Gonadal WAT
GPAT	glycerol 3-phosphate acyltransferase
GPO	glycerol-phosphate-oxidase
Gpx1	glutathione peroxidase 1
GR	glucocorticoid receptor
Gs	G stimulatory proteins
GS	glycogen synthase
GSK3	glycogen synthase kinase-3
GTT	Glucose tolerance test

H

HCF	Host Cell Factor
HDACs	histone deacetylases
Hepes	4-(2-hydroxyethyl)-1-piperazineethanesulfonic acid
HFD	High fat diet
HNF1B	hepatocyte nuclear factor 1 homeobox B
HNF4α	hepatocyte nuclear factor 4 α
HOMA-IR	homeostatic model assessment of insulin resistance
HRP	horseradish peroxidase
HSL	hormone sensitive lipase

I

IBMX	3-Isobutyl-1-methylxanthine
Idh3a	isocitrate dehydrogenase 3 (NAD+) alpha
Idh3b	isocitrate dehydrogenase 3 (NAD+) beta
IGF-1	Insulin growth factor
IKKβ	NF-κβ kinase
IL-10	Interleukin 10
IL-1Ra	interleukin-1 receptor antagonist
IL-1β	Interleukin-1 beta
IL-6	Interleukin 6
Ing. WAT	Inguinal WAT
IR	insulin receptor
IRE-1α	inositol requiring enzyme-1
IRS 1-4	insulin receptor substrate proteins 1 to 4
ITT	insulin tolerance test

	IU	International units
J	**JNK**	c-jun N-terminal Kinase
	kDa	kilo (unified atomic mass unit or dalton)
	KO	knock-out
K	**KRB Buffer**	Krebs-Ringer Bicarbonate Buffer
L	**LBD**	carboxy-terminal ligand-binding domain
	Lep	leptin
	Lipe	lipase, hormone sensitive
	LoxP	Locus of X-over P1phage
	LPA	lysophosphatidic acid
	LPL	lipoprotein lipase
	LXXLL	leucine-rich motifs
M	**MAG**	monoacylglycerols
	MAPK kinase	Mitogen-activated protein kinases
	MCK	muscle creatine kinase promoter
	MCP-1	chemo-attractant protein-1
	Mdh2	malate dehydrogenase 2, NAD (mitochondrial)
	MEFA	3-methy-N-ethyl-N(β-hydroxyethyl)-aniline
	MF	Molecular function
	MGL	monoacylglycerol lipase
	min	minutes
	mRNA	Messenger RNA
	MRS	magnetic resonance spectroscopy
	mt-Co2	cytochrome c oxidase II, mitochondrial
	mt-Nd2	NADH dehydrogenase 2, mitochondrial
	myf5	Macrophage migration inhibitory factor 5
N	**NADH**	Nicotinamide adenine dinucleotide reduced
	NAFLD	non-alcoholic fatty liver disease
	NCS	Newborn Calf Serum
	nDNA	nuclear DNA
	Ndufa4	NADH dehydrogenase (ubiquinone) 1 alpha subcomplex, 4
	Ndufab1	NADH dehydrogenase (ubiquinone) 1, alpha/beta subcomplex, 1
	Ndufb6	NADH dehydrogenase (ubiquinone) 1 beta subcomplex, 6
	Ndufb9	NADH dehydrogenase (ubiquinone) 1 beta subcomplex, 9
	NEFA	Non-esterified fatty acids
	nPKC	novel protein kinase C
	Nrf1	nuclear respiratory factor 1

Nrf2/Gabpa	GA repeat binding protein, alpha [Mus musculus
NT-PGC-1α	truncated isoforms of PGC-1α

O

ob/ob mice	mice with mutation in the leptin gene
OD	optical density (absorbance)
OLEFT rats	Otsuka Long-Evans Tokushima Fatty rats
OxPhos system	oxidative phosphorylation system

P

p38 MAPK	p38 mitogen activated protein kinase
PA	phosphatidic acid
PAI-1	Plasminogen activator inhibitor-1
PAP	phosphatidic acid phosphatase
PBS	phosphate buffered saline
PCR	polymerase chain reaction
PDE	phosphodiesterase
PDH	acetyl-CoA by pyruvate dehydrogenase
PDK1	phosphoinositide-dependent protein kinase 1
Pdk4	pyruvate dehydrogenase kinase
PEI	Polyethylenimine
PEPCK	phosphoenolpyruvate carboxykinase
PERK	PKR-like ER kinase
PGC-1α	Peroxisome Proliferator–Activated Receptor Gamma Coactivator 1α
PGC1β-FAT-KO	knockout mice for PGC-1β in adipose tissues
PGE2	prostaglandin E2
PGK	Phosphoglycerate kinase
PI	phosphatidylinositol
PI3K	phosphoinositide 3-kinase
PIP2	lipid 4,5-bisphosphate
PIP3	phosphatidylinositol 3,4,5-trisphosphate
PKA	protein kinase A
PKB	protein kinase B
PKCζ	atypical PKC isoform
PLIN	perilipin
PMSF	Phenylmethanesulfonyl fluoride
POD	peroxidase
POLRMT	mitochondrial RNA polymerase
Ppara	peroxisome proliferator activated receptor alpha
Pparg	peroxisome proliferator activated receptor gamma
Ppargc1a	peroxisome proliferative activated receptor, gamma, coactivator 1 alpha
Ppargc1b	peroxisome proliferative activated receptor, gamma, coactivator 1 beta
Pprc1	peroxisome proliferative activated receptor, gamma, coactivator-related 1

PPRE	PPAR Responsive Elements
Prdm16	PR domain containing 16 [Mus musculus
Pref1/Dlk1	delta-like 1 homolog (Drosophila)
Primer F	Reverse primer
Primer R	Forward primer
PRMT1	protein arginine methyltransferase 1
PVDF	polyvinyl difluoride

Q

qPCR	Quantitative PCR

R

Rab	member of the Ras superfamily of monomeric G proteins
RBP4	Retinol binding protein 4
Ret. WAT	Retroperitoneal WAT
Retn	resistin
Rip11	Rab11 effector
Rip140/Nrip1	nuclear receptor interacting protein 1
ROS	reactive oxygen species
Rosig.	rosiglitazone
rpm	Revolutions per minute
RRM	RNA recognition motif
RS	short argenine/serine-rich areas
RT-PCR	Reverse transcription polymerase chain reaction
RXR	retinoid X receptor

S

S phase	DNA synthesis phase
S6K1	ribosomal s6 kinase
Sdhb	succinate dehydrogenase complex, subunit B, iron sulfur (Ip)
Sdhd	succinate dehydrogenase complex, subunit D, integral membrane protein
SDS	Sodium dodecyl sulfate
SEM	the standard error of the mean
shRNA	short hairpin RNA
siControl	non-targeting siRNA
siGapdh	siRNA targeted to glyceraldehyde-3-phosphate dehydrogenase
siGLO	transfection indicator
siPGC-1α	siRNA targeted to Ppargc1a
siPGC-1β	siRNA targeted to Ppargc1b
siRNA	small interference RNA
SIRT1	sirtuin 1
Sod2	superoxide dismutase 2, mitochondrial
SOX9	Sry-related HMG box-9
SPF	Specific Patogen Free
SREBP-1	sterol regulatory element-binding protein 1

	ssDNA	single-stranded DNA
	SVF	stromal vascular fraction
T		
	TAE	Tris-Acetate-EDTA
	TAG	triacylglycerol
	TBS	Tris-buffered saline
	TBS-T	Tris-buffered saline-Tween
	TCA cycle	tricarboxylic acid cycle
	Td	dissociation temperature
	TdT	terminal deoxynucleotidyl transferase
	TE buffer	Tris-EDTA buffer
	TEMED	Tetramethylethylenediamine
	Tfam	transcription factor A, mitochondrial
	Tfb1m	transcription factor B1, mitochondrial
	Tfb2m	transcription factor B2, mitochondrial
	TG	triglycerides
	THR	thyroid hormone receptor
	TLRs	Toll-like receptots
	TNB	
	Tnfa	tumor necrosis factor
	Tris	2-Amino-2-hydroxymethyl-propane-1,3-diol
	tRNA	transfer RNA
T		
	TZDs	thiazolidinediones
	TAE buffer	Tris Acetate EDTA
U		
	Ucp1	uncoupling protein 1 (mitochondrial, proton carrier)
	Ucp2	uncoupling protein 2 (mitochondrial, proton carrier)
	Ucp3	uncoupling protein 3 (mitochondrial, proton carrier)
	UDG	uracil DNA glycosylase
	UPR	unfolded protein response
	Uqcrc2	ubiquinol cytochrome c reductase core protein 2 [Mus musculus
	Uqcrh	ubiquinol-cytochrome c reductase hinge protein
	Uqcrq	ubiquinol-cytochrome c reductase, complex III subunit VII
	UV	Ultraviolet
V		
	Vehic.	vehicle
	VLDL	very low-density lipoproteins
W		
	WAT	white adipose tissue
	Wt	Wild type

ABSTRACT

ABSTRACT

RESUM

CONTENTS

CONTENTS

1. INTRODUCTION

1.1. Pathogenesis of type 2 diabetes and adipose tissue

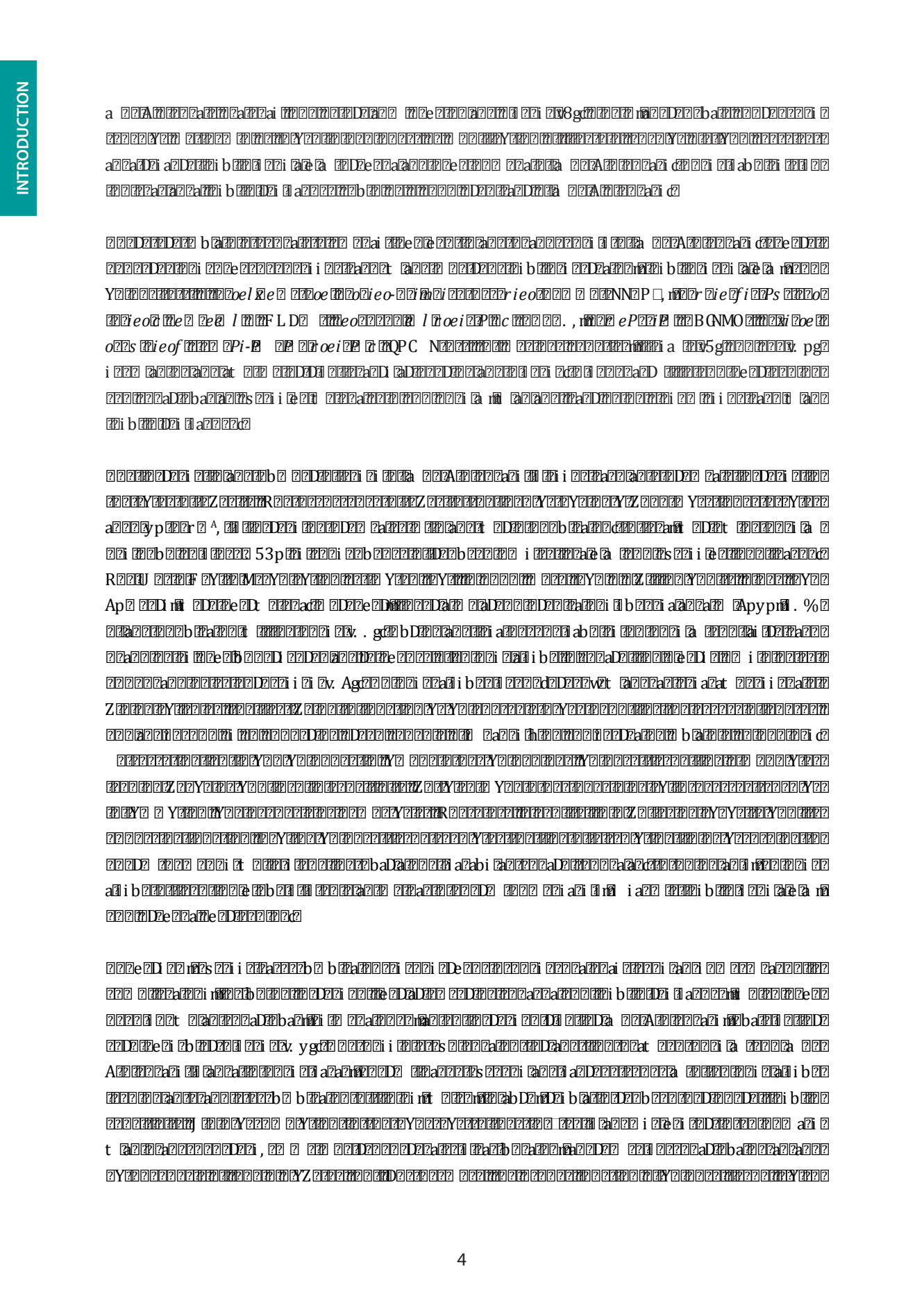

1.2. Adipose tissue

1.2.1. White adipose tissue

1.2.1.1. Morphology and anatomical distribution of white adipose tissue

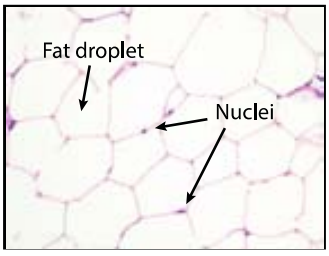

Figure 1. Histological section of white adipose tissue stained with hematoxylin/eosin.

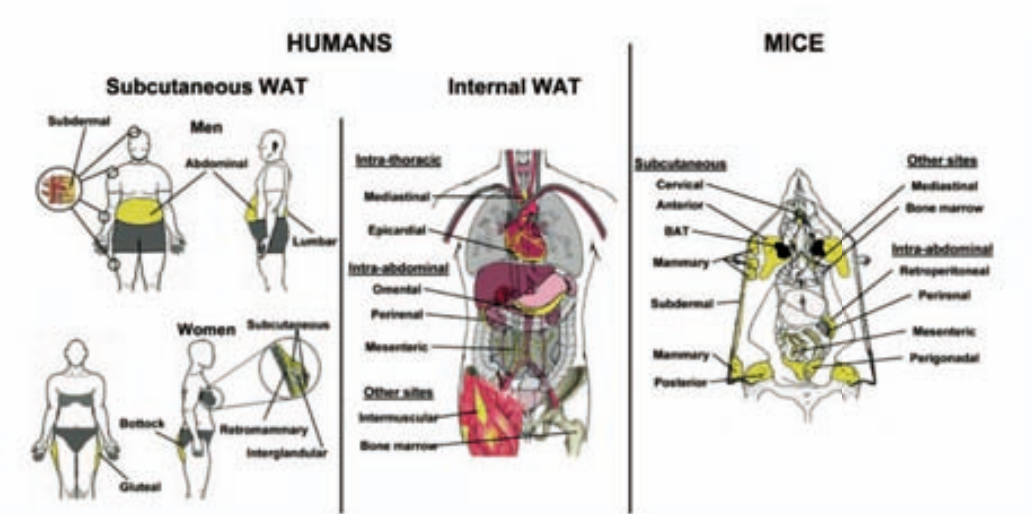

Figure 2. White adipose tissue distribution in humans and mice. Image extracted from [18].

1.2.1.2. Metabolic function of WAT

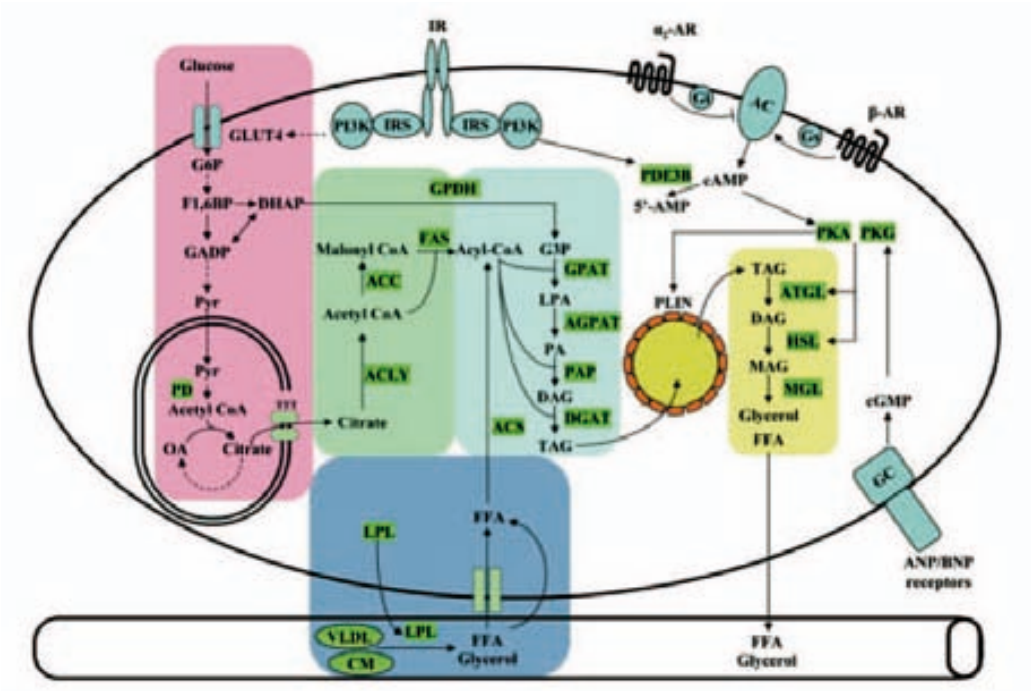

Figure 3. Metabolic functions of WAT. Uptake and metabolism of glucose is represented in the pink box. *De novo* lipogenesis is represented in the green box. Triglyceride synthesis is represented in the turquoise box. Lipolysis is represented in the yellow box. Fatty acid uptake from circulation is represented in the blue box. Image obtained from [18].

1.2.1.3. Endocrine function of WAT

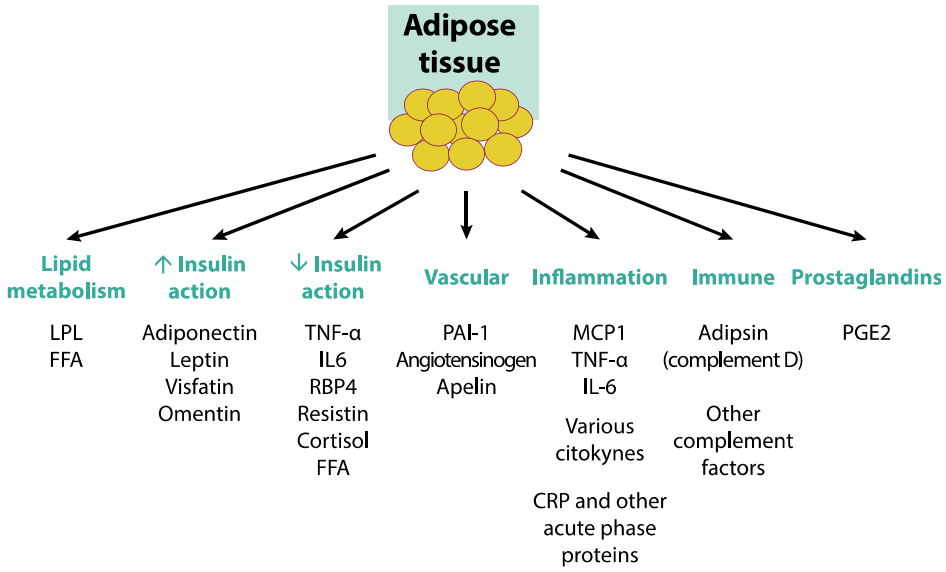

Figure 4. Adipokines and other adipocyte products that affect insulin action, nutrient homeostasis and cardiovascular function. Image adapted from [28].

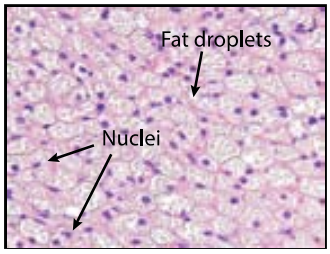

Figure 5. Histological section of brown adipose tissue stained with hematoxylin/eosin.

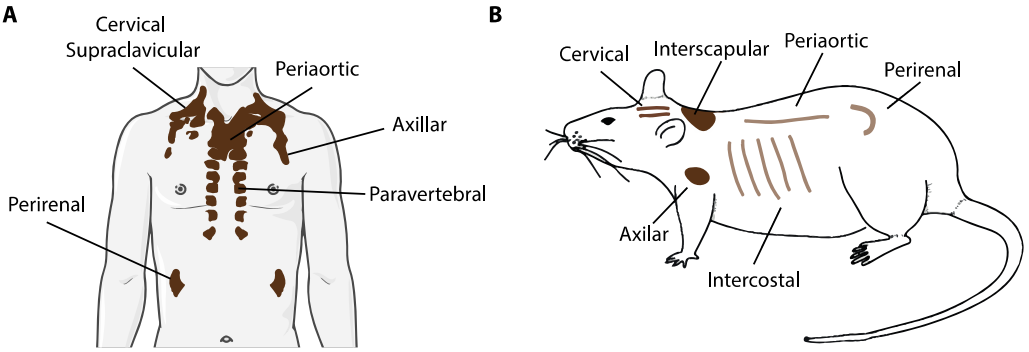

Figure 6. Distribution of major brown adipose tissue depots in (A) humans and (B) rodents. Adapted from [48].

1.2.2.2. Thermogenic function of brown adipose tissue

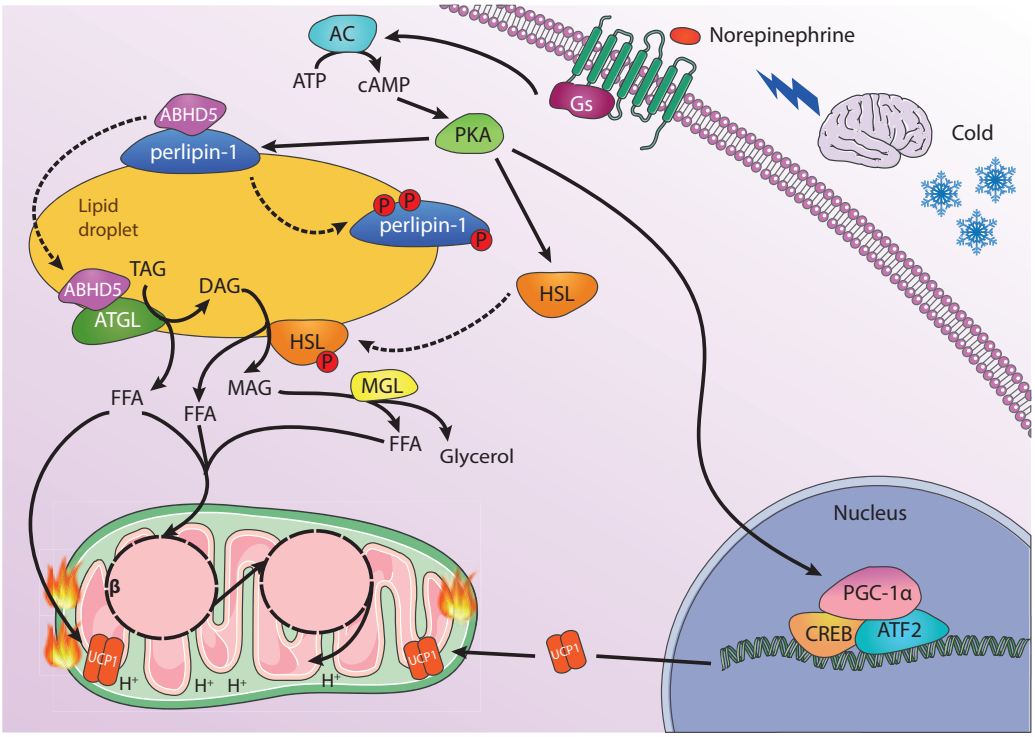

Figure 7. Overview of the regulatory mechanisms involved in cold-induced non-shivering adaptive thermogenesis in BAT. Image adapted from [48].

1.2.2.3. Brite adipocytes

TABLE 1. Differences between brown and beige adipocytes.
Table adapted from [56].

	Developmental origin in mice	Enriched markers	Key transcription factors	Activators
Brown adipocytes	Myf5+ cells (dermomyotome)	*Zic1* *Lhx8* *Eva1* *Pdk4* *Epsti1* *miR-206* *miR-133b*	*C/ebpβ* *Prdm16* *Pgc-1α* *Ppara* *Ebf2* *TR*	Cold Thiazolidinediones Natriuretic peptides Thyroid hormone Fgf21, Bmp7 Bmp8b Orexin
Brite adipocytes	Myf5- cells Pdgfr-α+ (dermomyotome)	*Cd137* *Tbx1* *Tmem26* *Cited1* *Shox2*	*C/ebpβ* *Prdm16* *Pgc-1α* *(Ppara)*	Cold Thiazolidinediones Natriuretic peptides Thyroid hormone Fgf21 Irisin

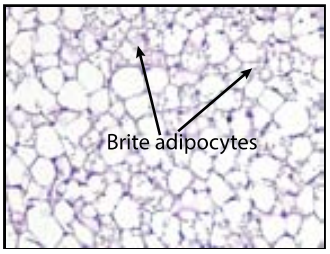

Figure 8. Histological section of white adipose tissue stimulated with a □3-adregergic agonist. Brite adipocytes can be found among white adipocytes. Tissue stained with hematoxylin/eosin.

1.3. Regulation of adipogenesis

1.3.1. Hormones and signal transduction pathways regulating adipogenesis

1.3.2. Transcriptional regulation of adipocyte differentiation

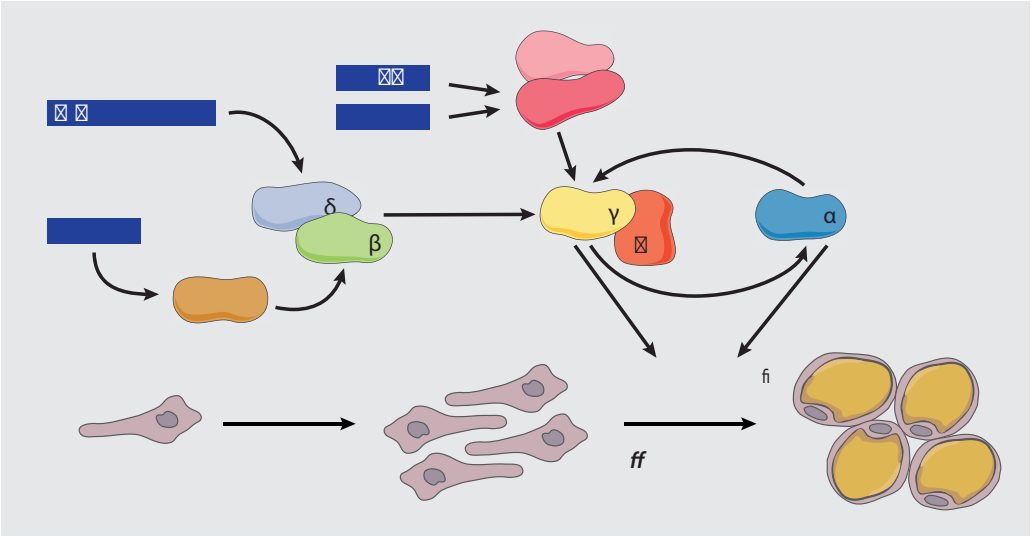

Figure 9. Schematic overview of the transcriptional and hormonal induction of adipogenesis. Scheme adapted from [72].

1.4. Mechanisms of insulin resistance

1.4.1. Insulin signaling pathway

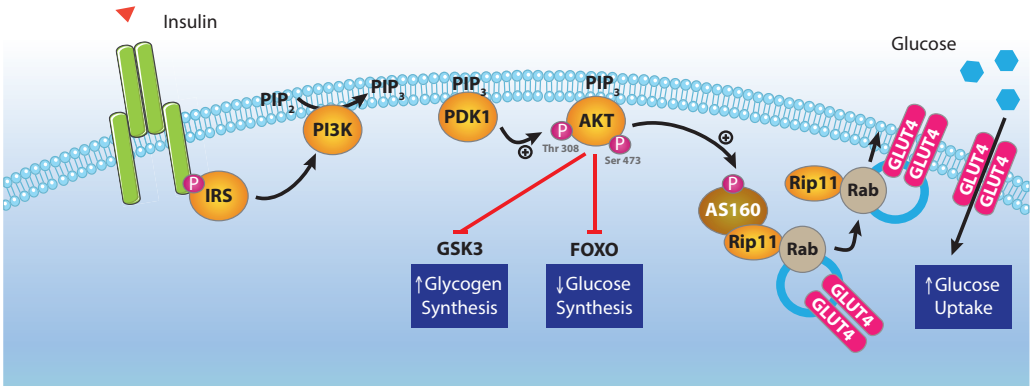

Figure 10. Abbreviated insulin signaling pathway. Image adapted from [104].

1.4.2. Mechanisms of insulin resistance

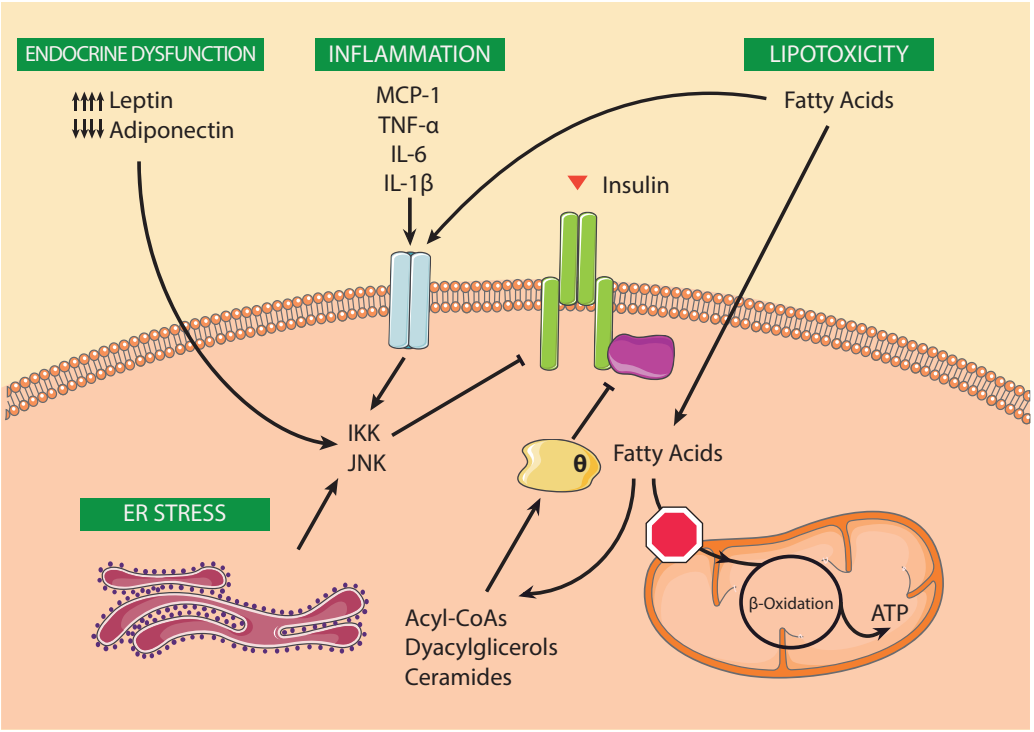

Figure 11. Scheme of the mechanisms mediating insulin resistance in obesity. Image from [105].

1.4.2.1. Lipotoxicity

1.4.2.2. Inflammation

1.4.2.3. Endoplasmic reticulum stress

1.4.2.4. Mitochondrial dysfunction

1.5. Regulation of mitochondrial biogenesis

1.5.1. Mitochondrial functions

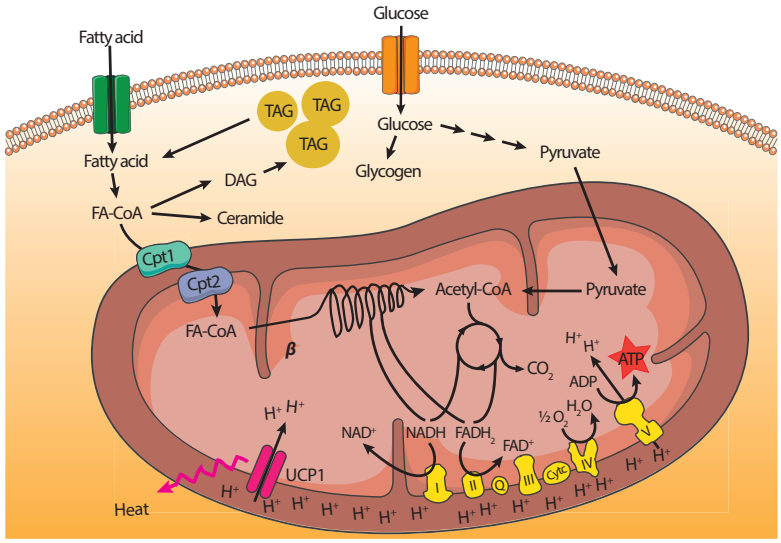

Figure 12. Schematic overview of metabolic oxidative pathways that take place in mitochondria. Image adapted from [153].

1.5.2. Transcriptional control of mitochondrial biogenesis

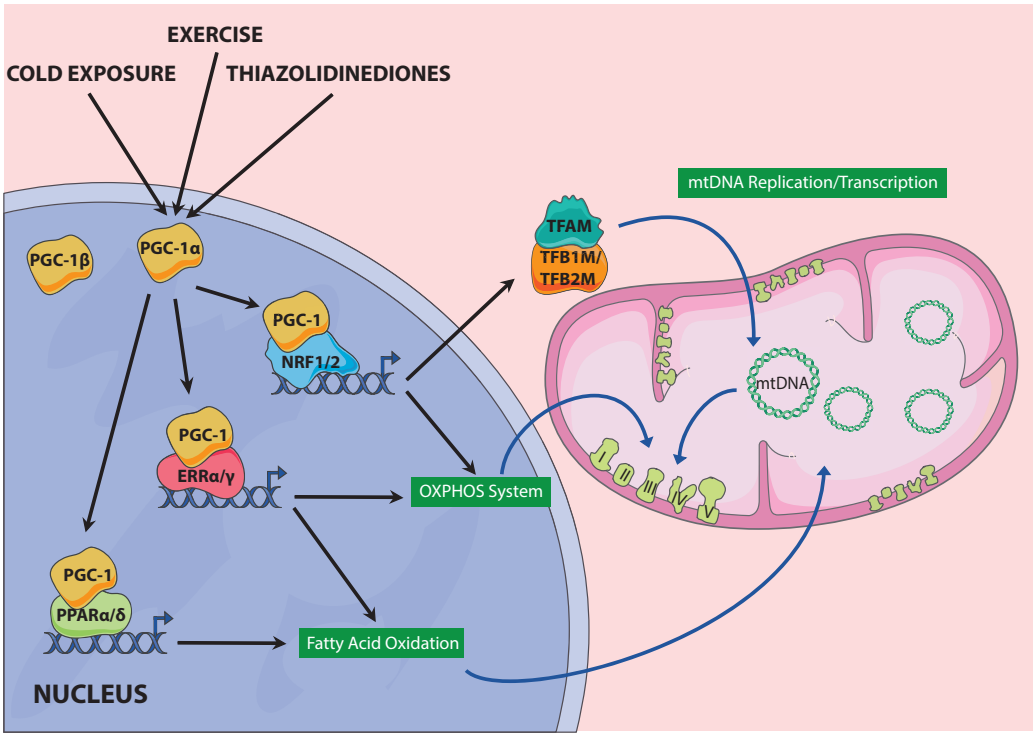

Figure 13. Overview of transcriptional control of mitochondrial biogenesis. Image a from [105].

1.5.2.1. Transcriptional regulators of mtDNA gene expression

1.5.2.2. Transcriptional regulators of mitochondrial genes encoded in the nuclear genome

[illegible]

Peroxisome Proliferator-Activated Receptors

[illegible]

[illegible]

[illegible]

[illegible]

[illegible]

[illegible]

[illegible]

[illegible]

[

1.5.2.3. Transcriptional coregulators of mitochondrial gene expression

[illegible]

[illegible]

1.6. PGC-1 family coactivators

1.6.1. Structure and mode of action

[illegible]

[illegible]

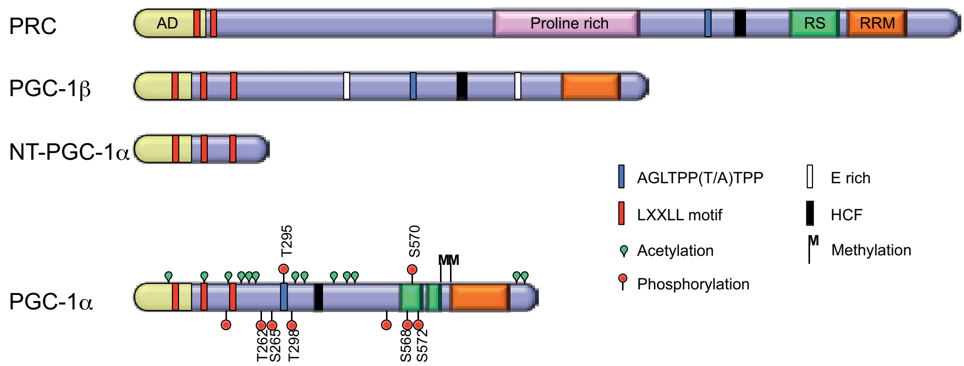

Figure 14. Structural domains of PGC-1 family members.

[illegible]

[illegible]

[illegible]

[illegible]

[illegible]

1.6.2. Regulation of PGCs activity by post-translational modifications

1.6.3. Function of PGC1 coactivators in different tissues

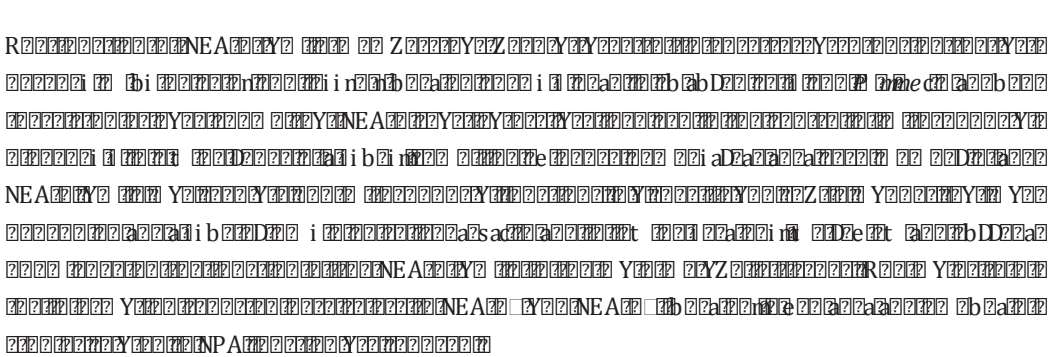

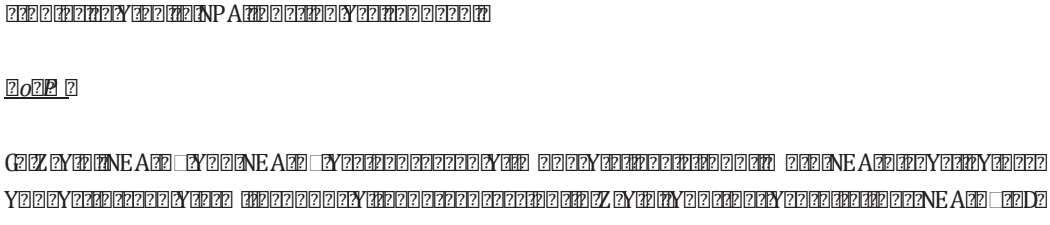

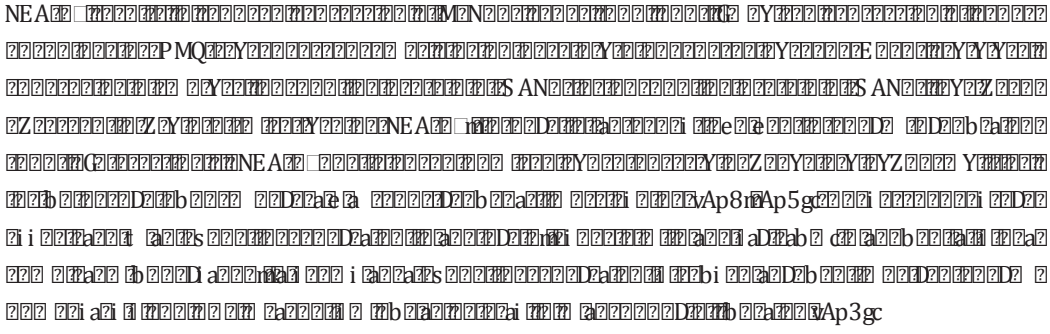

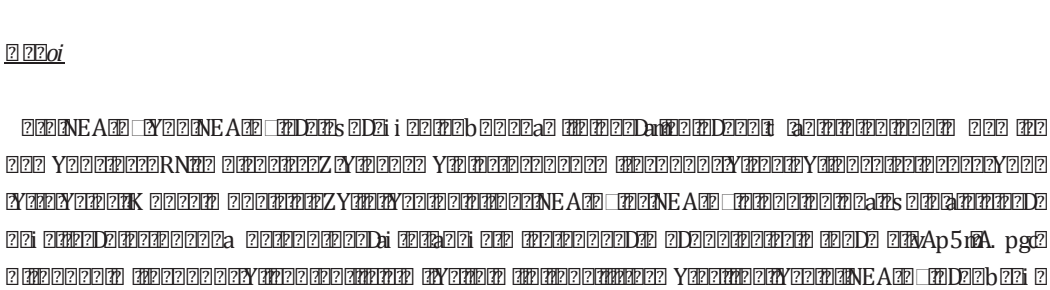

2. OBJECTIVES

3.MATERIALS AND METHODS

3.1. Animal studies

3.1.1. PGC1β-FAT-KO mice generation

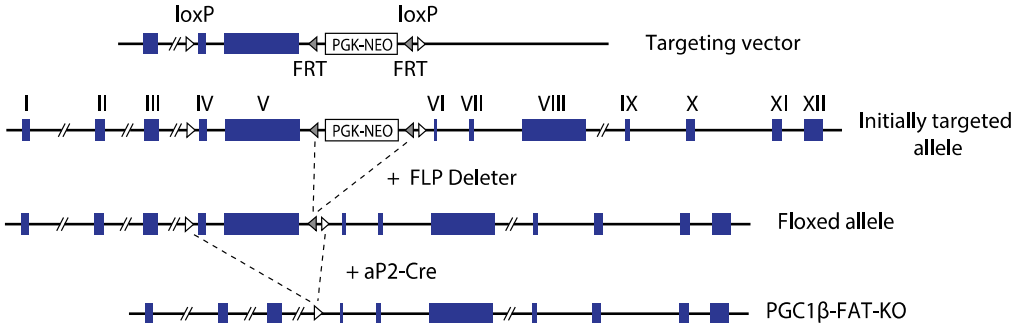

Figure 1. Scheme of PGC1β-FAT-KO mice generation.

3.1.2. Mice genotyping

[illegible]

bfs fr fs f[illegible]

[illegible]

[illegible]

sf [illegible]

rf [illegible]

bf [illegible]

xf [illegible]

. f [illegible]

3f [illegible]

1f [illegible]

2f [illegible]

Df [illegible]

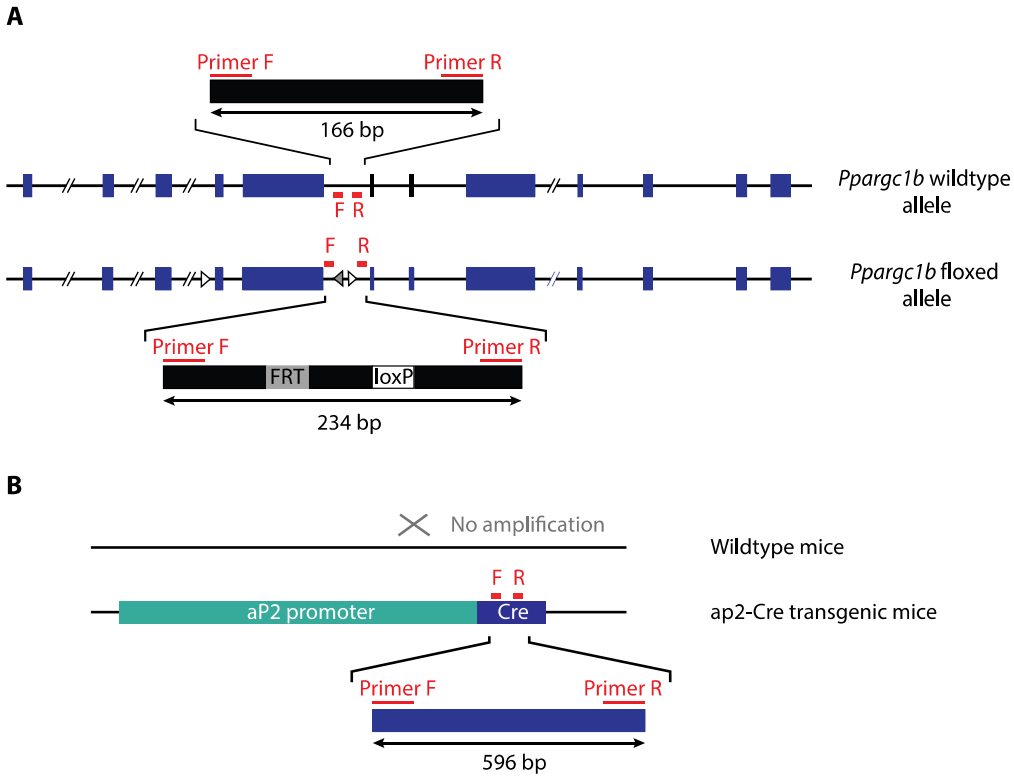

Figure 2. (A) Scheme of *Ppargc1b* wildtype and floxed allele and location of primers used for mice genotyping. (B) Scheme of aP2-Cre insert and location of primers used for mice genotyping.

1. Prepare the PCR master mix on ice in a sterile microcentrifuge tube. Add the components in the order listed in Table 1.

2. Gently mix the reaction by pipetting up and down. Briefly centrifuge to collect the contents at the bottom of the tube.

Component	Volume	Final concentration
Water	17.15 µL	
10X PCR Buffer	2.5 µL	2 mM $MgCl_2$
dNTP mix (10 mM each)	0.5 µL	200 µM (of each dNTP)
Forward primer (10 µM)	1.3 µL	0.52 µM
Reverse primer (10 µM)	1.3 µL	0.52 µM
Taq DNA Polymerase (5U/µL)	0.25 µL	0.05 U/µL

3. Add 2 µL of DNA template to the master mix. Gently mix by pipetting up and down.

4. Add DNA template to the master mix. Gently mix by pipetting up and down.

5. Transfer the reaction tubes to the thermal cycler. Ensure the lid is closed tightly.

6. Set the thermal cycler to the following conditions. Adjust the annealing temperature and extension time as needed based on the primer Tm and the length of the target amplicon.

Step	Temperature	Time	Cycles
Denaturation/Activation	94°C	2 min	1
Denaturation	94°C	30 sec	35
Annealing	58°C	30 sec	
Extension	72°C	45 sec	
Final extension	72°C	5 min	1
Cooling	4°C	∞	1

Troubleshooting common PCR issues

If you encounter problems with your PCR reaction, such as no amplification, non-specific bands, or low yield, consider the following troubleshooting steps. First, check the quality and concentration of your DNA template using a spectrophotometer or gel electrophoresis. Ensure that the primers are specific to the target sequence and have appropriate melting temperatures. Optimize the annealing temperature by performing a gradient PCR, where different temperatures are tested in a single run. Adjust the magnesium chloride concentration, as it can affect the stringency of primer binding and the activity of the DNA polymerase. Increase the number of cycles if the yield is low, but be cautious not to exceed 40 cycles, as this can lead to non-specific amplification. If you suspect contamination, prepare fresh reagents and use dedicated pipettes and workspaces for PCR setup. Finally, consider using a hot-start DNA polymerase to reduce non-specific amplification during the initial heating step.

For more information on PCR troubleshooting, refer to the following resources:

- Bio-Rad PCR Troubleshooting Guide
  - https://www.bio-rad.com/webroot/web/pdf/lsr/literature/Bulletin_2895.pdf
  - https://www.bio-rad.com/webroot/web/pdf/lsr/literature/Bulletin_2895.pdf

- [illegible]

[illegible] bmp [illegible]

[illegible]

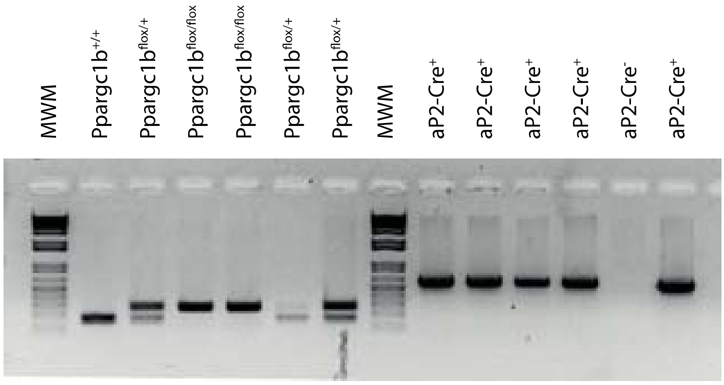

Figure 3. Example of a PCR of tail genomic DNA to detect loxP flanked *Ppargc1b* alleles and the presence of aP2-Cre transgene. DNA amplified samples were electrophoresed on a 2% agarose gel.

3.1.3. Mice housing conditions

[illegible]

[illegible]

[illegible]

[illegible]

3.1.4. Efficiency of *Ppargc1b* gene recombination

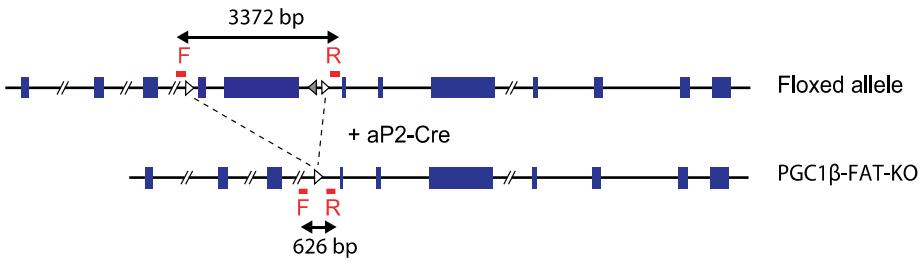

Figure 4. Location of primers to detect recombination in *Ppargc1b* floxed allele.

Step	Temperature	Time	Cycles
Denaturation/Activation	94°C	2 min	1
Denaturation	94°C	30 sec	35
Annealing	58°C	30 sec	
Extension	72°C	45 sec	
Final extension	72°C	5 min	1
Cooling	4°C	∞	1

3.1.5. Measurement of food intake

3.1.6. Pharmacological treatments

3.1.6.1. Rosiglitazone treatment

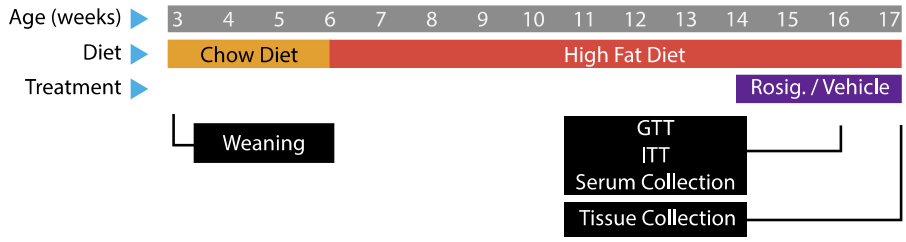

Figure 5. Overwiew of rosiglitazone experiment setup.

3.1.6.2. β_3-adrenergic agonist (CL-316,243) treatment

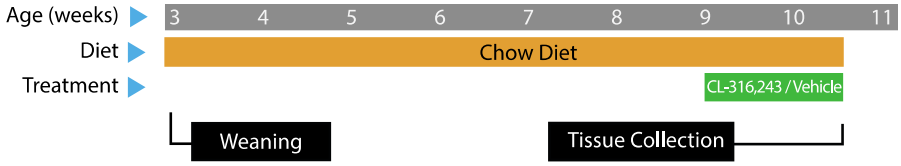

Figure 6. Overwiew [illegible] ergic agonist experiment setup.

3.1.7. Intraperitoneal glucose tolerance test

[illegible]

[illegible]

- [illegible]
- [illegible]
- [illegible]
- [illegible]
- [illegible]
- [illegible]

[illegible]

3.1.8. Intraperitoneal insulin tolerance test

[illegible]

3.1.9. Tissue collection

3.2. Isolation of mature adipocytes and stromal vascular fraction

MATERIALS AND METHODS

[illegible]

[illegible]

[illegible]

[illegible]

[illegible]

[illegible]

[illegible]

[illegible]

3.3. Gene expression analysis

3.3.1. Total RNA isolation

[illegible]

[illegible]

[illegible]

3.3.1.1. RNA isolation by isopropanol precipitation

I

- a
- r
- o
- t
- -
- h
- m
- e
- z
- ag
- aa
- ar
- ao
- at
- a-

3.3.1.2. RNA isolation from fatty tissues or cells using the RNeasy Lipid Tissue Mini Kit

3.3.2. RNA quality control

3.3.3. Reverse transcription

3.3.4. Real-time quantitative PCR

[1,2]

1. Prepare the reaction mix (Table 1) and add 18 µL to each well of a 96-well plate.

Component	Volume	Final concentration
Water	6 µL	
2X SYBR Green Master Mix	10 µL	1X
Forward primer (10 µM)	1 µL	0.5 µM
Reverse primer (10 µM)	1 µL	0.5 µM

2. Add 2 µL of cDNA (10 ng/µL) to each well. Include a non-template control (NTC) for each primer pair.
3. Seal the plate with optical adhesive film and centrifuge briefly (1000 rpm, 1 min).
4. Run the qPCR using the following thermal cycling conditions (Table 2).
5. Export the raw data (Ct values) for analysis using the $2^{-\Delta\Delta Ct}$ method.

TABLE 1. List of primers used for real-time quantitative PCR in this study.

Gene symbol	Entrez ID	Gene name	Forward primer	Reverse primer
Acaa2	52538	acetyl-Coenzyme A acyltransferase 2	TGTGTCAGAAATGTGCGCTTC	CAAGGCGTATCTGTCACAGTC
Acadm	11364	acyl-Coenzyme A dehydrogenase, medium chain	AAGCCACGAAGTATGCCCTG	CCATAGCCTCCGAAAATCTG
Aco2	11429	aconitase 2	TCTCTAACAACCTGCTCATCGG	TCATCTCCAATCACCACCCACC
Acss1	68738	acyl-CoA synthetase short-chain family member 1	TGCAAGGCTGTTATCACCTTC	TCTTCACTGCTCATGCTCTCA
Adipoq	11450	adiponectin, C1Q and collagen domain containing	TGTTCCTCTTAATCCTGCCCA	CCAACCTGCACAAGTTCCCTT
Atgl/ Pnpla2	66853	patatin-like phospholipase domain containing 2	CCTGATGACCACCCTTTCCAAC	ACCCGTCTGCTCTTTCATCCAC
Atp5a1	11946	ATP synthase, H+ transporting, mitochondrial F1 complex, alpha subunit 1	TTAGAGACAACGGCAAGCACG	ACATCTGGCGGTAAGCGACAG

Atp5b	11947	ATP synthase, H+ transporting mitochondrial F1 complex, beta subunit	GCAAGGCAGGGACAGCAGA	CCCAAGGTCTCAGGACCAACA
Atp5o	28080	ATP synthase, H+ transporting, mitochondrial F1 complex, O subunit	AAGGACCCCAAAGTGTCTCTG	TAGGCGACCATTTTCAGCAAG
Cat	12359	catalase	TGGCACACTTTGACAGAGAGC	CCTTTGCCTTGGAGTATCTGG
Cebpa	12606	CCAAT/enhancer binding protein (C/EBP), alpha	CGCTGTTGCTGAAGGAACTTG	GGCAGACGAAAAAACCCAAAC
Cidea	12683	cell death-inducing DNA fragmentation factor, alpha subunit-like effector A	CCTCGGCTGTCTCAATGTC	GGCTGCTCTTCTGTATGC
Cideb	12684	cell death-inducing DNA fragmentation factor, alpha subunit-like effector B	TTTCAGCCTTCAACCCCAATG	GTCCACAGCAGTCCATCCTC
Cox4i1	12857	cytochrome c oxidase subunit IV isoform 1	ATGTCACGATGCTGTCTGCC	GTGCCCCTGTTCATCTCGGC
Cox5a	12858	cytochrome c oxidase subunit Va	AACAAGCCAGACATTGATGCC	CAACCTCCAAGATGCGAACAG
Cox5b	12859	cytochrome c oxidase subunit Vb	GCTACTGGGCTGGAGAGGGAG	CTTGTTGCTGATGGACGGGAC
Cox7a1	12865	cytochrome c oxidase subunit VIIa 1	GACAATGACCTCCCAGTACAC	GCCCAGCCCAAGCAGTATAAG
Cox8b	12869	cytochrome c oxidase subunit VIIIb	CGAAGTTCACAGTGGTTCCC	TCTCCAAGTGGGCTAAGACC
Cpt1b	12895	carnitine palmitoyltransferase 1b, muscle	TCTAGGCAATGCCGTTCAC	GAGCACATGGGCACCATAC
Cs	12974	citrate synthase	AGAGGCATGAAGGGACTTGTGTA	TGTTCCTCTGTGGGCATCTGT
Cyc1	66445	cytochrome c-1	ATTTCAACCCTTACTTTCCCG	CCACTTATGCCGCTTCATGGC
Cycs	13063	cytochrome c, somatic	CACGGCTCTCCCTTTCTCAAG	ACAGTTGCCTCCTGGTGGTTA
Cypa/Ppia	268373	peptidylprolyl isomerase A	CAAGACTGAATGGCTGGATG	ATGGGGTAGGGACGCTCTCC
Dio2	13371	deiodinase, iodothyronine, type II	CAGCTTCCTCCTAGATGCCTA	CTGATTCAGGATTGGAGACGTG
Elovl6	170439	ELOVL family member 6, elongation of long chain fatty acids (yeast)	CGAGAACGAAGCCATCCAATG	GCAAGAGTCAGCGACCAGAGC
Esrra	26379	estrogen related receptor, alpha	GGAGGACGGCAGAAGTACAAA	GCGACACCAGAGCGTTCAC
Esrrg	26381	estrogen-related receptor gamma	TCCCCGACAGTGACATCAAA	GTGTGGAGAAGCCTGGAATA
Fabp3	14077	fatty acid binding protein 3, muscle and heart	GGAATAGAGTTCGACGAGGTGA	CTCCCTAGTTAGTGTTGTCTCCT
Fabp4	11770	fatty acid binding protein 4, adipocyte	TGTGTGATGCCTTTGTGGGAACC	CTTCACCTTCCTGTCGTCTGCGG
Gpx1	14775	glutathione peroxidase 1	GGTTTCCCGTGCAATCAGTT	CCACCAGGTCGGACGTACTT
Idh3a	67834	isocitrate dehydrogenase 3 (NAD+) alpha	AGGACTGATTGGAGGTCTTGG	ATCACAGCACTAAGCAGGAGG
Idh3b	170718	isocitrate dehydrogenase 3 (NAD+) beta	GCCGTCCATAAAGCCAACATC	GAGCACCCGTCTCAAAAACTG
Lep	16846	leptin	GACACCAAAACCCTCATCAAGAC	GGTGAAGCCCAGGAATGAAGT
Lipe	16890	lipase, hormone sensitive	AAGAGGCCAGGGAGGGCCTCAG	TCCAGCCCCAGTGCCTGTTCC
Mdh2	17448	malate dehydrogenase 2, NAD (mitochondrial)	GCCCAGGAAACCAGGAATG	GATGGGGATGGTGGAGTTCA
mt-Atp6	17705	ATP synthase 6, mitochondrial	AGGATTCCCAATCGTTGTAGCC	CCTTTTGGTGTGTGGATTAGCA
mt-Co2	17709	cytochrome c oxidase II, mitochondrial	TCTCCCCTCTCTACGCATTCTA	ACGGATTGGAAGTTCTATTGGC
mt-Co3	17710	cytochrome c oxidase III, mitochondrial	TCCAAGTCCATGACCATTAACTG	TATTGGTGAGTAGGCCAAGGG
mt-Nd2	17717	NADH dehydrogenase 2, mitochondrial	ATACTTCGTCACACAAGCAACA	GGCCTAGTTTTATGGATAGGGCT
Ndufa4	17992	NADH dehydrogenase (ubiquinone) 1 alpha subcomplex, 4	CTGGAGCAGCACTGTATGTGA	CTGGGCCTTCTTTCTTCAGTT
Ndufab1	70316	NADH dehydrogenase (ubiquinone) 1, alpha/beta subcomplex, 1	GGAATCAAGGACCGAGTTCTG	TCCAAACTGTCTAAGCCCAGG
Ndufb6	230075	NADH dehydrogenase (ubiquinone) 1 beta subcomplex, 6	TGGAAGAACATGGTCTTTAAGGC	AAGCACATGAGAAACAGCGAA
Ndufb9	66218	NADH dehydrogenase (ubiquinone) 1 beta subcomplex, 9	AAGGTGCTGCGGCTGTATAAG	TACGGCTGAGGATGCTGATTC

Nrf1	18181	nuclear respiratory factor 1	CCACGTTGGATGAGTACACG	CTGAGCCTGGGTCATTTTGT
Nrf2/ Gabpa	14390	GA repeat binding protein, alpha [Mus musculus	CCGCTACACCGACTACGATT	ACCTTCATCACCAACCCAAG
Ppargc1a	19017	peroxisome proliferative activated receptor, gamma, coactivator 1 alpha	GGAGCCGTGACCACTGACA	TGGTTTGCTGCATGGTTC TG
Ppargc1b	170826	peroxisome proliferative activated receptor, gamma, coactivator 1 beta	AGTGGGTGCGGAGACACAGATG	GTATGGAGGTGTGGTGGGTGGC
Pprc1	226169	peroxisome proliferative activated receptor, gamma, coactivator-related 1	TGGACGCCTCCCTTATATCCC	TGTGAGCAGCGACATTTCATTC
Ppara	19013	peroxisome proliferator activated receptor alpha	AAGGCTATCCCAGGCTTTGC	TTTAGAAGGCCAGGCCGATCTC
Pparg	19016	peroxisome proliferator activated receptor gamma	ATTGAGTGCCGAGTCTGTGGG	AGCAAGGCACTTCTGAAACCG
Prdm16	70673	PR domain containing 16 [Mus musculus	AAGATGGAAATCGGGGAGAGG	CAGGAACACGCTACACGGATG
Pref1/Dlk1	13386	delta-like 1 homolog (Drosophila)	CGTCCTCTTGCTCCTGCTGGC	TCCCGTCCCAGCCATCCTTGC
Retn	57264	resistin	AAGAACCTTTCATTTCCCCTCCT	GTCCAGCAATTTAAGCCAATGTT
Rip140/ Nrip1	268903	nuclear receptor interacting protein 1	TCCCCGACACGAAAAAGAAAG	ACATCCATTCAAAAGCCCAGG
Sdhb	67680	succinate dehydrogenase complex, subunit B, iron sulfur (Ip)	TACCGATGGGACCCAGACA	CGTGTGCACGCCAGAGTAT
Sdhd	66925	succinate dehydrogenase complex, subunit D, integral membrane protein	TGGTCAGACCCGCTTATGTG	GAGCAGGGATTCAAGTACCCA
Sod2	20656	superoxide dismutase 2, mitochondrial	AACGCCACCGAGGAGAAGTA	AATATGTCCCCCACCATTGAAC
Tfam	21780	transcription factor A, mitochondrial	CCAGGAGGCAAAGGATGATTC	CTTCGTCCAATTCAGCCATC
Tfb1m	224481	transcription factor B1, mitochondrial	AAGGACACTCGCTTTATCCCA	CCATGAACAATTCGGAGTTTTCC
Tfb2m	15278	transcription factor B2, mitochondrial	TATAGAGCCGTTGCCTGATTCT	GCCGCTTTCTTACATGCTATGTG
Tnfa	21926	tumor necrosis factor	CTTCTCATTCCTGCTTGTGGC	ACTTGGTGGTTTGCTACGACG
Ucp1	22227	uncoupling protein 1 (mitochondrial, proton carrier)	CACCTTCCCGCTGGACACTGC	GATTTGCCTCTGAATGCCCGC
Ucp2	22228	uncoupling protein 2 (mitochondrial, proton carrier)	GCATTGGCCTCTACGACTCTG	AGCGGACCTTTACCACATCTG
Ucp3	22229	uncoupling protein 3 (mitochondrial, proton carrier)	ACAGAGGGACTATGGATGCCT	TGATGTCGTAGGTCACCATCT
Uqcrc2	67003	ubiquinol cytochrome c reductase core protein 2	AAAGTTGCCCCGAAGGTTAAA	CAGAGAAGCAATCACCAAACCA
Uqcrh	66576	ubiquinol-cytochrome c reductase hinge protein	GGACTAGAGGACGAACGAAAGA	GGCCTTTACACACTTCTCCAG
Uqcrq	22272	ubiquinol-cytochrome c reductase, complex III subunit VII	CCTACAGCTTGTCGCCCTTT	GCCTTTGCTGAAATAGCTTGGG

3.3.5. Primer design

[illegible]

- [illegible]
- [illegible]
- [illegible]
- [illegible]

3.3.6. Gene expression profiling

3.4. Protein extraction and protein analysis by Western Blot
3.4.1. Total protein extraction and quantification

oa	I M2U UV
yoa	ya e d
yM uwa	y e d
o p d	y e d p d
o	V V R V MD V R V S T R MX R yg w I V R I C I HV V I V R

. g e F

- yg X V VU H S V XR d g
- mg s a ed dwA g
- sg r 7 d R LVRXV V IV T X X IV UV R X V V V R V
- wg i i r 7 d R LVRXV V IV T
- og TV R VU R A

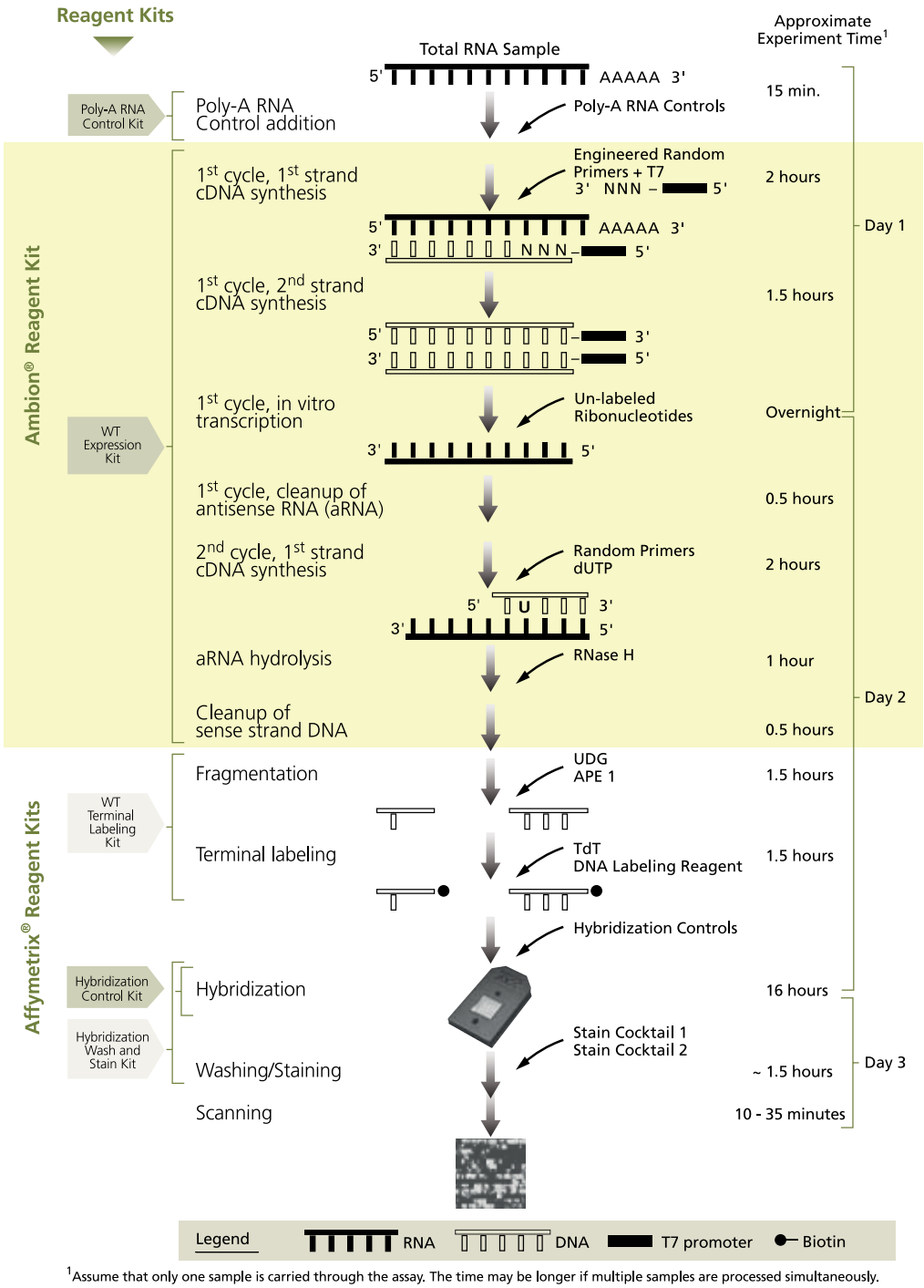

[1]Assume that only one sample is carried through the assay. The time may be longer if multiple samples are processed simultaneously.

Figura 7. Scheme of microarray assay. Image from extracted from GeneChip® WT Terminal Labeling and Hybridization User Manual.

3.4.2. SDS-polyacrylamide gel electrophoresis

3.4.3. Western Blot

TABLE 2. LIST OF ANTIBODIES USED IN THIS STUDY

Antibody	Type	Source	Working dilution	Incubation solution	Supplier	Cat. Number
Primary Antibodies						
α-TUBULIN	Monoclonal	Rabbit	1:2000	BSA	Cell Signaling	2125
NDUFB9	Polyclonal	Rabbit	1:1000	Milk	Abcam	ab106699
SDHB	Polyclonal	Rabbit	1:1000	Milk	Abcam	ab84620
CYCS	Polyclonal	Rabbit	1:1000	Milk	Cell Signaling	4272
COX4I1	Polyclonal	Rabbit	1:1000	Milk	Cell Signaling	4844
ATP5B	Polyclonal	Rabbit	1:1000	Milk	Abcam	ab85068
ACO2	Polyclonal	Rabbit	1:500	Milk	Abcam	ab71440
UCP1	Polyclonal	Rabbit	1:1000	Milk	Abcam	ab10983
AKT	Polyclonal	Rabbit	1:1000	BSA	Cell Signaling	9272
P-AKT Ser473	Polyclonal	Rabbit	1:1000	BSA	Cell Signaling	9271
PGC-1β*	Polyclonal	Rabbit	50 ng/μL	Milk	Dr. Kralli	-----
Secondary Antibody						
Rabbit IgG	----	Goat	1:10.000	Milk	Cell Signaling	7074

Table 2. Antibodies used in this study. (*) PGC-1β antibody was generated by immunizing rabbits with a bacterially expressed protein having aminoacids 91–426 of PGC-1β fused to GST.

3.4.4. Stripping of PVDF membranes

[illegible]

[illegible]

3.5. Mitochondrial DNA quantification

[illegible]

[illegible]

[illegible]

3.6. Mitochondrial activity

3.6.1. Citrate synthase activity

1g [illegible]

5g [illegible]

Lg [illegible]

bg [illegible]

ug [illegible]

5gbgdgLg [illegible]

[illegible]

[illegible]

[illegible]

[illegible]

[illegible]

dg [illegible]

1g [illegible]

5g [illegible]

Lg [illegible]

ug [illegible]

bg [illegible]

3.6.2. Respiratory chain complexes enzymatic activity

Spectrophotometric techniques described by Degli [251] were used for performing *in vitro* redox assays to functionally dissect a single respiratory enzyme within the biological preparation. Mitochondria-enriched fractions were obtained from inguinal WAT as described in section 3.6.1.1.

All assays were performed using a UV-2401 PC (Shimadzu) spectrophotometer.

3.6.2.1. Complex I (NADH-ubiquinone oxidoreductase) enzymatic activity

$$NADH + H^{+} + Q \rightarrow NAD^{+} + QH_2$$

- Reagent solution: 25 mM potassium phosphate buffer, 5 mM MgCl2, 2 mM EDTA, 2 mM KCN, 2 mg/ml BSA, pH 7.5
- Substrate solution: 10 mM NADH in reagent solution
- Activator solution: 10 mM decylubiquinone in 96% ethanol
- Inhibitor solution: 10 mM rotenone in 96% ethanol

- [illegible]
- [illegible]
- [illegible]
- [illegible]

[illegible]

1. [illegible]
2. [illegible]
3. [illegible]
5. [illegible]
6. [illegible]
7. [illegible]
8. [illegible]

[illegible]

[illegible]

[illegible]	[illegible]	[illegible]
[illegible]	[illegible]	[illegible]
[illegible]	[illegible]	[illegible]
[illegible]	[illegible]	[illegible]
[illegible]	[illegible]	[illegible]
[illegible]	[illegible]	[illegible]
[illegible]	[illegible]	[illegible]
[illegible]	[illegible]	[illegible]
[illegible]	[illegible]	[illegible]

3.6.2.2. Complex II (succinate dehydrogenase (ubiquinone)) enzymatic activity

3.6.2.3. Complex II + Complex III (Succinate-Cytochrome c oxidoreductase) enzymatic activity

3.6.2.4. Complex IV (Cytochrome c oxidase) enzymatic activity

- i
- i
- Te
- y

i e

- e
- He
- Ce
- le
- , e
- pe

f

D N V N X V D A U V N N V V V V V N U N S C I O N X m

L V V V N V V
V N O X N
N X V
L S U X N
X X X 1 1 m
F N V V V S V S S U m
m X 1 1 X i m

3.7. Fatty acid oxidation assay ex vivo

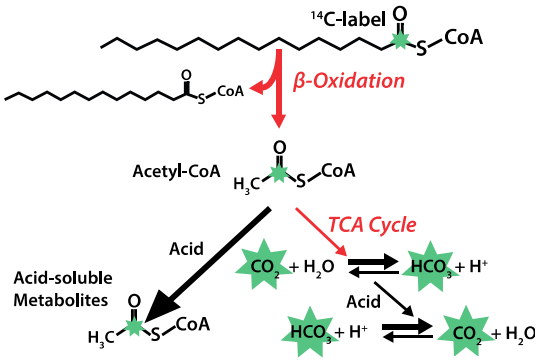

Figure 8. Schematic representation of radiolabeled palmitate oxidation. One molecule of [1-^{14}C] palmitate enters β-oxidation cycle and after one round of oxidation one radiolabeled Acetyl-CoA molecule is produced. This Acetyl-CoA molecule is directly used as an energy source within the TCA cycle. During TCA cycle $^{14}CO_2$ is liberated and dissolved in the medium as bicarbonate. After medium acidification, $^{14}CO_2$ is released and trapped with a CO_2 chelator.

	Stock solution	Info	For 10 mL of stock solution
FA-free BSA	1 mM	Mw: 66338 g/mol	666.34 mg
Sodium palmitate	5 mM	Mw: 278.41 g/mol	13.92 mg
Palmitic Acid [1-^{14}C]	8.33 µCi/mL (138 µM)	Stock: 0.1 mCi/mL	833.3 µL

- [illegible]
- [illegible]
- [illegible]

[illegible]

[illegible]

[

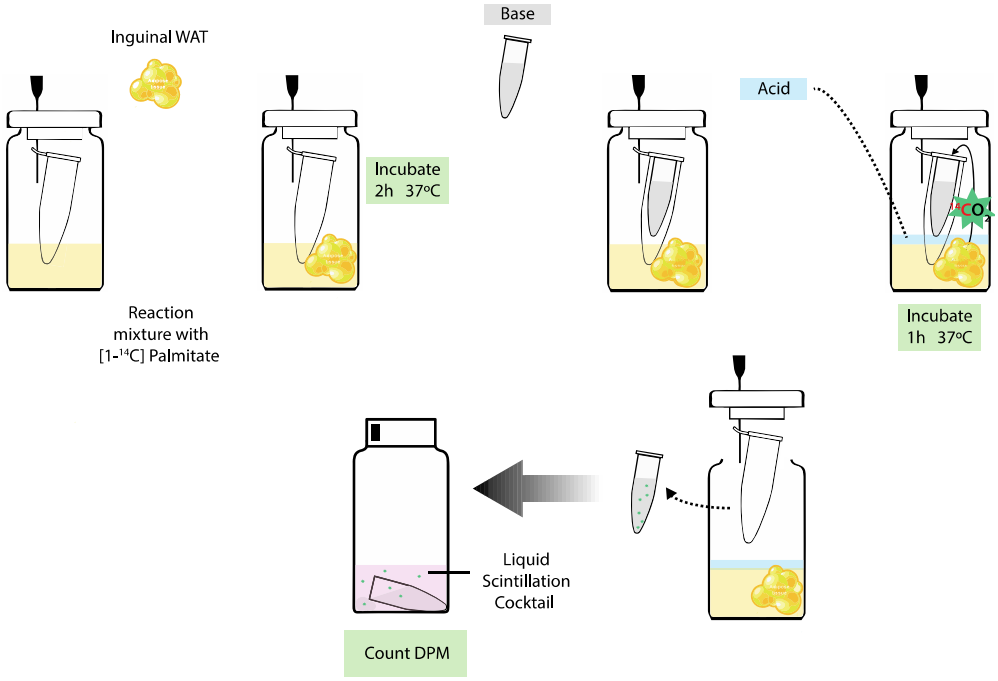

Figure 9. Schematic representation of fatty acid oxidation assay *ex vivo*.

3.8. Study of insulin-stimulated phosphorylation of AKT

[illegible]

[illegible]

	Insulin	Ketamine	Xylazyne
Product/Supplier	Actrapid; Lab. Novo Nodisk	Ketolar; Grupo Pfizer	Xilagesic; Lab. Calier
Stock solution	100 U/mL	50 mg/mL	20 mg/mL
Working solution	1U/mL in 0.9% NaCl	Ketamine/Xylazine ratio 200:54 (vol/vol)	
Mice dose	5U/kg	100 mg/kg	11 mg/kg
		2.2 µL de anesthesic cocktail/g of mouse	

vt [illegible]

it [illegible]

gt [illegible]

ht [illegible]

st [illegible]

dt [illegible]

- [illegible]
- [illegible]
- [illegible]

ut [illegible]

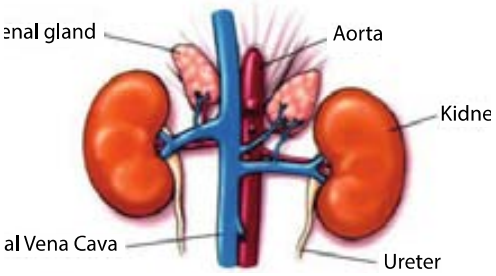

Figure 10. Illustration of anatomical location of Caudal Vena Cava (Image property of Drs. Kenneth S. Latimer and Ashley L. Ayoob 2000).

3.9. Serological parameters

gtl tvt [illegible]

[illegible]

nlwlnl

M W R W R W R

3.10. Histological analysis

-
-
-
-
-
-

[illegible]

[illegible] M[illegible]X[illegible]V[illegible]L[illegible]LX[illegible]V

- [illegible]
- [illegible]
- [illegible]
- [illegible]
- [illegible]
- [illegible]

adi[illegible]

- ESaLM[illegible] MKM[illegible]ML[illegible] [illegible]MT [illegible]V[illegible] VX[illegible]VS[illegible]V[illegible]XM[illegible]V[illegible]
  l[illegible]
- [illegible]

cdi[illegible]

- [illegible]
- [illegible]
- ESaLM[illegible] MKM[illegible]ML[illegible] [illegible]MV[illegible] VX[illegible]VS[illegible]V[illegible]VX[illegible]T [illegible]M[illegible]
- [illegible]
- 0. %[illegible]
- [illegible]
- [illegible]

hdi[illegible]

- [illegible]

3.11. Cell culture procedures of 3T3-L1 cells

[illegible]

[illegible]

[illegible]

3.11.1. Cell culture media for 3T3-L1 fibroblasts

[illegible]

3.11.2. Resurrection of frozen 3T3-L1 cell stocks from liquid nitrogen

1. Incubate the cryovial containing the cells in a water bath at 37°C for 2 minutes.
2. Transfer the cells into a 15 mL centrifuge tube containing 10 mL of pre-warmed culture medium (DMEM supplemented with 10% FBS and 1% penicillin/streptomycin).
3. Centrifuge the cell suspension at 1000 rpm for 5 minutes at room temperature.
4. Discard the supernatant and resuspend the cell pellet in 10 mL of fresh culture medium.
5. Transfer the cell suspension into a 75 cm² culture flask and incubate at 37°C in a humidified atmosphere containing 5% CO₂.

3.11.3 3T3-L1 fibroblasts subculturing protocol

1. When the cells reach 70-80% confluence, remove the culture medium from the flask.
2. Wash the cell monolayer with 5 mL of pre-warmed PBS to remove any residual serum.
3. Add 2 mL of trypsin-EDTA solution to the flask and incubate at 37°C for 5 minutes to detach the cells.
4. Neutralize the trypsin activity by adding 8 mL of culture medium to the flask.
5. Transfer the cell suspension into a 15 mL centrifuge tube and centrifuge at 1000 rpm for 5 minutes at room temperature.
6. Discard the supernatant and resuspend the cell pellet in 10 mL of fresh culture medium.
7. Count the cells using a hemocytometer and seed them into new culture flasks at a density of 2 × 10⁴ cells/cm².
8. Incubate the cells at 37°C in a humidified atmosphere containing 5% CO₂.

3.11.4. 3T3-L1 fibroblasts differentiation protocol

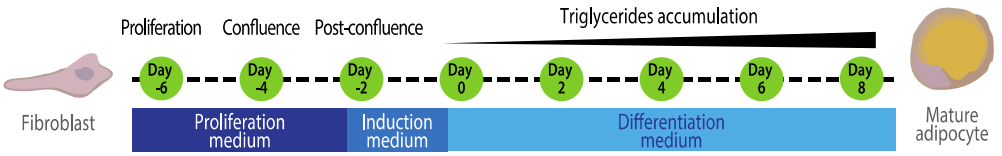

Figure 11. Scheme of protocol for adipocyte differentiation.

3.11.5. Preparation of 3T3-L1 fibroblast cells for freezing

- s
- w
- c
- -
- y
- d
- i
- v

3.12. siRNA transfection of 3T3-L1 adipocytes

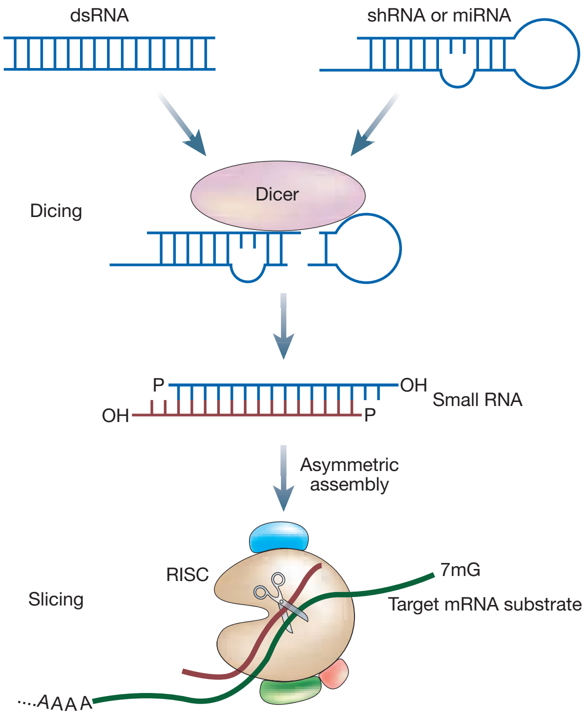

Figure 12. Mechanism of RNA silencing in different systems. Long dsRNA and miRNA precursors are processed to siRNA/miRNA duplexes by the RNase-III-like enzyme Dicer. These short dsRNAs are subsequently unwound and assembled into effector complexes, RISCs, which can direct RNA cleavage, mediate translational repression. Image and text extracted from [252].

[illegible]

[illegible]

TABLE 3. siRNAs used in this study

Component	Catalog number	Description
siGLO Red	D-001630-02-20	Fluorescent siRNA transfection indicator
ON-TARGETplus Non-targeting siRNA #2	D-001810-02-20	Negative control siRNA
ON-TARGETplus GAPD	D-001830-02-20	Positive control siRNA targeting GAPDH
ON-TARGETplus SMARTpool siRNA, PPARGC1B	L-040905-01-0020	Pool of 4 different siRNA targeting PPARGC1B
ON-TARGETplus SMARTpool siRNA, PPARGC1A	L-040773-01-0020	Pool of 4 different siRNA targeting PPARGC1A

3.12.1. Transfection of adhered 3T3-L1 adipocytes. Optimization protocol.

[illegible]

[illegible]

[illegible]

		0.7 µL/cm² Dharmafect		1.4 µL/cm₂ Dharmafect	
		siRNA 25 nM	siRNA 100 nM	siRNA 25 nM	siRNA 100 nM
Tube 1	DharmaFECT 4	2.8 µL	2.8 µL	5.6 µL	5.6 µL
	OptiMEM	77.2 µL	77.2 µL	74.4 µL	74.4 µL
Tube 2	siRNA 5 µM	5 µL	20 µL	5 µL	20 µL
	OptiMEM	75 µL	60 µL	75 µL	60 µL

[illegible]

3.12.2. Transfection of 3T3-L1 adipocytes on suspension. Optimization protocol.

[illegible]

[illegible]

[illegible]

[illegible]

[illegible]

[illegible]

[illegible]

		0.7 µL/cm^{2} Dharmafect		1.4 µL/cm$_{2}$ Dharmafect	
		siRNA 25 nM	siRNA 100 nM	siRNA 25 nM	siRNA 100 nM
Tube 1	DharmaFECT 4	2.8 µL	2.8 µL	5.6 µL	5.6 µL
	OptiMEM	77.2 µL	77.2 µL	74.4 µL	74.4 µL
Tube 2	siRNA 5 µM	5 µL	20 µL	5 µL	20 µL
	OptiMEM	75 µL	60 µL	75 µL	60 µL

[illegible]

3.12.3. siRNA transfection of 3T3-L1 adipocytes to knockdown PGC-1[illegible] [illegible] PGC-1[illegible]

[illegible]

[illegible]

[illegible]

MATERIALS AND METHODS

pl E M M N T G N M P A TM MC M R O M S N
1 l

		siControl 100 nM	siPGC-1α 50 nM + siControl 50 nM	siPGC-1β 50 nM + siControl 50 nM	siPGC-1α 50 nM + siPGC-1β 50 nM
Tube 1	DharmaFECT 4	5.6 µL	5.6 µL	5.6 µL	5.6 µL
	Opti-MEM	74.4 µL	74.4 µL	74.4 µL	74.4 µL
Tube 2	siRNA 5 µM (Control)	20 µL	10 µL	10 µL	---
	siRNA 5 µM (Test)	--	10 µL	10 µL	10 µL+10 µL
	Opti-MEM	60 µL	60 µL	60 µL	60 µL

M
1
w e e p
1 2 1
1 l
E
1 p p
1 M
1 p TO l
1 e 1 l
w e
1 M O 1
1
c OO
1 2 h 2 lOOO t
E h n 2 o M p TuMm 1
d e 1 e e
p m c u h M 1 l

3.13. ATP production measurement

1 E E u p e 1 1 e
e l 1 1 e 1
1 e 1
O N M M P N M M A O R M P N M A O R T M M N M P O R M
1 I T M O I M S T O T
e 1 i

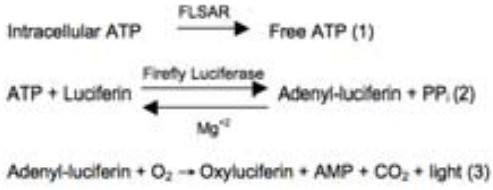

P O M R O P I D I D N T
M M P M P T F S M A F M P O N P O
eu 1 d e e e e r w e p OOO e t
1 1 e e 1 1 e e 1

3.14. ROS production measurement

3.15. Oxygen consumption

3.16. Fatty acid oxidation assay *in vitro*

- [illegible]
- [illegible]
- [illegible]
- [illegible]

[illegible]

1. [illegible]
   - [illegible]
   - [illegible]
   - [illegible]
2. [illegible]
3. [illegible]

[illegible]

4. [illegible]
5. [illegible]
6. [illegible]
7. [illegible]
8. [illegible]

[illegible]

[illegible]

[illegible]

3.17. Statistical analysis

4.RESULTS

4.1. Generation of a mouse model lacking PGC-1β specifically in adipocytes

4.1.1. *Ppargc1b* expression in white adipocytes

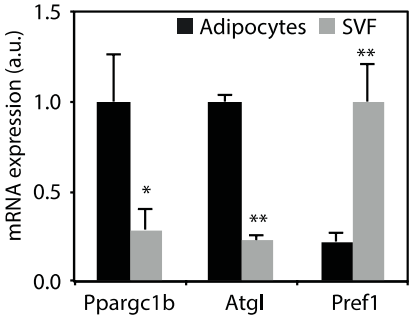

Figure 1. mRNA expression of *Ppargc1b*, *Atgl* and *Pref1* in adipocytes and SVF isolated by collagenase digestion from inguinal WAT. mRNA expression was assessed by real-time quantitative PCR. Results are expressed as means ± SEM (n=4-5 animals). * indicates statistical significance between adipocytes and SVF. * P≤0.05; ** P≤0.01.

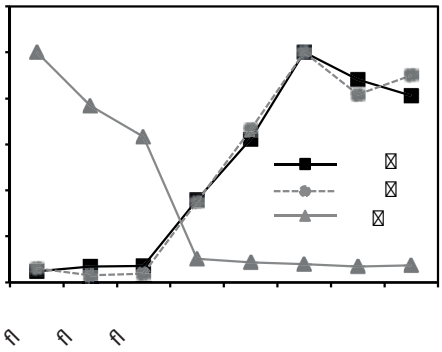

ff

Figure 2. mRNA expression of *Ppargc1b*, *PPARg* and *Pref1* during differentiation of 3T3-L1 cells. mRNA expression was assessed by real-time quantitative PCR. A Representative experiment out of 3 is shown in this figure.

4.1.2. Generation of a PGC1β-FAT-KO mouse model to study the role of PGC-1β in WAT

RESULTS

4.1.3. Efficiency of *Ppargc1b* gene disruption in adipose tissues

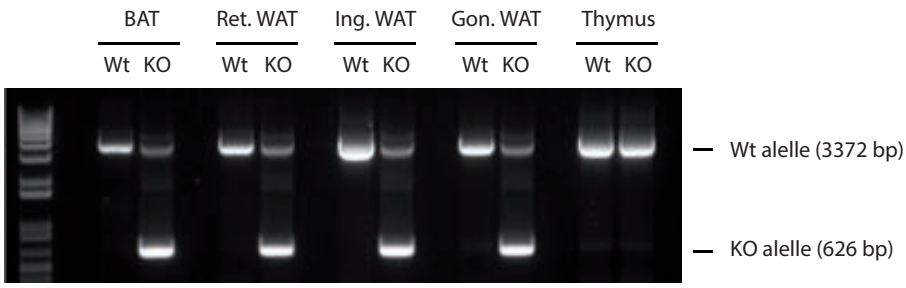

Figure 3. Recombination of *Ppargc1b* gene in different tissues of Wt and PGC1β-FAT-KO mice. The recombination was assessed by PCR using genomic DNA of BAT, several WAT depots and thymus. Primer forward and reverse were situated upstream and downstream respectively the loxP regions flanking exons 4 and 5 of the *Ppargc1b* gene. Amplification of the Wt allele yields a band of 3372 bp, while the recombined allele yields a shorter band of 626 bp.

4.1.4. Effect of *Ppargc1b* gene disruption on PGC-1β mRNA levels

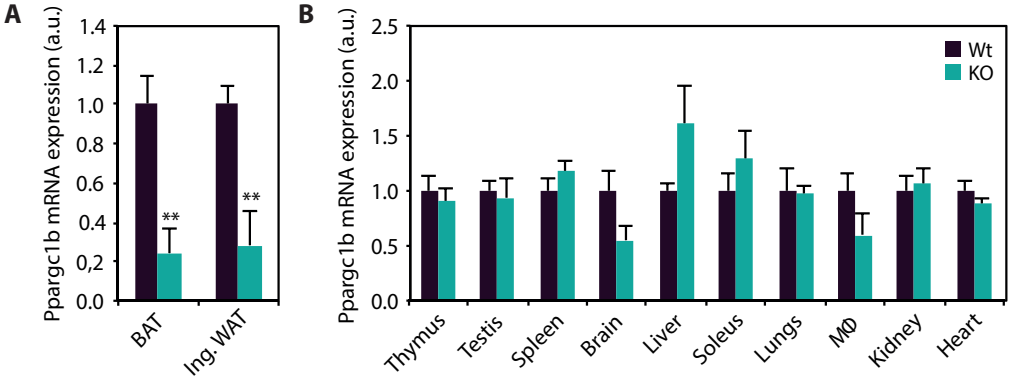

Figure 4. *Ppargc1b* mRNA levels in tissues of male mice fed a chow diet and housed at 21ºC. The expression of PGC-1β mRNA in (A) adipose tissues and (B) non-adipose tissues of PGC1β-FAT-KO mice and Wt littermates was assessed by real-time quantitative PCR. MΦ stands for macrophages. Results are expressed as means ± SEM (n=4-7 animals/group, ** P≤ 0.01).

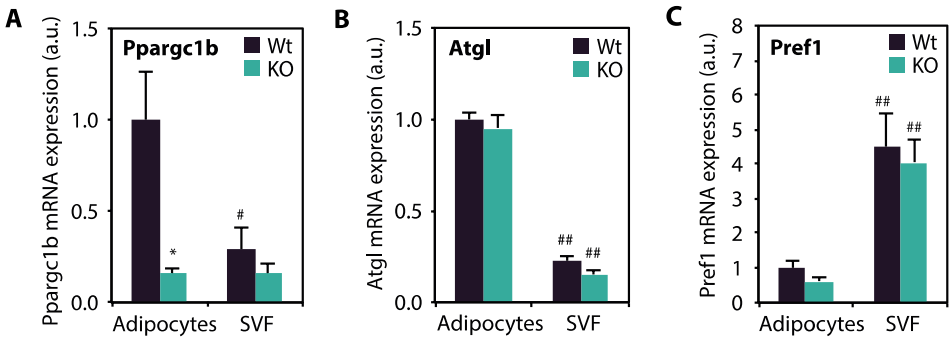

Figure 5. Expression of (A) (B) *Atgl* and (C) *Pref1* was assessed by real-time quantitative PCR in white adipocytes and SVF isolated from inguinal WAT of Wt and PGC1β-FAT-KO mice fed a standard diet and housed at 21ºC. Results are expressed as means ± SEM (n=4-5 animals/group). * Indicates statistical significance between Wt and PGC1β-FAT-KO mice; # indicates statistical significance between adipocytes and SVF. *, # P≤0.05; **, ## P≤0.01.

4.1.5. Effect of *Ppargc1b* gene disruption on PGC-1β protein levels

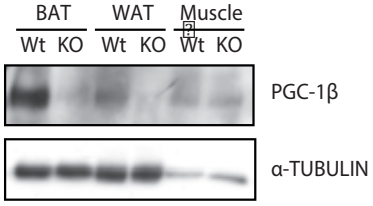

Figure 6. Western Blot analysis of PGC-1β protein levels in interscapular BAT, retroperitoneal WAT and gastrocnemius muscle of Wt and PGC1β-FAT-KO mice fed a chow diet and housed at 21ºC. α-TUBULIN protein was detected as a loading control.

4.1.6. Physiological characterization of PGC1β-FAT-KO mice housed at 21ºC

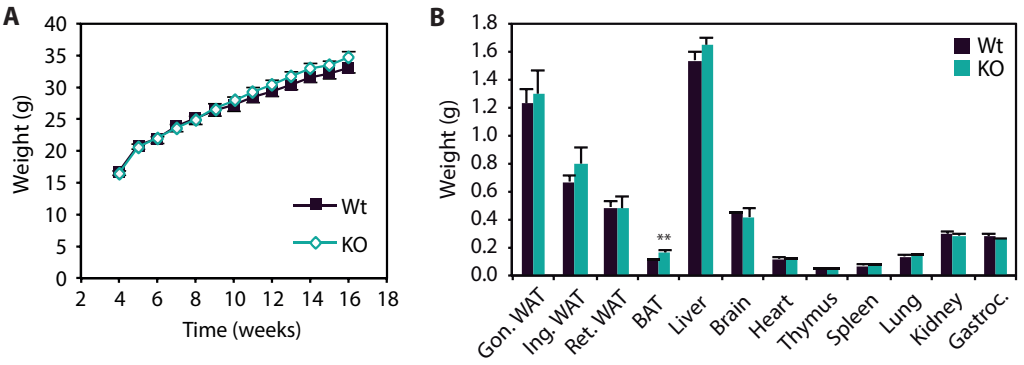

Figure 7. (A) Body weight and (B) tissue weight of wild type and PGC1β-FAT-KO male mice fed chow diet and housed at 21ºC. Results are expressed as means ± SEM (n=4-5 animals/group). * Indicates statistical significance between Wt and PGC1β-FAT-KO mice. ** P≤0.01.

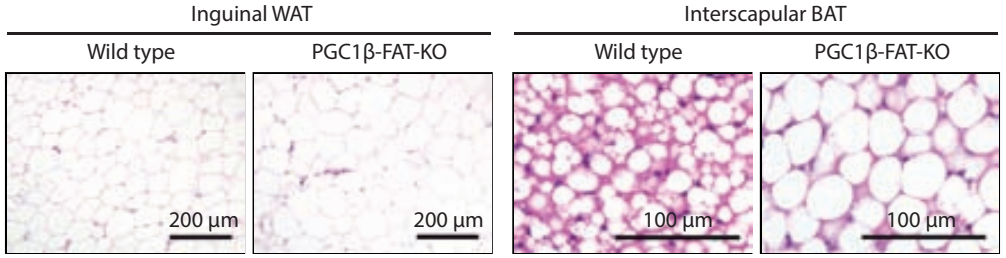

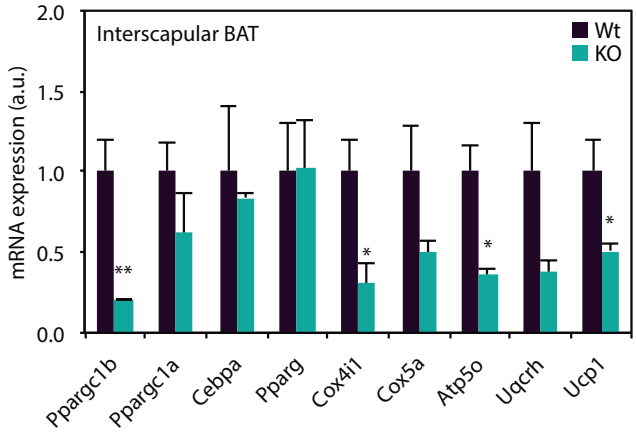

Figure 9. mRNA expression levels in BAT of mice housed 21ºC and fed a chow diet assessed by quantitative PCR. Results are expressed as means ± SEM (n=4-5 animals/group). * Indicates statistical significance between Wt and PGC1β-FAT-KO mice. * P≤0.05; ** P≤0.01.

4.2. Study of the cellular process regulated by PGC-1β in white adipose tissue

4.2.1. Gene expression profile analysis of retroperitoneal WAT from PGC1β-FAT-KO mice housed at 30ºC

RESULTS

TABLE 1. LIST OF UP-REGULATED GENES IN PGC1β-FAT-KO MICE IN THE MICROARRAY ANALYSIS

Entrez ID	Symbol	Gene Name	logFC	P.Value
26938	St6galnac5	ST6 (alpha-N-acetyl-neuraminyl-2,3-beta-galac-tosyl-1,3)-N-acetylgalactosaminide alpha-2,6-sialyltrans-ferase 5	0.992	2.43E-03
18979	Pon1	paraoxonase 1	0.867	3.17E-03
13107	Cyp2f2	cytochrome P450, family 2, subfamily f, polypeptide 2	0.856	2.16E-02
12053	Bcl6	B-cell leukemia/lymphoma 6	0.797	1.49E-03
19416	Rasd1	RAS, dexamethasone-induced 1	0.781	5.06E-04
237175	Gpr64	G protein-coupled receptor 64	0.761	2.35E-02
20860	Sult1e1	sulfotransferase family 1E, member 1	0.719	1.36E-03
320974	Lrrn4	leucine rich repeat neuronal 4	0.696	5.29E-04
22414	Wnt2b	wingless related MMTV integration site 2b	0.656	3.69E-04
100647	Upk3b	uroplakin 3B	0.637	8.33E-04
19872	Rny1	RNA, Y3 small cytoplasmic (associated with Ro protein); RNA, Y1 small cytoplasmic, Ro-associated	0.630	3.34E-04
17528	Mpz	myelin protein zero	0.599	3.53E-02
234267	Gpm6a	glycoprotein m6a	0.590	6.56E-03
22223	Uchl1	ubiquitin carboxy-terminal hydrolase L1	0.589	2.89E-02
21743	Inmt	indolethylamine N-methyltransferase	0.550	9.62E-05
192190	Pkhd1l1	polycystic kidney and hepatic disease 1-like 1	0.548	1.30E-02
70676	Gulp1	GULP, engulfment adaptor PTB domain containing 1	0.540	2.72E-02
17933	Myt1l	myelin transcription factor 1-like	0.532	2.43E-04
14264	Fmod	fibromodulin	0.504	7.17E-03
55987	Cpxm2	carboxypeptidase X 2 (M14 family)	0.500	3.95E-03
235281	Scn3b	sodium channel, voltage-gated, type III, beta	0.499	1.36E-02
79362	Bhlhe41	basic helix-loop-helix family, member e41	0.498	6.59E-03
319229	Sctr	secretin receptor; similar to Sctr protein	0.482	3.41E-02
13170	Dbp	D site albumin promoter binding protein	0.469	1.56E-02
18619	Penk	preproenkephalin	0.461	9.31E-03
192199	Rspo1	R-spondin homolog (Xenopus laevis)	0.459	1.98E-03
230157	Tmeff1	transmembrane protein with EGF-like and two follista-tin-like domains 1	0.458	4.65E-02
12797	Cnn1	calponin 1	0.449	2.20E-02
15483	Hsd11b1	hydroxysteroid 11-beta dehydrogenase 1	0.449	1.61E-02
14734	Gpc3	glypican 3	0.445	9.60E-03
330695	Ctxn1	cortexin 1	0.444	8.62E-03
12737	Cldn1	claudin 1	0.440	1.39E-02
18823	Plp1	proteolipid protein (myelin) 1	0.438	3.65E-02
11568	Aebp1	AE binding protein 1	0.437	3.68E-03
56332	Amotl2	angiomotin-like 2	0.435	7.74E-03
13731	Emp2	epithelial membrane protein 2	0.430	2.20E-02

380967	Tmem106c	transmembrane protein 106C	0.421	1.57E-03
94214	Spock2	sparc/osteonectin, cwcv and kazal-like domains proteoglycan 2	0.416	1.10E-03
399558	Flrt2	fibronectin leucine rich transmembrane protein 2	0.408	2.99E-03
23967	Osr1	odd-skipped related 1 (Drosophila)	0.400	1.03E-02
21345	Tagln	transgelin	0.400	2.69E-02
58804	Cdc42ep5	CDC42 effector protein (Rho GTPase binding) 5	0.400	2.58E-02
13497	Drp2	dystrophin related protein 2	0.391	4.97E-02
269037	Ctif	CBP80/20-dependent translation initiation factor	0.391	2.46E-02
217166	Nr1d1	nuclear receptor subfamily 1, group D, member 1	0.390	1.27E-02
100217418	Snora44	small nucleolar RNA, H/ACA box 44	0.387	3.00E-02
269831	Tspan12	tetraspanin 12	0.386	3.06E-02
19871	Rnu73b	U73B small nuclear RNA; U73A small nuclear RNA	0.385	3.17E-02
272428	Acsm5	acyl-CoA synthetase medium-chain family member 5	0.383	3.43E-02
14546	Gdap10	ganglioside-induced differentiation-associated-protein 10	0.382	1.17E-02

Table 1. List of the first 50 up-regulated genes obtained in a microarray analysis comparing mRNA expression levels in retroperitoneal WAT from wild type and PGC1β-FAT-KO mice housed at 30ºC and fed a standard diet. Genes are listed in descending order of logarithm of fold change.

TABLE 2. LIST OF UP-REGULATED GENES IN PGC1β-FAT-KO MICE IN THE MICROARRAY ANALYSIS

Entrez ID	Symbol	Gene Name	logFC	P.Value
14077	Fabp3	acid binding protein 3, muscle and heart	-1.351	2.7E-04
12895	Cpt1b	carnitine palmitoyltransferase 1b, muscle	-1.277	9.6E-05
12683	Cidea	cell death-inducing DNA fragmentation factor, alpha subunit-like effector A	-1.261	2.7E-04
12865	Cox7a1	cytochrome c oxidase, subunit VIIa 1	-1.252	6.1E-05
12700	Cish	cytokine inducible SH2-containing protein	-0.974	1.3E-02
620807	Mup6	major urinary protein 6	-0.937	3.3E-02
12869	Cox8b	cytochrome c oxidase, subunit VIIIb	-0.895	1.9E-04
103172	Chchd10	coiled-coil-helix-coiled-coil-helix domain containing 10	-0.866	6.0E-04
12684	Cideb	cell death-inducing DNA fragmentation factor, alpha subunit-like effector B	-0.802	4.7E-02
67426	Cabc1	aarF domain containing kinase 3	-0.801	7.7E-04
18775	Prl3d1	prolactin family 3, subfamily d, member 1	-0.779	2.8E-02
15484	Hsd11b2	hydroxysteroid 11-beta dehydrogenase 2	-0.774	3.6E-02
63993	Slc5a7	solute carrier family 5 (choline transporter), member 7	-0.754	2.0E-02
27273	Pdk4	pyruvate dehydrogenase kinase, isoenzyme 4	-0.720	3.2E-03
385643	Kng2	kininogen 2	-0.711	1.4E-02
232493	Gys2	glycogen synthase 2	-0.588	4.4E-02
18406	Orm2	orosomucoid 2	-0.565	2.2E-02
75552	Paqr9	progestin and adipoQ receptor family member IX	-0.537	1.9E-02

26970	Pla2g2e	phospholipase A2, group IIE	-0.523	3.5E-02
73656	Ms4a6c	membrane-spanning 4-domains, subfamily A, member 6C	-0.512	4.7E-02
19013	Ppara	peroxisome proliferator activated receptor alpha	-0.499	2.8E-02
17294	Mest	mesoderm specific transcript	-0.494	1.3E-02
229791	D3Bwg0562e	DNA segment, Chr 3, Brigham & Women's Genetics 0562 expressed	-0.482	8.0E-03
246728	Oas2	2'-5' oligoadenylate synthetase 2	-0.482	4.4E-03
77219	Ptgr2	prostaglandin reductase 2	-0.473	5.0E-03
11429	Aco2	aconitase 2, mitochondrial	-0.462	8.0E-04
20510	Slc1a1	solute carrier family 1 (neuronal/epithelial high affinity glutamate transporter, system Xag), member 1	-0.457	4.5E-02
13063	Cycs	cytochrome c, somatic	-0.452	6.8E-03
75735	Pank1	pantothenate kinase 1	-0.437	4.7E-03
18430	Oxtr	oxytocin receptor	-0.433	4.5E-02
170718	Idh3b	isocitrate dehydrogenase 3 (NAD+) beta	-0.428	6.9E-04
11555	Adrb2	adrenergic receptor, beta 2	-0.426	6.1E-03
66925	Sdhd	succinate dehydrogenase complex, subunit D, integral membrane protein	-0.423	9.3E-04
21906	Otop1	otopetrin 1	-0.422	7.7E-03
435804	Olfr1335	olfactory receptor 1335	-0.413	2.6E-02
67775	Rtp4	receptor transporter protein 4	-0.409	7.8E-03
99899	Ifi44	interferon-induced protein 44	-0.396	1.1E-02
170439	Elovl6	ELOVL family member 6, elongation of long chain fatty acids (yeast)	-0.395	3.4E-02
105675	Ppif	peptidylprolyl isomerase F (cyclophilin F)	-0.394	1.0E-02
16832	Ldhb	lactate dehydrogenase B	-0.394	4.6E-03
23960	Oas1g	2'-5' oligoadenylate synthetase 1G	-0.392	7.8E-03
18655	Pgk1	phosphoglycerate kinase 1	-0.391	2.2E-03
216783	Olfr320	olfactory receptor 320	-0.384	7.4E-03
64136	Sdf2l1	stromal cell-derived factor 2-like 1	-0.372	1.4E-02
66218	Ndufb9	NADH dehydrogenase (ubiquinone) 1 beta subcomplex, 9	-0.364	3.1E-03
12858	Cox5a	cytochrome c oxidase, subunit Va	-0.361	4.4E-03
13004	Ncan	neurocan	-0.356	4.0E-02
20916	Sucla2	succinate-Coenzyme A ligase, ADP-forming, beta subunit	-0.354	1.8E-03
666907	Ms4a4a	membrane-spanning 4-domains, subfamily A, member 4A	-0.348	3.5E-02
21877	Tk1	thymidine kinase 1	-0.346	1.7E-02

Table 2. List of the first 50 down-regulated genes obtained in a microarray analysis comparing mRNA expression levels in retroperitoneal WAT from wild type and PGC1β-FAT-KO mice housed at 30ºC and fed a standard diet. Genes are listed in descending order of logarithm of fold change. Mitochondrial genes are highlighted in dark color.

[illegible]

TABLE 3. GENE ENRICHEMENT ANALYSIS OF UP-REGULATED GENES

Category	GO Term	# genes	P.Value
GOTERM_BP_FAT	GO:0035295~tube development	13	2.58E-05
GOTERM_BP_FAT	GO:0048729~tissue morphogenesis	12	4.86E-05
GOTERM_BP_FAT	GO:0006355~regulation of transcription, DNA-dependent	33	5.81E-05
GOTERM_BP_FAT	GO:0051252~regulation of RNA metabolic process	33	7.85E-05
GOTERM_BP_FAT	GO:0060562~epithelial tube morphogenesis	8	1.84E-04
GOTERM_BP_FAT	GO:0001501~skeletal system development	12	2.40E-04
GOTERM_BP_FAT	GO:0048706~embryonic skeletal system development	7	2.56E-04
GOTERM_BP_FAT	GO:0001656~metanephros development	6	3.76E-04
GOTERM_BP_FAT	GO:0045449~regulation of transcription	41	4.36E-04
GOTERM_BP_FAT	GO:0048598~embryonic morphogenesis	13	4.65E-04
GOTERM_BP_FAT	GO:0035239~tube morphogenesis	9	4.93E-04
GOTERM_BP_FAT	GO:0048704~embryonic skeletal system morphogenesis	6	5.94E-04
GOTERM_BP_FAT	GO:0060429~epithelium development	11	6.55E-04
GOTERM_BP_FAT	GO:0006350~transcription	34	8.60E-04
GOTERM_BP_FAT	GO:0001655~urogenital system development	8	9.62E-04
GOTERM_CC_FAT	GO:0005578~proteinaceous extracellular matrix	12	2.50E-04
GOTERM_CC_FAT	GO:0031012~extracellular matrix	12	3.51E-04
GOTERM_MF_FAT	GO:0030528~transcription regulator activity	28	5.19E-05
GOTERM_MF_FAT	GO:0043565~sequence-specific DNA binding	17	1.36E-04
GOTERM_MF_FAT	GO:0003705~RNA polymerase II transcription factor activity, enhancer binding	5	2.15E-04
GOTERM_MF_FAT	GO:0003700~transcription factor activity	20	2.58E-04

Table 3. Gene enrichment analysis of up-regulated genes in WAT from PGC1β-FAT- KO mice using DAVID bioinformatics source (GOTERM_CC_FAT, cellular component; GOTERM_BP_FAT, biological process; GOTERM_MF_FAT, molecular function). An EASE Score threshold of 0.001 was used in the analysis.

TABLE 4. GENE ENRICHEMENT ANALYSIS OF DOWN-REGULATED GENES

Category	GO Term	# genes	P.Value
GOTERM_BP_FAT	GO:0006091~generation of precursor metabolites and energy	43	3.32E-47
GOTERM_BP_FAT	GO:0022900~electron transport chain	25	1.13E-29
GOTERM_BP_FAT	GO:0006084~acetyl-CoA metabolic process	14	8.67E-21
GOTERM_BP_FAT	GO:0045333~cellular respiration	16	5.32E-20
GOTERM_BP_FAT	GO:0055114~oxidation reduction	34	1.04E-19

GOTERM_BP_FAT	GO:0015980~energy derivation by oxidation of organic compounds	17	6.03E-18
GOTERM_BP_FAT	GO:0006732~coenzyme metabolic process	18	1.33E-16
GOTERM_BP_FAT	GO:0006099~tricarboxylic acid cycle	11	2.02E-16
GOTERM_BP_FAT	GO:0046356~acetyl-CoA catabolic process	11	3.43E-16
GOTERM_BP_FAT	GO:0009060~aerobic respiration	11	1.45E-15
GOTERM_BP_FAT	GO:0009109~coenzyme catabolic process	11	3.40E-15
GOTERM_BP_FAT	GO:0051186~cofactor metabolic process	18	8.38E-15
GOTERM_BP_FAT	GO:0051187~cofactor catabolic process	11	1.08E-14
GOTERM_BP_FAT	GO:0006119~oxidative phosphorylation	8	1.23E-07
GOTERM_BP_FAT	GO:0006096~glycolysis	7	6.04E-07
GOTERM_BP_FAT	GO:0006006~glucose metabolic process	10	6.13E-07
GOTERM_BP_FAT	GO:0019320~hexose catabolic process	7	1.66E-06
GOTERM_BP_FAT	GO:0006007~glucose catabolic process	7	1.66E-06
GOTERM_BP_FAT	GO:0046365~monosaccharide catabolic process	7	2.09E-06
GOTERM_BP_FAT	GO:0019318~hexose metabolic process	10	2.95E-06
GOTERM_BP_FAT	GO:0044275~cellular carbohydrate catabolic process	7	3.91E-06
GOTERM_BP_FAT	GO:0046164~alcohol catabolic process	7	6.27E-06
GOTERM_BP_FAT	GO:0005996~monosaccharide metabolic process	10	8.03E-06
GOTERM_BP_FAT	GO:0016052~carbohydrate catabolic process	7	2.25E-05
GOTERM_BP_FAT	GO:0022904~respiratory electron transport chain	5	4.21E-05
GOTERM_BP_FAT	GO:0042773~ATP synthesis coupled electron transport	4	2.58E-04
GOTERM_BP_FAT	GO:0006085~acetyl-CoA biosynthetic process	3	7.27E-04
GOTERM_BP_FAT	GO:0009144~purine nucleoside triphosphate metabolic process	6	9.15E-04
GOTERM_CC_FAT	GO:0005739~mitochondrion	62	9.16E-38
GOTERM_CC_FAT	GO:0044429~mitochondrial part	44	5.13E-35
GOTERM_CC_FAT	GO:0019866~organelle inner membrane	37	3.41E-34
GOTERM_CC_FAT	GO:0005743~mitochondrial inner membrane	36	1.44E-33
GOTERM_CC_FAT	GO:0005740~mitochondrial envelope	38	5.52E-32
GOTERM_CC_FAT	GO:0031966~mitochondrial membrane	37	1.39E-31
GOTERM_CC_FAT	GO:0031967~organelle envelope	39	4.32E-28
GOTERM_CC_FAT	GO:0031975~envelope	39	4.95E-28
GOTERM_CC_FAT	GO:0070469~respiratory chain	20	3.80E-26
GOTERM_CC_FAT	GO:0031090~organelle membrane	39	9.28E-22
GOTERM_CC_FAT	GO:0031980~mitochondrial lumen	10	3.00E-06
GOTERM_CC_FAT	GO:0005759~mitochondrial matrix	10	3.00E-06
GOTERM_CC_FAT	GO:0044455~mitochondrial membrane part	6	2.85E-05
GOTERM_CC_FAT	GO:0005746~mitochondrial respiratory chain	4	1.65E-04
GOTERM_CC_FAT	GO:0045259~proton-transporting ATP synthase complex	4	3.43E-04
GOTERM_CC_FAT	GO:0045271~respiratory chain complex I	3	7.88E-04
GOTERM_CC_FAT	GO:0030964~NADH dehydrogenase complex	3	7.88E-04
GOTERM_CC_FAT	GO:0005747~mitochondrial respiratory chain complex I	3	7.88E-04

GOTERM_MF_FAT	GO:0015078~hydrogen ion transmembrane transporter activity	11	3.01E-10
GOTERM_MF_FAT	GO:0015077~monovalent inorganic cation transmembrane transporter activity	11	5.47E-10
GOTERM_MF_FAT	GO:0022890~inorganic cation transmembrane transporter activity	11	2.26E-08
GOTERM_MF_FAT	GO:0005506~iron ion binding	15	1.38E-07
GOTERM_MF_FAT	GO:0051539~4 iron. 4 sulfur cluster binding	6	5.10E-07
GOTERM_MF_FAT	GO:0003954~NADH dehydrogenase activity	6	6.41E-07
GOTERM_MF_FAT	GO:0050136~NADH dehydrogenase (quinone) activity	6	6.41E-07
GOTERM_MF_FAT	GO:0008137~NADH dehydrogenase (ubiquinone) activity	6	6.41E-07
GOTERM_MF_FAT	GO:0016655~oxidoreductase activity. acting on NADH or NADPH. quinone or similar compound as acceptor	6	1.20E-06
GOTERM_MF_FAT	GO:0051536~iron-sulfur cluster binding	7	1.40E-06
GOTERM_MF_FAT	GO:0051540~metal cluster binding	7	1.40E-06
GOTERM_MF_FAT	GO:0051287~NAD or NADH binding	6	1.46E-05
GOTERM_MF_FAT	GO:0004129~cytochrome-c oxidase activity	5	1.96E-05
GOTERM_MF_FAT	GO:0016676~oxidoreductase activity. acting on heme group of donors. oxygen as acceptor	5	1.96E-05
GOTERM_MF_FAT	GO:0015002~heme-copper terminal oxidase activity	5	1.96E-05
GOTERM_MF_FAT	GO:0016675~oxidoreductase activity. acting on heme group of donors	5	1.96E-05
GOTERM_MF_FAT	GO:0016651~oxidoreductase activity. acting on NADH or NADPH	6	3.04E-05
GOTERM_MF_FAT	GO:0048037~cofactor binding	9	2.11E-04
GOTERM_MF_FAT	GO:0009055~electron carrier activity	8	6.04E-04
GOTERM_MF_FAT	GO:0001730~2'-5'-oligoadenylate synthetase activity	3	7.45E-04
GOTERM_MF_FAT	GO:0050662~coenzyme binding	7	9.98E-04

Table 4. Gene enrichment analysis of down-regulated genes in WAT from PGC1β-FAT- KO mice using DAVID bioinformatics source (GOTERM_CC_FAT, cellular component; GOTERM_BP_FAT, biological process; GOTERM_MF_FAT, molecular function). An EASE Score threshold of 0.001 was used in the analysis.

4.2.2. Expression of genes in retroperitoneal WAT by real-time quantitative PCR

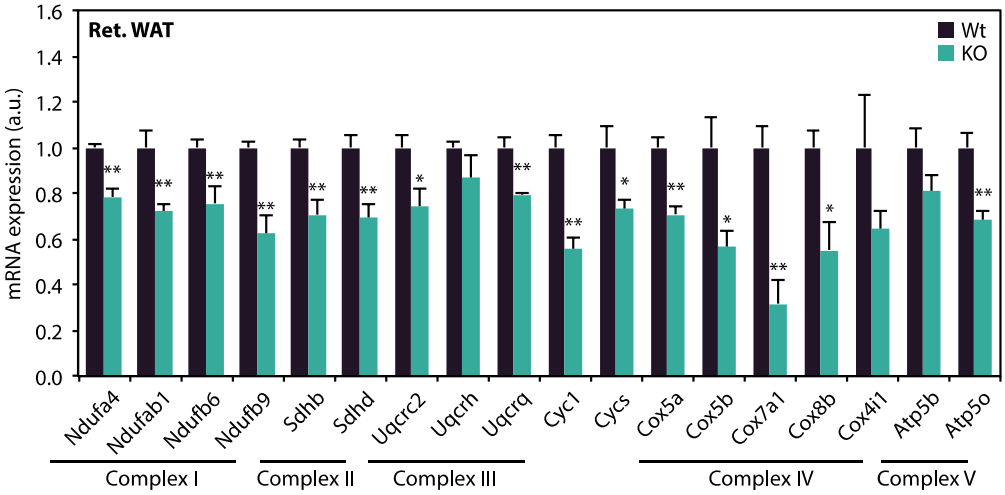

Figure 10. mRNA expression levels of genes involved in oxidative phosphorylation in retroperitoneal WAT from Wt and KO mice housed at thermoneutrality and fed a chow diet. mRNA levels were determined by quantitative RT-PCR. Results are expressed as means ± SEM (n=5-8 animals/group, * P≤ 0.05** P≤ 0.01).

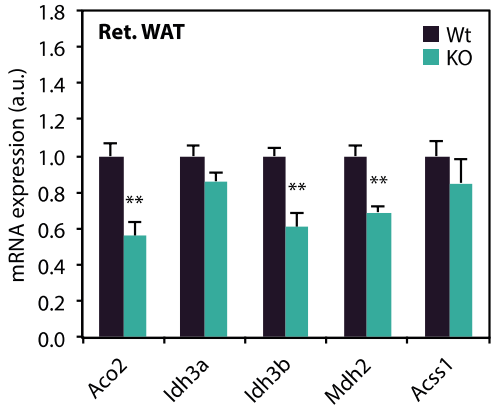

Figure 11. mRNA expression levels of genes involved in TCA cycle in retroperitoneal WAT from Wt and KO mice housed at thermoneutrality and fed a chow diet. mRNA levels were determined by quantitative RT-PCR. Results are expressed as means ± SEM (n=5-8 animals/group, ** P≤ 0.01).

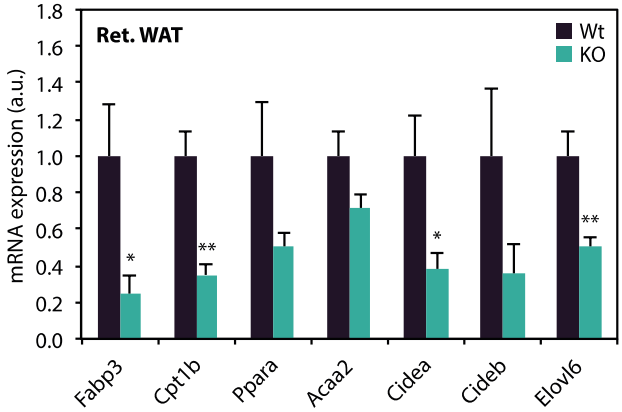

Figure 12. mRNA expression levels of genes involved in lipid metabolism in retroperitoneal WAT from Wt and KO mice housed at thermoneutrality and fed a chow diet. mRNA levels were determined by quantitative RT-PCR. Results are expressed as means ± SEM (n=5-8 animals/group, * P≤ 0.05** P≤ 0.01).

4.2.3. Gene expression analysis of PGC-1β target genes in subcutaneous WAT and interscapular BAT of PGC1β-FAT-KO mice

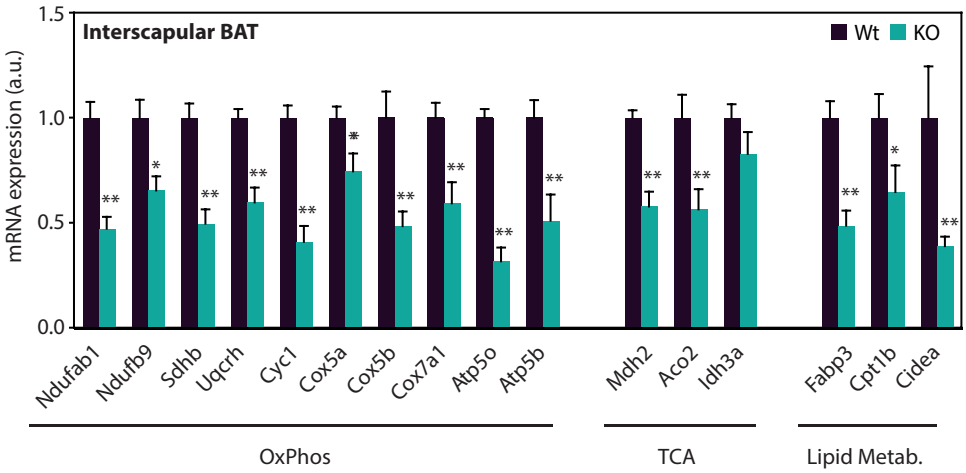

Figure 13. mRNA expression levels of mitochondrial genes involved in OxPhos, TCA or lipid metabolism in inguinal WAT of Wt and PGC1β-FAT-KO mice housed at thermoneutrality and fed a regular chow diet were determined by real-time quantitative RT-PCR. Results are expressed as mean ± SEM, n=5–8 animals/ group, *P≤0.05 **P≤0.01.

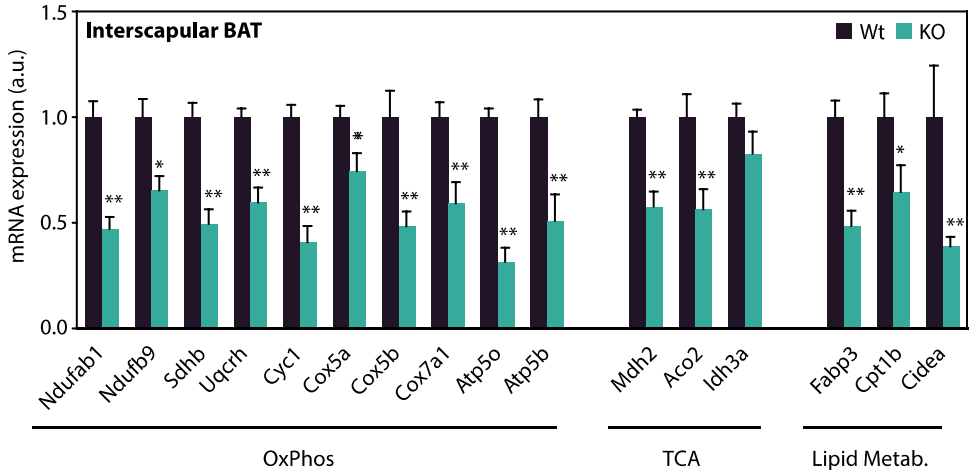

Figure 14. mRNA expression levels of mitochondrial genes involved in OxPhos, TCA or lipid metabolism in interscapular BAT of Wt and PGC1β-FAT-KO mice housed at thermoneutrality and fed a regular chow diet were determined by real-time quantitative RT-PCR. Results are expressed as mean ± SEM, n=5–8 animals/group, *P≤0.05 **P≤0.01.

4.2.4. Western Blot analysis of proteins coded by PGC-1β target genes in WAT of PGC1β-FAT-KO mice

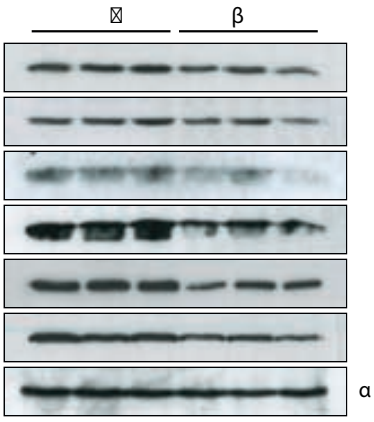

Figure 15. Western Blot analysis of proteins involved in OxPhos and TCA cycle in retroperitoneal WAT from Wt and PGC1β-FAT-KO mice fed a chow diet and housed at 30ºC. α-Tubulin protein was used for loading control.

4.2.5. Analysis of mitochondrial function in WAT of PGC1β-FAT-KO mice

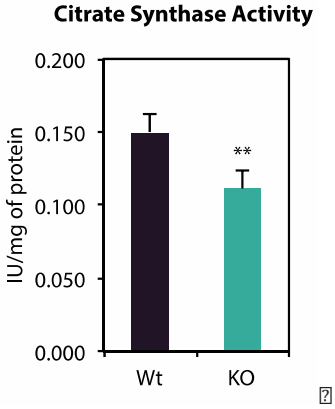

Figure 16. Citrate synthase activity was measured spectrophotometrically in protein extracts of inguinal WAT from Wt and PGC1β-FAT-KO mice fed a chow diet and housed at thermoneutrality. Results are expressed as means ± SEM (n=5-8 animals/group, ** P≤ 0.01).

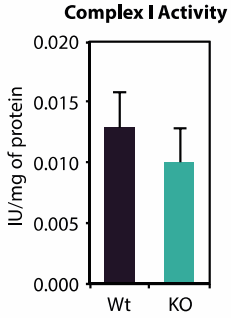

Figure 17. (A) NADH-ubiquinone oxidoreductase (B) succinate dehydrogenase (C) Succinate-Cytochrome c oxidoreductase and (D) Cytochrome c oxidase activity were measured spectrophotometrically in inguinal WAT protein extracts from Wt and PGC1β-FAT-KO mice fed a chow diet and housed at thermoneutrality. Results are expressed as means ± SEM (n=5-8 animals/group, ** P≤ 0.01).

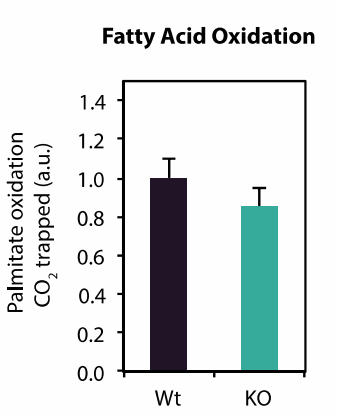

Figure 18. Palmitate oxidation was assessed in inguinal WAT explants dissected from mice housed at 30°C and fed a HFD for 9 months. Tissue samples were incubated in KRB buffer containing [1-^{14}C] palmitate and the utilization of palmitate was monitored by the production of $^{14}CO_2$. $^{14}CO_2$ [illegible] esults are expressed as means ± SEM (n=7-12 animals/group).

4.2.6. Effect of PGC-1β deficiency on mitochondrial biogenesis in WAT

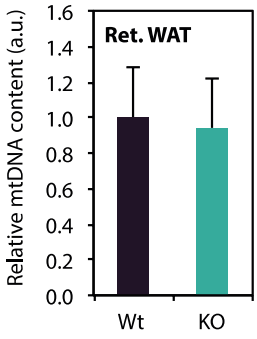

Figure 19. Relative mitochondrial DNA copy number was determined by quantitative RT-PCR. DNA isolated from inguinal WAT from mice housed at 30ºC and fed a chow diet was used to determine ratio between mtCo2 (mtDNA) and Rip140 (nDNA) relative copy number. Results are expressed as means ± SEM (n=6-8 animals/group).

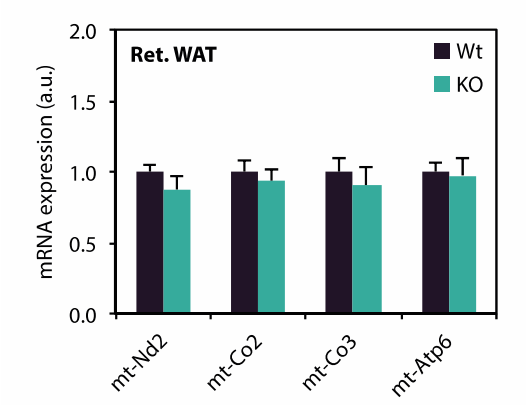

Figure 20. mRNA expression levels of genes coded in mitochondrial genome in retroperitoneal WAT from Wt and KO mice housed at thermoneutrality and fed a chow diet. mRNA levels were determined by quantitative RT-PCR. Results are expressed as means ± SEM (n=5-8 animals/group).

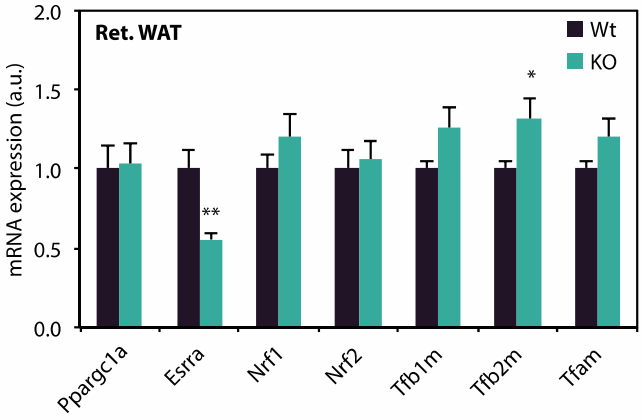

Figure 21. mRNA expression of well-established regulators of mitochondrial gene expression assessed in retroperitoneal WAT from Wt and KO mice housed at thermoneutrality and fed a chow diet. mRNA levels were determined by quantitative RT-PCR. Results are expressed as means ± SEM (n=5-8 animals/group, ** P≤ 0.01).

4.3. Effects of PGC-1β knocdown in cultured 3T3-L1 adipocytes

4.3.1. Lipid-based siRNA transfection of 3T3-L1 adipocytes

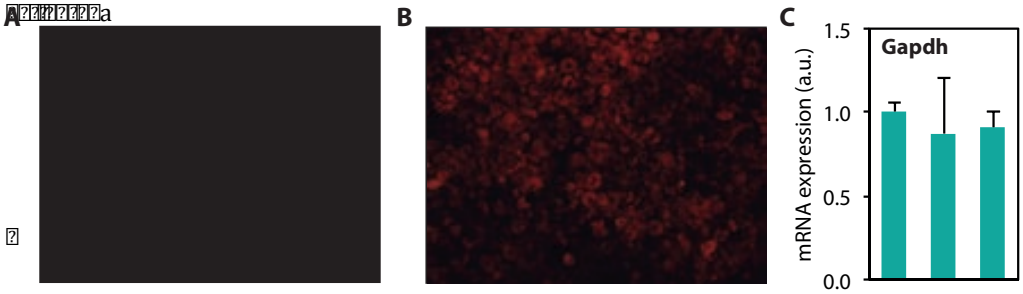

Figure 22. (A) Image of 3T3-L1 adipocytes transfected with siControl. (B) Image of 3T3-L1 adipocytes transfected with siGLO (red staining). (C) Knockdown of *Gapdh* was assayed via qPCR in triplicate. Knockdown of specific genes in 3T3-L1 adipocytes was assayed 48 hours post-transfection using 100 nM nontargeting siRNA (siControl), 100 nM transfection indicator siGLO and 100 nM siRNA targeted to Gapdh (siGapdh). Transfection reagent was used at a concentration of 1.4 µL/cm^2. Transfection was carried out on attached adipocytes (classical transfection). Results are expressed as means ± SEM (n=3).

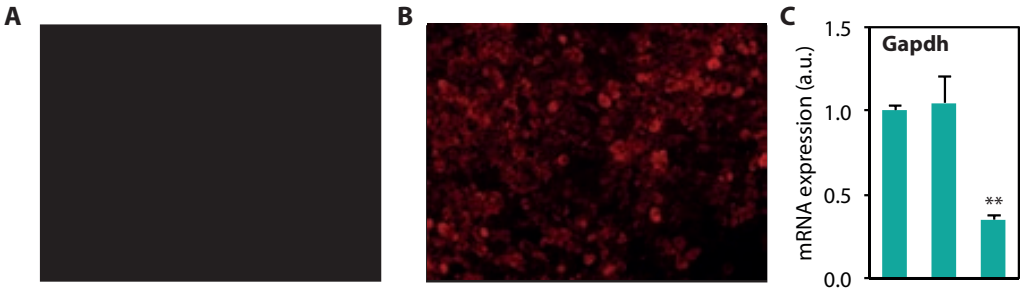

Figure 23. (A) Image of 3T3-L1 adipocytes transfected with siControl. (B) Image of 3T3-L1 adipocytes transfected with siGLO (red staining). (C) Knockdown of Gapdh was assayed via qPCR in triplicate. Knockdown of specific genes in 3T3-L1 adipocytes was assayed 48 hours post-transfection using 100 nM nontargeting siRNA (siControl), 100 nM transfection indicator siGLO and 100 nM siRNA tartgeted to Gapdh (siGapdh). Transfection reagent was used at a concentration of 1.4 µL/cm^2. Transfection was carried on adipocytes in suspension. Results are expressed as means ± SEM (n=3).

4.3.2. Optimization of the conditions for siRNA transfection of 3T3-L1 adipocytes

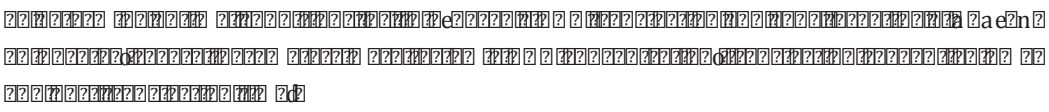

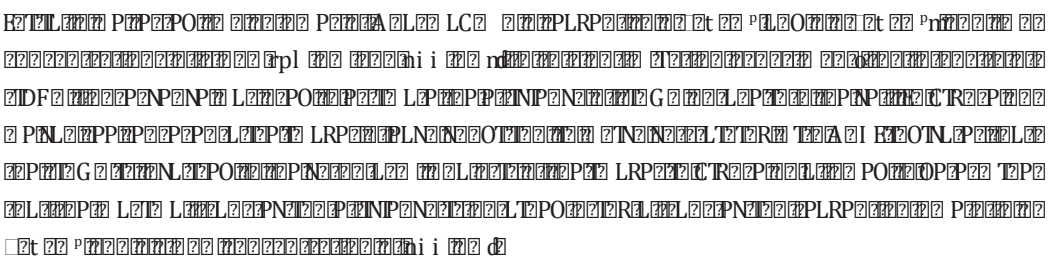

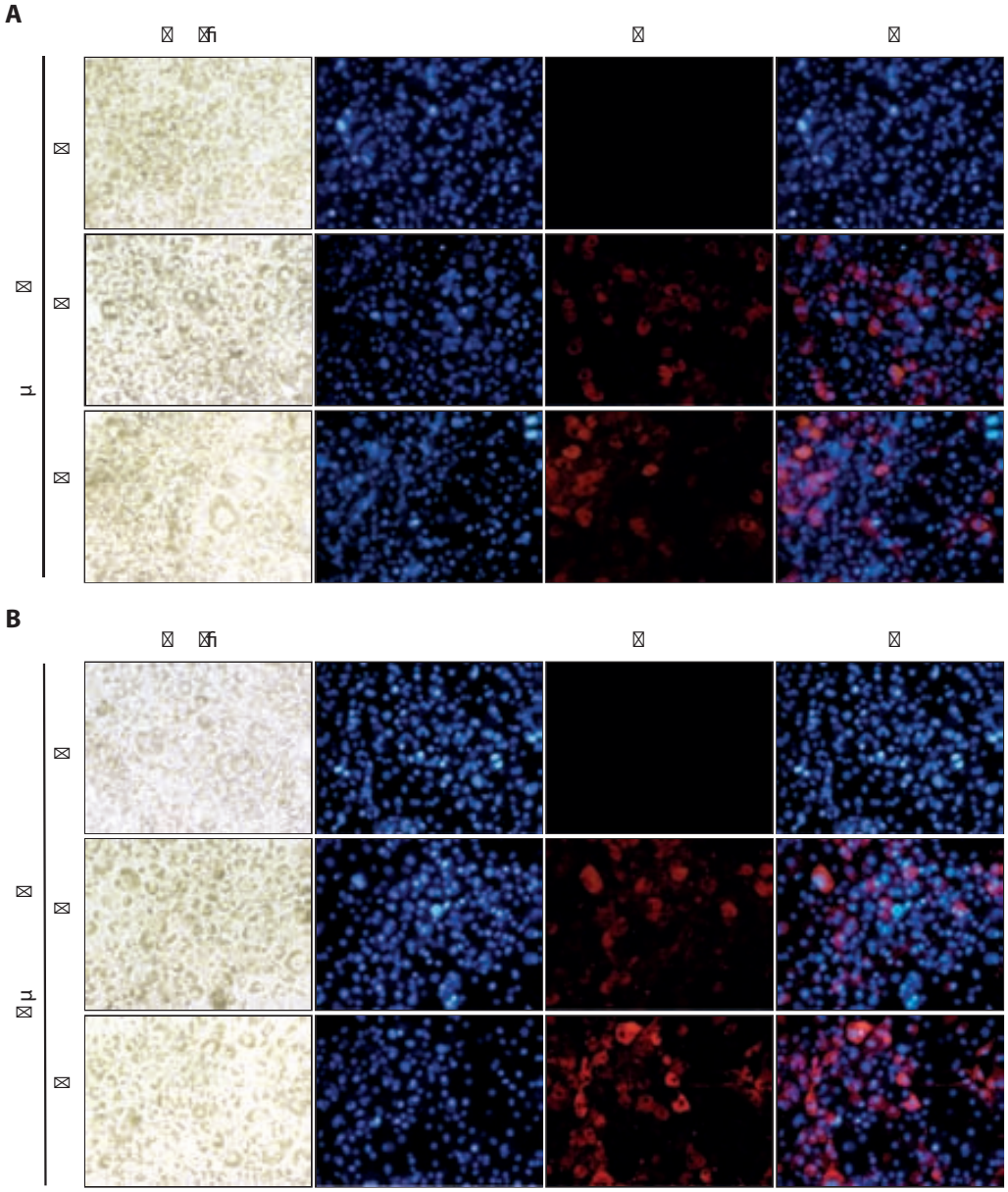

Figure 24. 3T3-L1 adipocytes transfected in suspension with siGLO red. Uptake of the fluorescent-labeled molecule siGLO was assayed at 48 hours post transfection of adipocytes. Brightfield and fluorescent images of adipocytes transfected with (A) 0.7 µL/cm^2 or (B) 1.4 µL/cm^2 of DharmaFECT in combination with two concentrations of siGLO (25 nM and 100 nM). Nuclei were co-stained with DAPI.

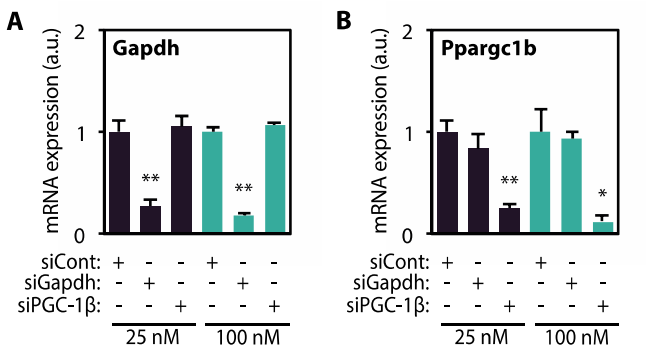

Figure 25. Knockdown of specific genes in 3T3-L1 adipocytes was assayed 48 hours post-transfection using the non-targeting siRNA (siControl), the siRNA tartgeted to Gapdh (siGapdh) and the siRNA targeted to Ppargc1b (siPGC-1β). Transfection was carried out on adipocytes in suspension using two concentrations of siRNA (25 nM and 100 nM). mRNA levels of (A) Gapdh and (B) Ppargc1b were assayed via qPCR in triplicate. Results are expressed as means ± SEM.

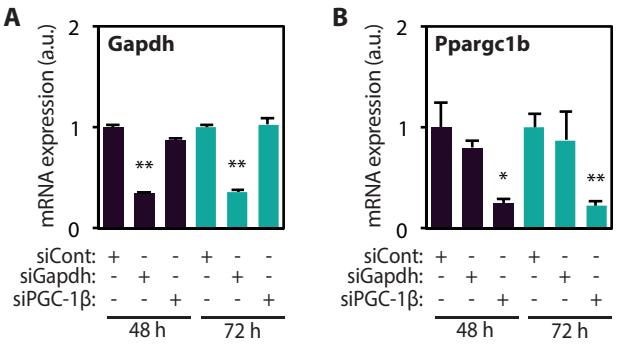

Figure 26. Knockdown of specific genes in 3T3-L1 adipocytes was assayed 48 hours or 72 hours post-transfection using the non-targeting siRNA (siControl), the siRNA tartgeted to Gapdh (siGapdh) and the siRNA targeted to PGC-1β (siPGC-1β). Transfection was carried out on adipocytes in suspension using 100 nM siRNA. mRNA levels of (A) Gapdh and (B) PGC-1β were assayed by qPCR in triplicate. Results are expressed as means ± SEM.

4.3.3. Analysis of mitochondrial gene expression in 3T3-L1 adipocytes lacking PGC-1β

[illegible]

[illegible]

[illegible]

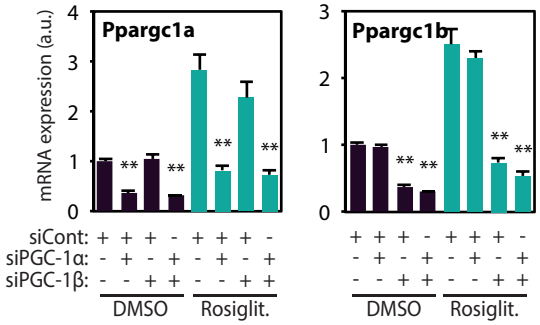

Figure 27. 3T3-L1 adipocytes were transfected with siRNAs targeting PGC-1β and/or PGC-1α and then treated with vehicle or 1 µM Rosiglitazone for 48 hours. Transfection was carried out on adipocytes in suspension using 100 nM siRNA. mRNA levels of PGC-1β and PGC-1α were assayed by qPCR. Results are expressed as means ± SEM of 3-4 experiments with triplicates. * Indicates statistical significance of the comparison between control adipocytes (siCont) and adipocytes in which any of the PGCs have been knocked down; * P≤ 0.05 ** P≤0.01.

RESULTS

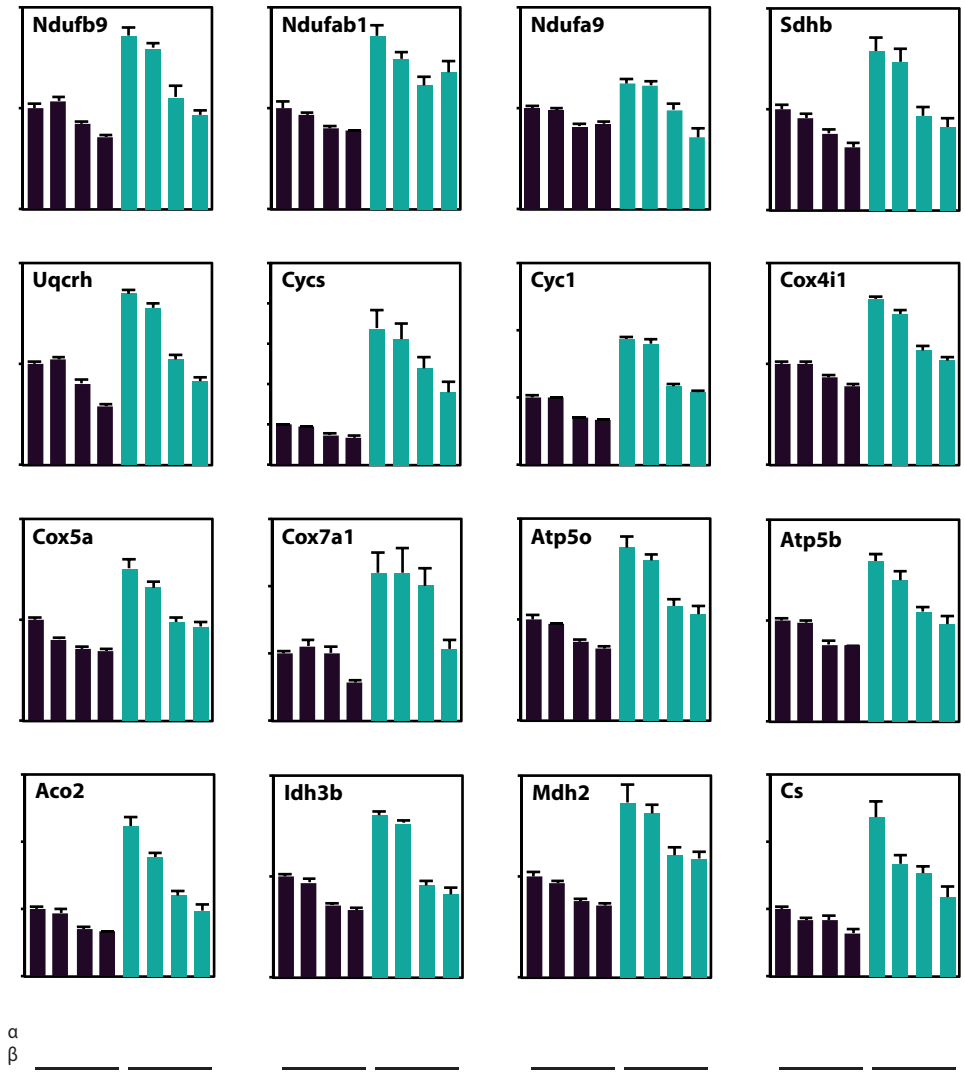

Figure 28. 3T3-L1 adipocytes were transfected with siRNAs targeting PGC-1β and/or PGC-1α and then treated with vehicle or 1 μM Rosiglitazone for 48 hours. Transfection was carried out on adipocytes in suspension using 100 nM siRNA. mRNA levels of OxPhos and TCA cycle genes were assayed by qPCR. Results are expressed as means ± SEM of 3-4 experiments with triplicates. * Indicates statistical significance of the comparison between control adipocytes (siCont) and adipocytes in which any of the PGCs have been knocked down; * P≤ 0.05 ** P≤0.01.

4.3.4. Study of the role of PGC-1β in fatty acid re-esterification in 3T3-L1 adipocytes

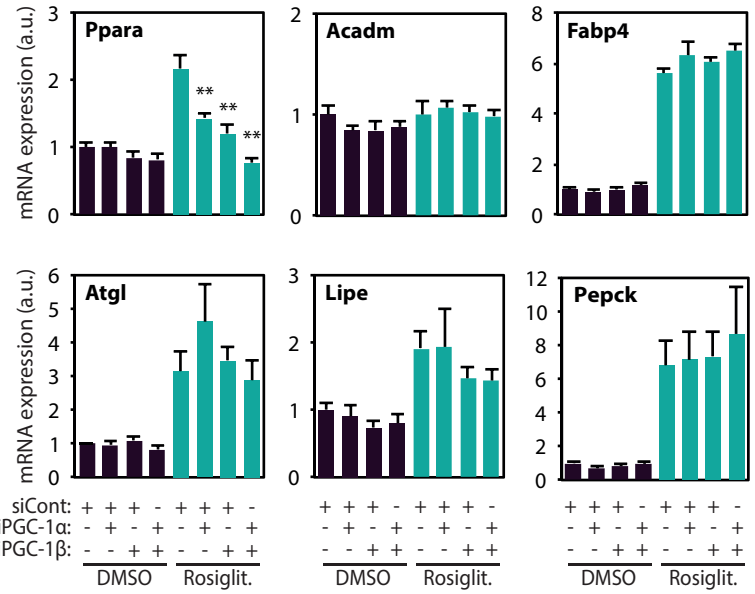

Figure 29. 3T3-L1 adipocytes were transfected with siRNAs targeting PGC-1β and/or PGC-1α and then treated with vehicle or 1 µM Rosiglitazone for 48 hours. Transfection was carried out on adipocytes in suspension using 100 nM siRNA. mRNA levels of lipid metabolism genes were assayed by qPCR. Results are expressed as means ± SEM of 3-4 experiments with triplicates. * Indicates statistical significance of the comparison between control adipocytes (siCont) and adipocytes in which any of the PGCs have been knocked down; * P≤ 0.05 ** P≤0.01.

4.3.5. Assessment of mitochondrial function in 3T3-L1 adipocytes lacking PGC-1β

I [illegible] L [illegible] OF G [illegible] A [illegible] LT [illegible] L OGGCA [illegible] s [illegible] s [illegible] w [illegible] w [illegible] ts [illegible] w [illegible] dm [illegible] RLR L [illegible] c [illegible] lo [illegible] tl loc [illegible] w [illegible] t a [illegible] w [illegible] i [illegible] w [illegible] c [illegible] i [illegible] w [illegible] s [illegible] l d m [illegible] s [illegible] dm t [illegible] dm [illegible] w [illegible] w c [illegible] s [illegible] n w [illegible] s [illegible] i [illegible] m e

4.3.5.1. Fatty acid oxidation

[illegible] w [illegible] l [illegible] w [illegible] ts [illegible] t [illegible] w [illegible] lo [illegible] e [illegible] c [illegible] w [illegible] t [illegible] lo [illegible] c [illegible] R L R [illegible] R l L [illegible] R P l [illegible] L T R [illegible] L P [illegible] d [illegible] t [illegible] w [illegible] l [illegible] lo [illegible] w [illegible] t a [illegible] d o [illegible] c [illegible] ts [illegible] c [illegible] w [illegible] n ts [illegible] s [illegible] R R R R L R [illegible]

L [illegible] BRP [illegible] RP TR [illegible] L [illegible] TL T [illegible] L [illegible] n [illegible] d [illegible] ts [illegible] l [illegible] lo [illegible] dm t [illegible] dm [illegible] w [illegible] w c [illegible] w [illegible] l [illegible] w [illegible] a [illegible] dm [illegible] c [illegible] d o [illegible] w [illegible] a [illegible] l d m [illegible] nf l ue [illegible] R R [illegible] BRP [illegible] L T [illegible] L [illegible] OGG [illegible] a [illegible] s [illegible] s e [illegible] a [illegible] t [illegible] c [illegible] d o [illegible] t [illegible] w [illegible] c [illegible] a c [illegible] w [illegible] a [illegible] s d [illegible] w [illegible] c [illegible] dm [illegible] h [illegible] dm [illegible] RLR L [illegible] L T [illegible] L [illegible] L R [illegible] A L L T L R [illegible] w [illegible] w [illegible] t [illegible] w [illegible] n [illegible] w [illegible] c [illegible] w [illegible] c [illegible] d o [illegible] a [illegible] ct w [illegible] w [illegible] ts [illegible] dm [illegible] dm [illegible] w [illegible] lo [illegible] l d m [illegible] e

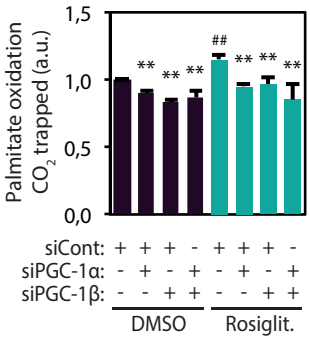

Figure 30. 3T3-L1 adipocytes were transfected with siRNAs targeting PGC-1β and/or PGC-1α and then treated with DMSO or 1 μM Rosiglitazone for 72 hours. Transfection was carried out on adipocytes in suspension using 100 nM siRNA. Cells were incubated at 37ºC in medium containing [1-^{14}C] palmitate and the utilization of palmitate was monitored by the production of $^{14}CO_2$. $^{14}CO_2$ trapped in hyamine hydroxide was quantified by liquid scintillation counting. Results are expressed as mean ± SEM of 3 independent experiments with triplicates. * Indicates statistical significance of the comparison between control adipocytes (siControl) and adipocytes in which any of the PGCs have been knocked down; * P≤ 0.05 ** P≤0.01. # Indicates statistical significance of comparison between vehicle- and rosiglitazone-treated cells; # P≤ 0.05 ## P≤0.01.

4.3.5.2. Respirometry

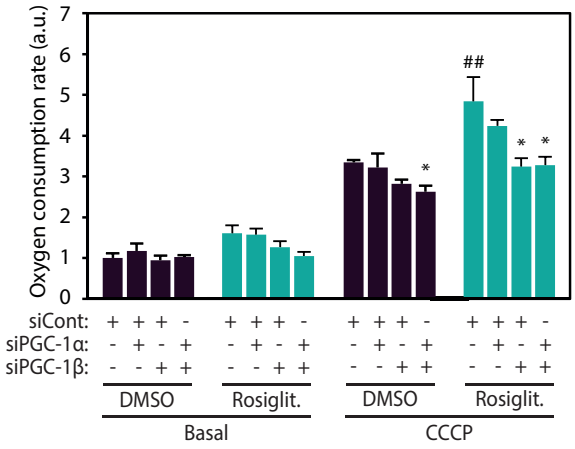

Figure 31. 3T3-L1 adipocytes were transfected with siRNAs targeting PGC-1β and/or PGC-1α and then treated with DMSO or 1 μM Rosiglitazone for 72 hours. Transfection was carried out on adipocytes in suspension using 100 nM siRNA. Basal and maximal (CCCP) cell respiration rates were measured in 3T3-L1 adipocytes using a Clark-type oxygen electrode. Results are expressed as mean ± SEM of 4 independent experiments with triplicates. * Indicates statistical significance of the comparison between control adipocytes (siCont) and adipocytes in which any of the PGCs have been knocked down; * P≤ 0.05 ** P≤0.01. # Indicates statistical significance of comparison between vehicle- and rosiglitazone-treated cells; # P≤ 0.05 ## P≤0.01.

4.3.5.3. Measurement of ATP levels

RESULTS

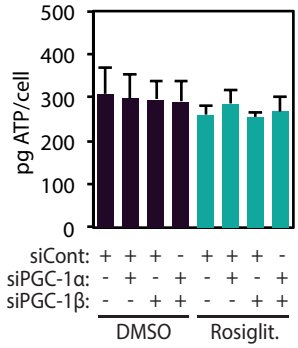

Figure 32. 3T3-L1 adipocytes were transfected with siRNAs targeting PGC-1β and/or PGC-1α and then treated with DMSO or 1 µM Rosiglitazone for 72 hours. Transfection was carried out on adipocytes in suspension using 100 nM siRNA. ATP production was assessed by measuring the light emitted in the reaction of intracellular ATP with the enzyme luciferase. Results are expressed as mean ± SEM of 4 independent experiments with triplicates.

4.3.5.4. ROS production

RESULTS

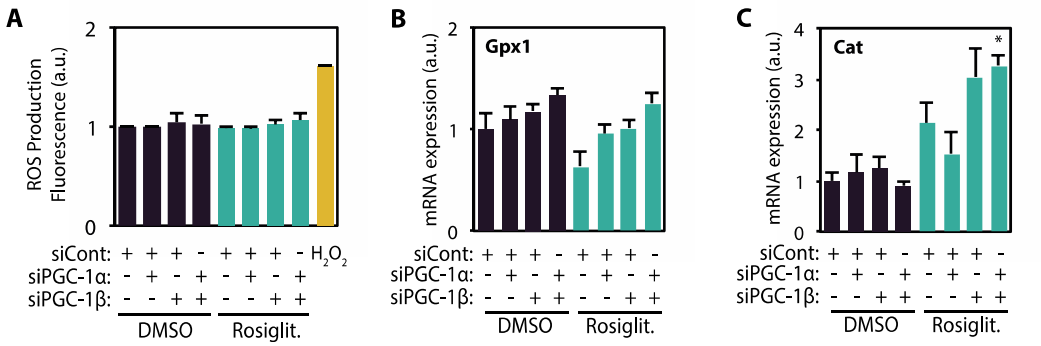

Figure 33. 3T3-L1 adipocytes were transfected with siRNAs targeting PGC-1β and/or PGC-1α and then treated with DMSO or 1 μM Rosiglitazone for 72 hours. Transfection was carried out on adipocytes in suspension using 100 nM siRNA. (A) Production of oxidant species was detected by measuring fluorescence emitted by the oxidation of the molecule Carboxy-H_2DCFDA. Hydrogen peroxide was used as positive control. mRNA levels of (B) Glutathione peroxidase 1 (Gpx1) and (C) catalase (Cat) were assayed by qPCR. Results are expressed as mean ± SEM of 3 independent experiments with triplicates. * Indicates statistical significance of the comparison between control adipocytes (siControl) and adipocytes in which any of the PGCs have been knocked down; * P≤ 0.05.

[illegible]

RESULTS

4.4. Effect of PGC-1β deletion on oxidative capacity of rosiglitazone in white adipose tissue

4.4.1. Effects of the lack of PGC-1β in WAT on rosiglitazone-induced expression of mitochondrial genes

[illegible]

[illegible]

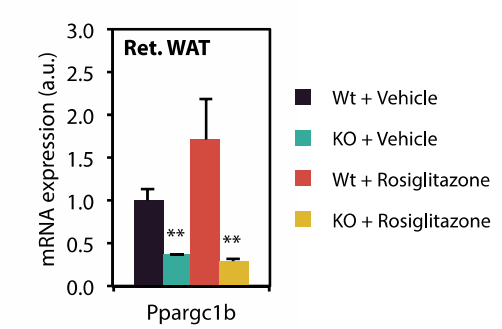

Figure 34. Expression levels of *Ppargc1b* gene in retroperitoneal WAT from wild type and PGC1β-FAT-KO male littermates housed at thermoneutrality that have been subjected to vehicle or rosiglitazone treatment for 21 days after a period of 8 weeks of feeding with a high fat diet. Gene expression was determined by real-time quantitative PCR. Results are expressed as means ± SEM (n=5-7 animals/group). * indicates statistical significance of the comparison between wild type and PGC1β-FAT-KO mice. ** P≤ 0.01.

[illegible]

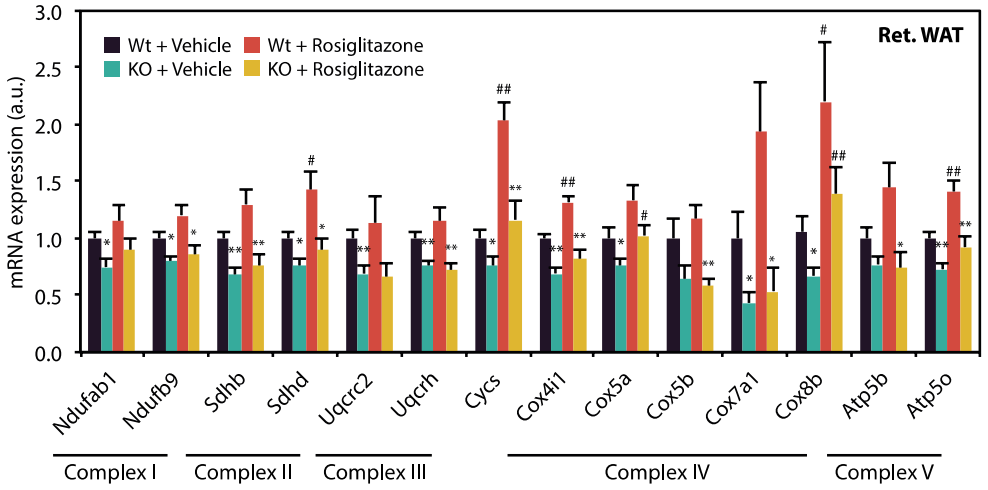

Figure 35. Expression levels of OxPhos genes in retroperitoneal WAT from wild type and PGC1β-FAT-KO male littermates housed at thermoneutrality that have been subjected to vehicle or rosiglitazone treatment for 21 days after a period of 8 weeks of feeding with a high fat diet. Gene expression was determined by real-time quantitative PCR. Results are expressed as means ± SEM (n=5-7 animals/group). * indicates statistical significance of the comparison between wild type and PGC1β-FAT-KO mice. # indicates statistical significance of the comparison between vehicle- and rosiglitazone-treated groups. *# P≤ 0.05; **## P≤ 0.01.

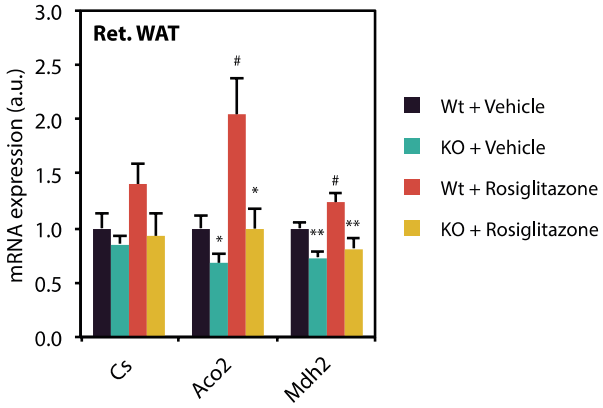

Figure 36. Expression levels of TCA cycle genes in retroperitoneal WAT from wild type and PGC1β-FAT-KO male littermates housed at thermoneutrality that have been subjected to vehicle or rosiglitazone treatment for 21 days after a period of 8 weeks of feeding with a high fat diet. Gene expression was determined by real-time quantitative PCR. Results are expressed as means ± SEM (n=5-7 animals/group). * indicates statistical significance of the comparison between wild type and PGC1β-FAT-KO mice. # indicates statistical significance of the comparison between vehicle- and rosiglitazone-treated groups. *# P≤ 0.05; **## P≤ 0.01.

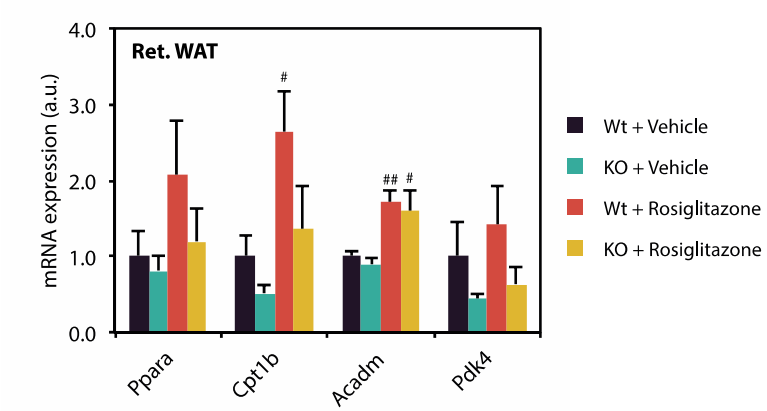

Figure 37. mRNA expression levels of lipid oxidation genes in retroperitoneal WAT from wild type and PGC1β-FAT-KO male littermates housed at thermoneutrality that had been subjected to vehicle or rosiglitazone treatment for 21 days after a period of 8 weeks of feeding with a high fat diet. Gene expression was determined by real-time quantitative PCR. Results are expressed as means ± SEM (n=5-7 animals/group). * indicates statistical significance of the comparison between wild type and PGC1β-FAT-KO mice. # indicates statistical significance of the comparison between vehicle- and rosiglitazone-treated groups. *# P≤ 0.05; **## P≤ 0.01.

4.4.2. Effect of the lack of PGC-1β on rosiglitazone-dependent induction of TCA cycle and OxPhos protein levels in WAT

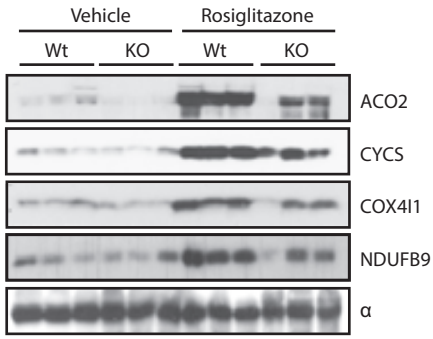

Figure 38. Levels of mitochondrial proteins encoded by PGC-1β target genes were determined by Western Blot analysis in retroperitoneal WAT of Wt and PGC1β-FAT-KO mice housed at thermoneutrality that had been subjected to vehicle or rosiglitazone treatment for 21 days after a period of 8 weeks of feeding with a high fat diet. α-Tubulin protein was detected for loading control.

4.4.3. Role of PGC-1β on rosiglitazone-induced lipogenesis and adipogenesis

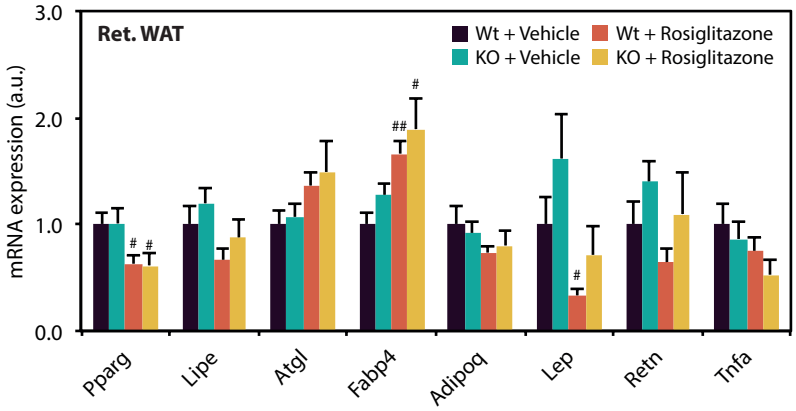

Figure 39. mRNA expression levels of genes coding for lipases and adipokines in retroperitoneal WAT from wild type and PGC1β-FAT-KO male littermates housed at thermoneutrality that have had subjected to vehicle or rosiglitazone treatment for 21 days after a period of 8 weeks of feeding with a high fat diet. Gene expression was determined by real-time quantitative PCR. Results are expressed as means ± SEM (n=5-7 animals/group). * indicates statistical significance of the comparison between wild type and PGC1β-FAT-KO mice. # indicates statistical significance of the comparison between vehicle- and rosiglitazone-treated groups. *# P≤ 0.05; **## P≤ 0.01.

4.4.4. Contribution of PGC-1β to rosiglitazone-enhancement of mitochondrial function

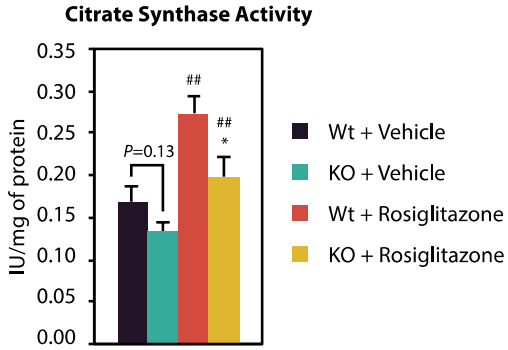

Figure 40. Citrate synthase activity was measured spectrophotometrically in protein extracts of retroperitoneal WAT from Wt and PGC1β-FAT-KO mice housed at thermoneutrality that had been subjected to vehicle or rosiglitazone treatment for 21 days after a period of 8 weeks of feeding with a high fat diet. Results are expressed as means ± SEM (n=5-7 animals/group). * indicates statistical significance of the comparison between wild type and PGC1β-FAT-KO mice. # indicates statistical significance of the comparison between vehicle- and rosiglitazone-treated groups. *# P≤ 0.05; **## P≤ 0.01.

RESULTS

4.4.5. Influence of PGC-1β on the transcriptional regulation of antioxidant enzymes

[illegible]

[illegible]

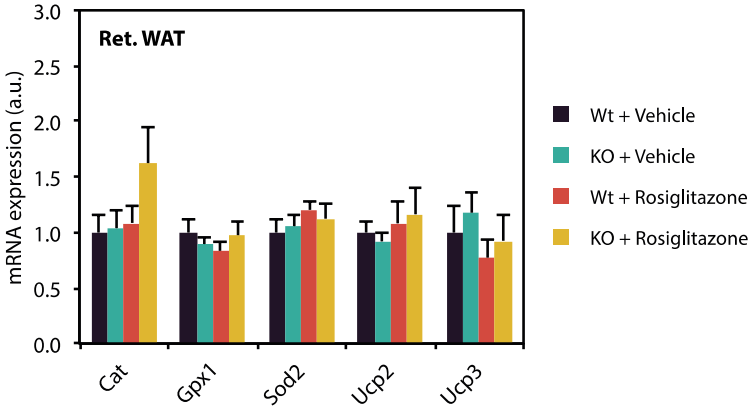

Figure 41. Expression levels of genes related to oxidative stress in retroperitoneal WAT from wild type and PGC1β-FAT-KO male littermates housed at thermoneutrality that have been subjected to vehicle or rosiglitazone treatment for 21 days after a period of 8 weeks of feeding with a high fat diet. Gene expression was determined by real-time quantitative PCR. Results are expressed as means ± SEM (n=5-7 animals/group). * indicates statistical significance of the comparison between wild type and PGC1β-FAT-KO mice. # indicates statistical significance of the comparison between vehicle- and rosiglitazone-treated groups. *# P≤ 0.05; **## P≤ 0.01.

4.4.6. Study of the contribution of PGC-1β to rosiglitazone-induced mitochondriogenesis

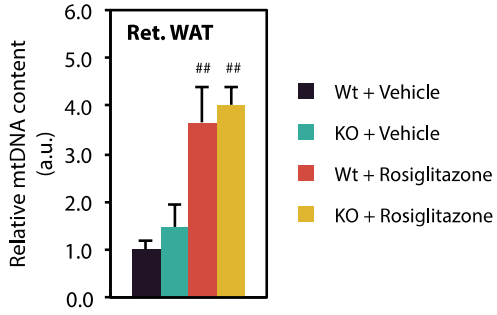

Figure 42. Relative mtDNA content analyzed in retroperitoneal WAT from Wt and PGC1β-FAT-KO mice housed at thermoneutrality that have been subjected to vehicle or rosiglitazone treatment for 21 days after a period of 8 weeks of feeding with a high fat diet. Results are expressed as means ± SEM (n=5-7 animals/group). # indicates statistical significance of the comparison between vehicle- and rosiglitazone-treated groups. ## P≤ 0.01.

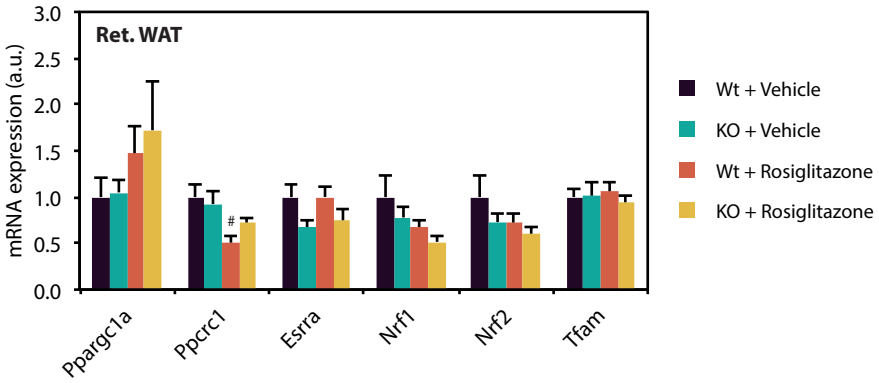

Figure 43. mRNA expression of well-established regulators of mitochondrial gene expression assessed in retroperitoneal WAT from Wt and KO mice housed at thermoneutrality that have been subjected to vehicle or rosiglitazone treatment for 21 days after a period of 8 weeks of feeding with a high fat diet. Results are expressed as means ± SEM (n=5-7 animals/group. # indicates statistical significance of the comparison between vehicle- and rosiglitazone-treated groups. *# P≤ 0.05; **## P≤ 0.01.

4.5. Effect of adipose PGC-1β deficiency on glucose homeostasis and insulin sensitivity

4.5.1. Effect of the lack of PGC-1β in body adiposity of mice fed a chow diet

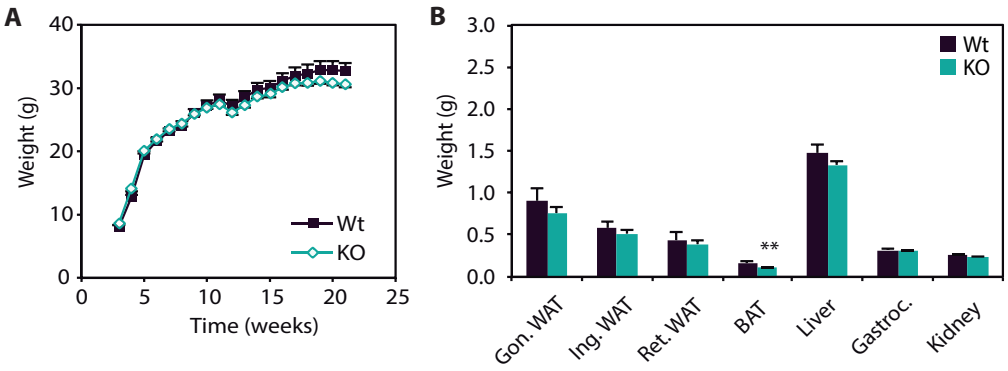

Figure 44. (A) Body weight and (B) tissue weight of 21 weeks-old mice housed at 30ºC and fed a chow diet. Results are expressed as means ± SEM (n=5-7 animals/group). * Indicates statistical significance between Wt and PGC1β-FAT-KO mice; ** P≤0,01.

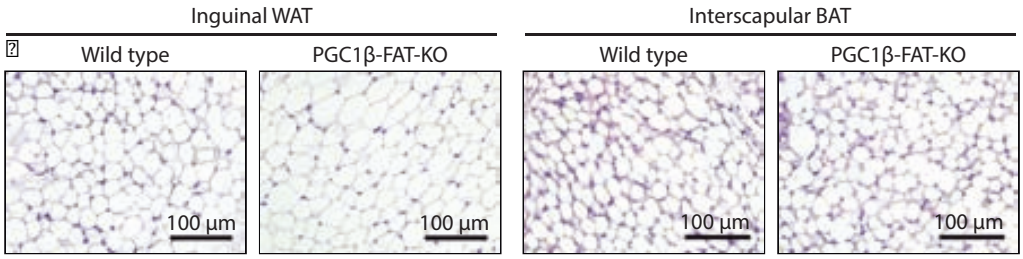

Figure 45. Histological sections of inguinal WAT and interscapular BAT stained with hematoxylin/eosin from mice housed at 30ºC and fed a chow diet.

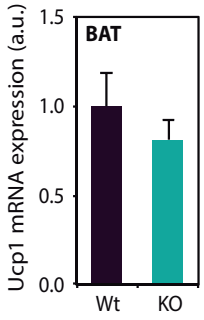

Figure 46. *Ucp1* mRNA expression in BAT from mice housed at 30ºC and fed a chow diet. mRNA expression was assessed by quantitative PCR. Results are expressed as means ± SEM (n=5-7 animals/group).

4.5.2. Effect of the lack of PGC-1β in white adipose tissue on glucose homeostasis

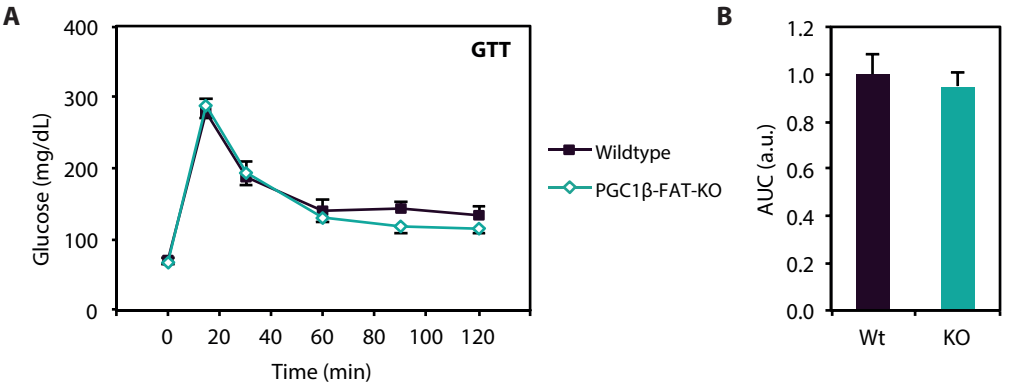

Figure 47. (A) Glucose tolerance test (GTT) was performed on 16h-fasted mice. Blood Glucose levels were measured at 0, 15, 30, 60, 90 and 120 minutes after an intraperitoneal injection of glucose (2 g/kg). (B) Area under the curve of GTT associated curves. Results are expressed as means ± SEM (n=5-7 animals/group).

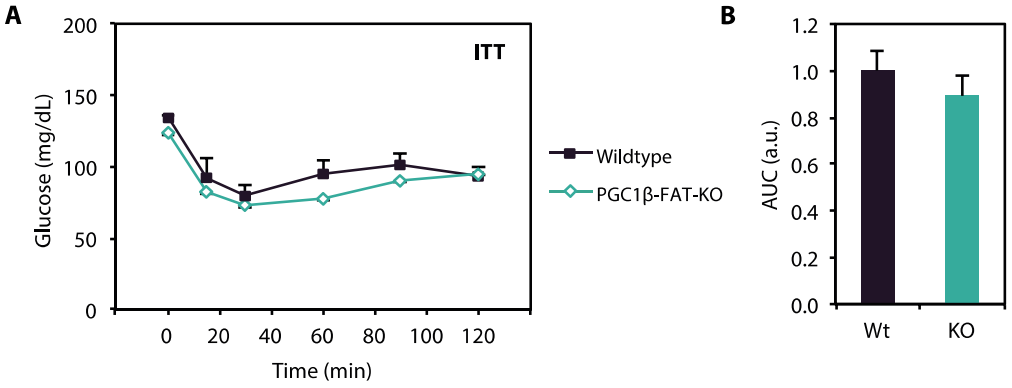

Figure 48. (A) Insulin tolerance test (ITT) was performed on 5h-fasted mice. Blood Glucose levels were measured at 0, 15, 30, 60, 90 and 120 minutes after an intraperitoneal injection of insulin (0.9 U/kg). (B) Area under the curve of ITT associated curves. Results are expressed as means ± SEM (n=5-7 animals/ group).

4.5.3. Effect of the lack of PGC-1β in body adiposity upon rosiglitazone treatment

RESULTS

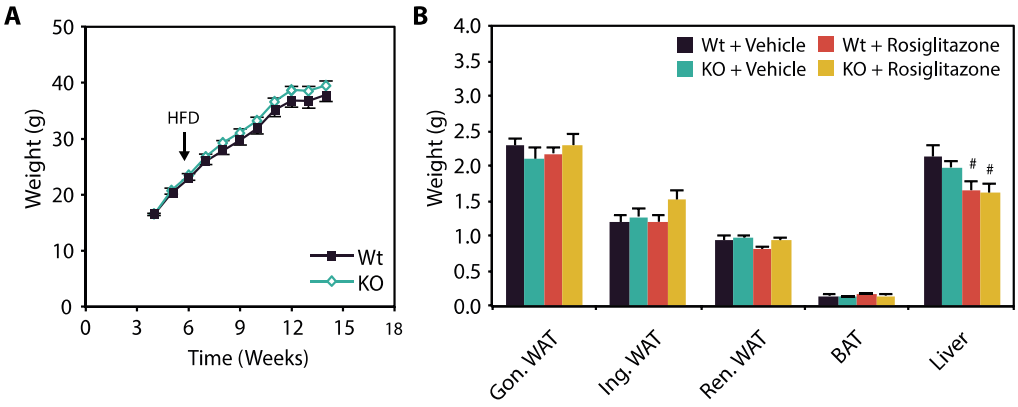

Figure 49. (A) Body weight of wild type and PGC1β-FAT-KO male littermates fed a high fat diet since age 6 weeks and housed at thermoneutrality. (B) Tissue weight of major adipose depots and liver from wild type and PGC1β-FAT-KO male littermates housed at thermoneutrality that have been subjected to vehicle or rosiglitazone treatment for 21 days after a period of 8 weeks of feeding with a high fat diet. Results are expressed as means ± SEM (n=5-7 animals/group). # indicates statistical significance of the comparison between vehicle- and rosiglitazone-treated groups. # P≤ 0.05.

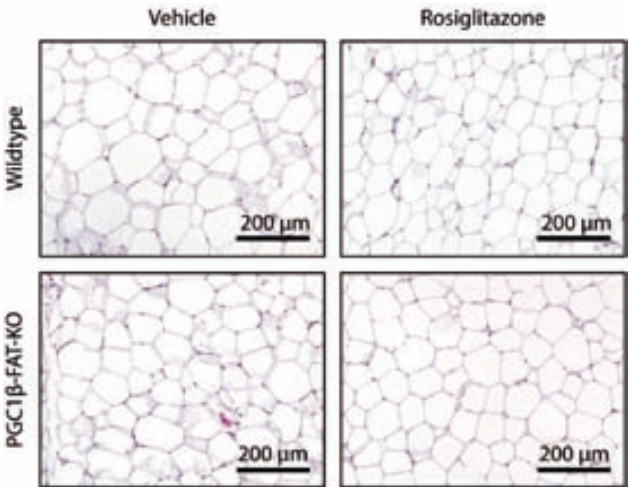

Figure 50. Histological sections of inguinal WAT stained with hematoxylin/eosin from wild type and PGC1β-FAT-KO male littermates housed at thermoneutrality that have been subjected to vehicle or rosiglitazone treatment for 21 days after a period of 8 weeks of feeding with a high fat diet.

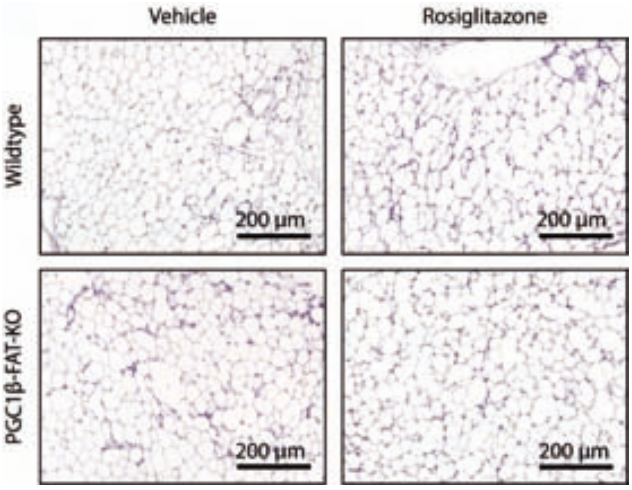

Figure 51. Histological sections of interscapular BAT stained with hematoxylin/eosin from wild type and PGC1β-FAT-KO male littermates housed at thermoneutrality that have been subjected to vehicle or rosiglitazone treatment for 21 days after a period of 8 weeks of feeding with a high fat diet.

4.5.4. Effect of adipose deletion of PGC-1β on glucose homeostasis upon rosiglitazone treatment

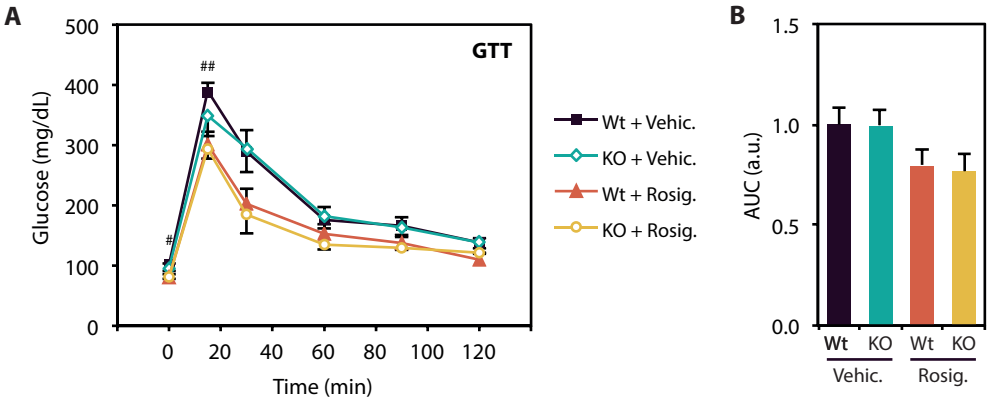

Figure 52. (A) Glucose tolerance test (GTT) was performed on 16h-fasted mice. Blood Glucose levels were measured at 0, 15, 30, 60, 90 and 120 minutes after an intraperitoneal injection of glucose (2 g/kg). (B) Area under the curve of GTT associated curves. Results are expressed as means ± SEM (n=5-7 animals/group). # indicates statistical significance of the comparison between vehicle- and rosiglitazone-treated groups. # P≤ 0.05; ## P≤ 0.01.

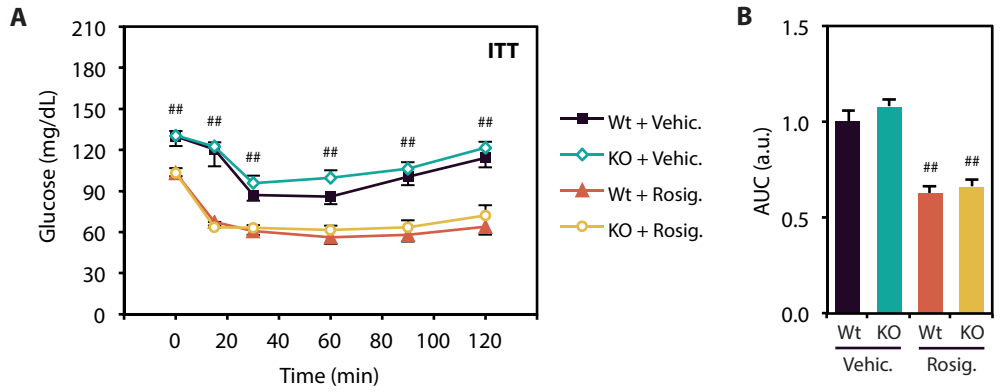

Figure 53. (A) Insulin tolerance test (ITT) was performed on 5h-fasted mice. Blood Glucose levels were measured at 0, 15, 30, 60, 90 and 120 minutes after an intraperitoneal injection of insulin (0.9 U/kg). (B) Area under the curve of ITT associated curves. Results are expressed as means ± SEM (n=5-7 animals/ group). # indicates statistical significance of the comparison between vehicle- and rosiglitazone-treated groups. ## P≤ 0.01.

RESULTS

4.5.5. Effect of adipose-targeted deletion of PGC-1β on the amelioration of the metabolic profile by rosiglitazone

	Vehicle		Rosiglitazone	
	Wildtype	PGC1β-FAT-KO	Wildtype	PGC1β-FAT-KO
Glucose (mg/dL)	129.8 ± 6.9	130.5 ± 3.1	103.2 ± 2.5 ##	103.2 ± 3.4 ##
FFA (mmol/L)	0.440 ± 0.05	0.446 ± 0.04	0.314 ± 0.04	0.341 ± 0.05
Triglyceride (mg/dL)	56.1 ± 3.7	54.7 ± 5.3	58.1 ± 3.8	61.5 ± 3.8
Cholesterol (mg/dL)	200.0 ± 3.7	188.4 ± 6.7	162.2 ± 8.1 ##	151.0 ± 7.9 ##
Insulin (ng/mL)	3.34 ± 0.36	3.38 ± 0.33	1.88 ± 0.20 ##	2.13 ± 0.29 ##
Leptin (ng/mL)	15.4 ± 3.4	17.9 ± 2.7	13.2 ± 2.2	16.2 ± 2.5
HOMA-IR	28.83 ± 3.42	31.04 ± 3.23	14.32 ± 1.52 ##	14.56 ± 1.99 ##

Table 5. Serum metabolites and hormone levels of Wt and PGC1β-FAT-KO mice that have been subjected to vehicle or rosiglitazone treatment for 21 days after a period of 8 weeks of feeding with a high fat diet. HOMA-IR was calculated using the following formula: fasting blood glucose (mg/dl) × fasting insulin (μU/ml)/405. Results are expressed as means ± SEM (n=5-7 animals/group). # Indicates statistical significance of the comparison between vehicle- and rosiglitazone-treated groups. ## P≤ 0.01.

4.5.6. Assessment of tissue-specific insulin signaling in PGC1β-FAT-KO mice

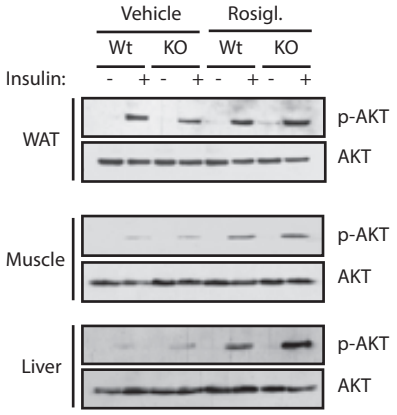

Figure 54. Total and phosphorylated AKT were detected by Western Blot in protein lysates of liver, inguinal WAT and gastrocnemius muscle from mice that were treated with an insulin bolus after an overnight fast.

4.6. Role of PGC-1β in brite adipocyte recruitment in wat

4.6.1. Role of PGC-1β in brite adipocyte recruitment in WAT by rosiglitazone treatment

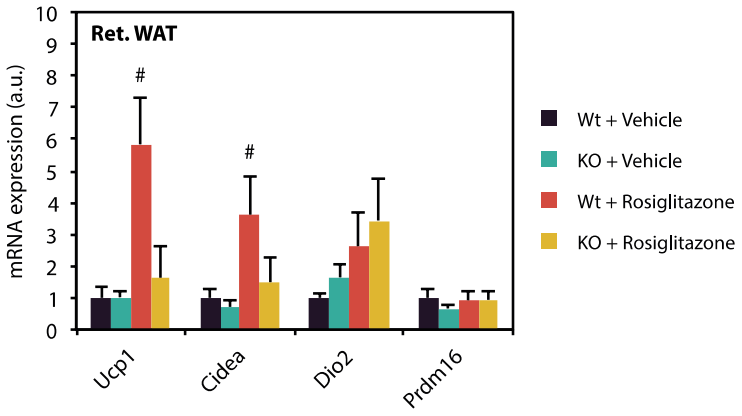

Figure 55. Expression brown adipocyte-specific genes in retroperitoneal WAT from wild type and PGC1β-FAT-KO male littermates housed at thermoneutrality that have been subjected to vehicle or rosiglitazone treatment for 21 days after a period of 8 weeks of feeding with a high fat diet. Gene expression was determined by real-time quantitative PCR. Results are expressed as means ± SEM (n=5-7 animals/group). * indicates statistical significance of the comparison between wild type and PGC1β-FAT-KO mice. # indicates statistical significance of the comparison between vehicle- and rosiglitazone-treated groups. *# P≤ 0.05; **## P≤ 0.01.

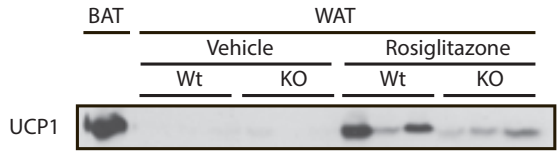

Figure 56. UCP1 protein levels were detected by Western Blot in retroperitoneal WAT from wild type and PGC1β-FAT-KO male littermates housed at thermoneutrality that have been subjected to vehicle or rosiglitazone treatment for 21 days after a period of 8 weeks of feeding with a high fat diet. BAT protein extract from Wt mice housed at 21ºC was used as a positive control for UCP1 protein expression.

4.6.2 Effect of β-adrenergic stimulation on brite adipocyte recruitment in WAT of PGC1β-FAT-KO mice

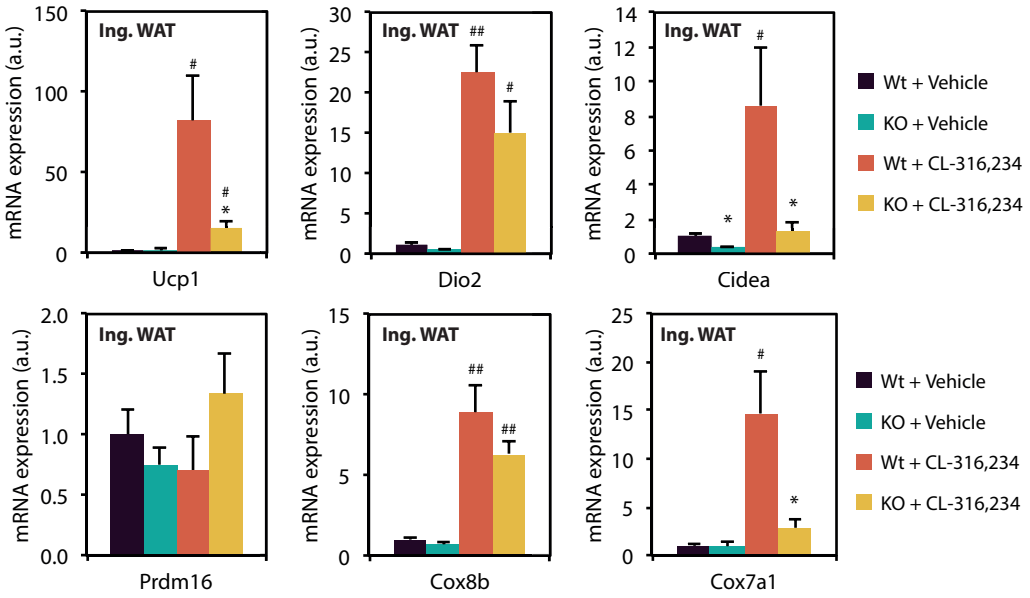

Figure 57. Expression brown adipocyte-specific genes in inguinal WAT from wild type and PGC1β-FAT-KO male littermates housed at thermoneutrality and fed chow diet that have been subjected to vehicle or CL-316,234 treatment for 10 days. Gene expression was determined by real-time quantitative PCR. Results are expressed as means ± SEM (n=5-7 animals/group). * indicates statistical significance of the comparison between wild type and PGC1β-FAT-KO mice. # indicates statistical significance of the comparison between vehicle- and CL-316,234-treated groups. *# P≤ 0.05; **## P≤ 0.01.

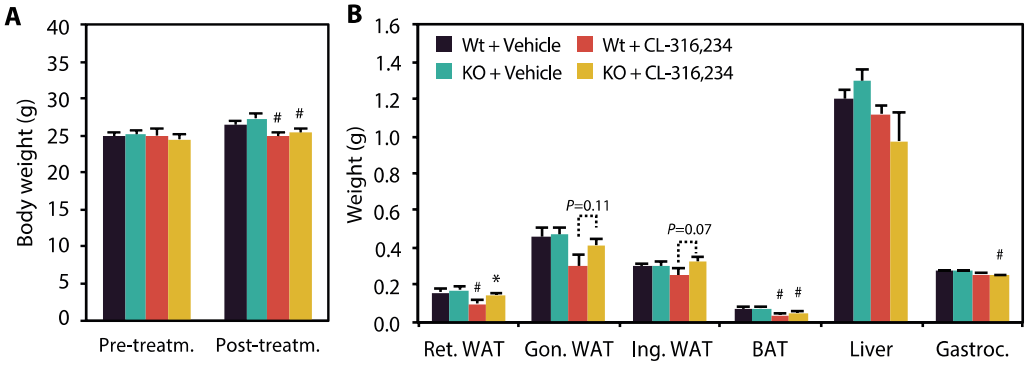

Figure 58. (A) Body weight of Wt and PGC1β-FAT-KO mice before and after CL-316,234 or vehicle treatment. (B) Adipose depots weight of Wt and PGC1β-FAT-KO male littermates housed at thermoneutrality and fed standard diet that have been subjected to vehicle or CL-316,243 treatment for 10 days. Results are

expressed as means ± SEM (n=5-7 animals/group). * indicates statistical significance of the comparison between wild type and PGC1β-FAT-KO mice. # indicates statistical significance of the comparison between vehicle- and CL-316,234-treated groups. *# P≤ 0.05; **## P≤ 0.01.

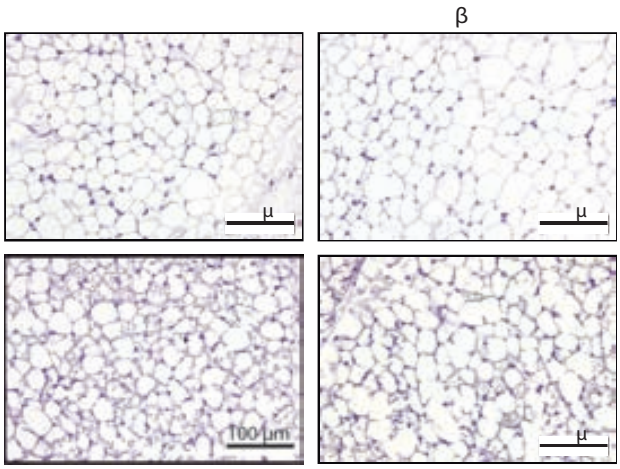

Figure 59. Histological sections of inguinal WAT stained with hematoxylin/eosin from wild type and PGC1β-FAT-KO male littermates housed at thermoneutrality and fed standard diet that have been subjected to vehicle or CL-316,243 treatment for 10 days.

4.6.3. Role of PGC-1β on the regulation of mitochondrial gene expression induced by CL-316,243 treatment

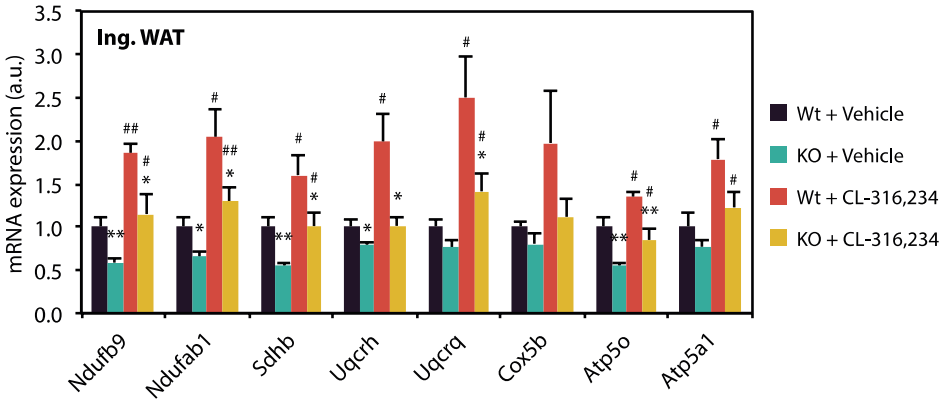

Figure 60. Expression OxPhos genes in inguinal WAT from wild type and PGC1β-FAT-KO male littermates housed at thermoneutrality and fed chow diet that have been subjected to vehicle or CL-316,234 treatment for 10 days. Gene expression was determined by real-time quantitative PCR. Results are expressed as means ± SEM (n=5-7 animals/group). * indicates statistical significance of the comparison between wild type and PGC1β-FAT-KO mice. # indicates statistical significance of the comparison between vehicle- and CL-316,234-treated groups. *# P≤ 0.05; **## P≤ 0.01.

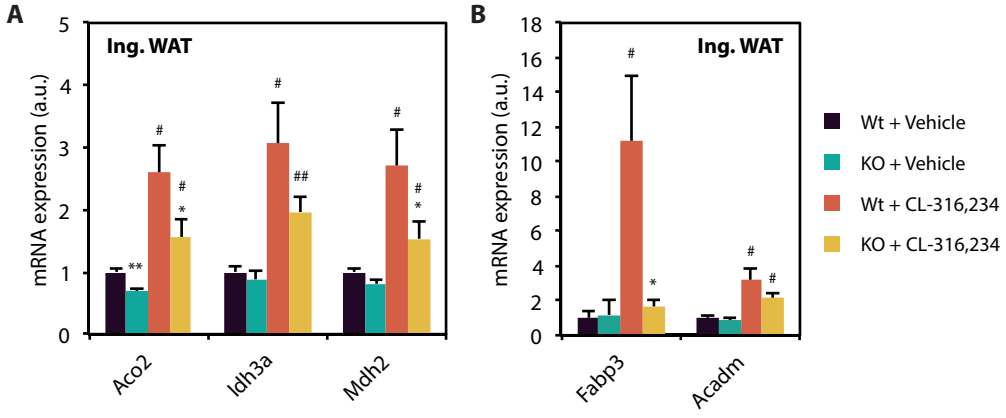

Figure 61. Expression of (A) TCA cycle and (B) lipid metabolism genes in inguinal WAT from wild type and PGC1β-FAT-KO male littermates housed at thermoneutrality and fed chow diet that have been subjected to vehicle or CL-316,234 treatment for 10 days. Gene expression was determined by real-time quantitative PCR. Results are expressed as means ± SEM (n=5-7 animals/group). * indicates statistical significance of the comparison between wild type and PGC1β-FAT-KO mice. # indicates statistical significance of the comparison between vehicle- and CL-316,234-treated groups. *# P≤ 0.05; **## P≤ 0.01.

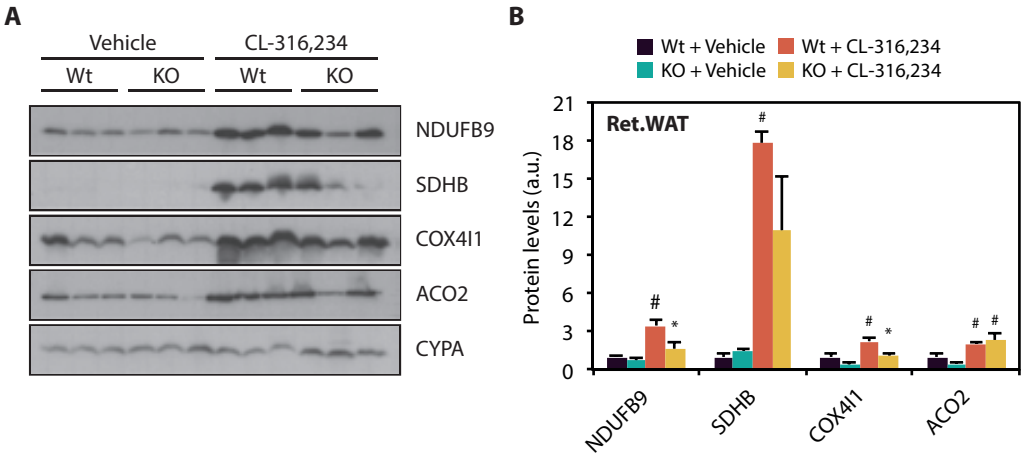

Figure 62. (A) Levels of mitochondrial proteins encoded by PGC-1β target genes were determined by Western Blot analysis in retroperitoneal WAT of Wt and PGC1β-FAT-KO mice housed at thermoneutrality that have been subjected to vehicle or CL-316,234 treatment for 10 days. Cyclophilin A protein was detected for loading control. (B) Protein expression levels normalized by Cyclophilin A expression were determined with the Image J software.

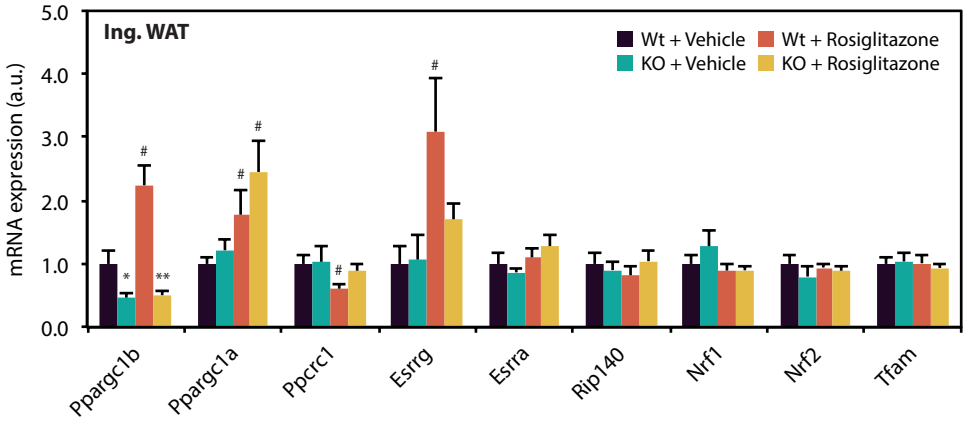

Figure 63. Expression of well-established regulators of mitochondrial gene expression in inguinal WAT from wild type and PGC1β-FAT-KO male littermates housed at thermoneutrality and fed chow diet that have been subjected to vehicle or CL-316,234 treatment for 10 days. Gene expression was determined by real-time quantitative PCR. Results are expressed as means ± SEM (n=5-7 animals/group). * indicates statistical significance of the comparison between wild type and PGC1β-FAT-KO mice. # indicates statistical significance of the comparison between vehicle- and CL-316,234-treated groups. *# P≤ 0.05; **## P≤ 0.01.

[illegible]

4.6.4. Role of PGC-1β on β-adrenergic stimulation in BAT

[illegible]

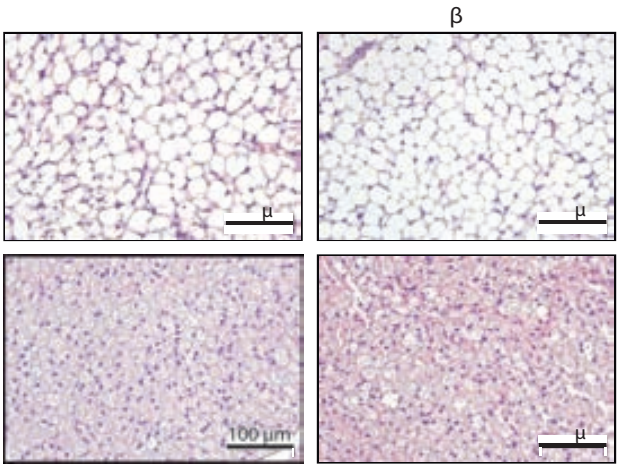

Figure 64. Histological sections of interscapular BAT stained with hematoxylin/eosin from wild type and PGC1β-FAT-KO male littermates housed at thermoneutrality and fed standard diet that have been subjected to vehicle or CL-316,243 treatment for 10 days.

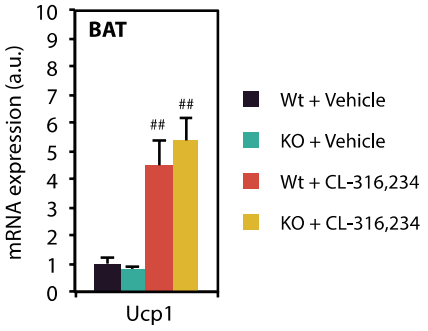

Figure 65. Expression of Ucp1 in interscapular BAT from wild type and PGC1β-FAT-KO male littermates housed at thermoneutrality and fed chow diet that have been subjected to vehicle or CL-316,234 treatment for 10 days. Gene expression was determined by real-time quantitative PCR. Results are expressed as means ± SEM (n=5-7 animals/group). # indicates statistical significance of the comparison between vehicle- and CL-316,234-treated groups. # P≤ 0.05; ## P≤ 0.01.

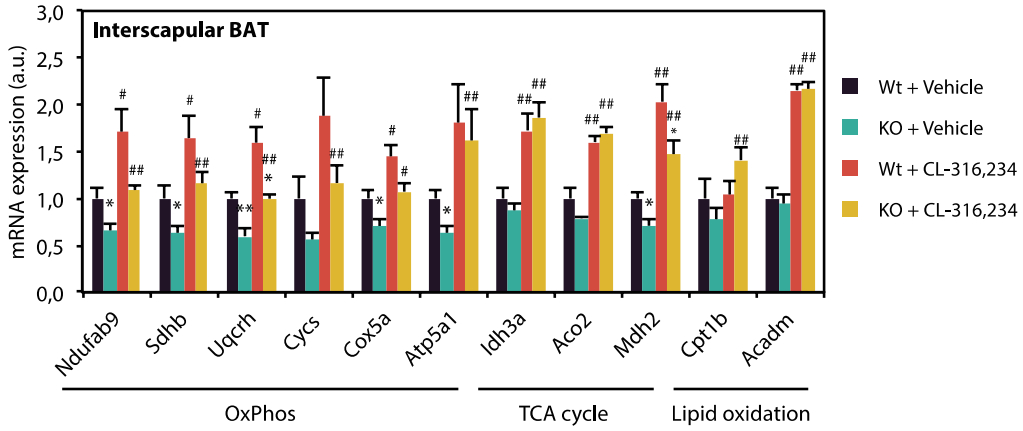

Figure 66. Expression of genes involved in oxidative metabolism in interscapular BAT from wild type and PGC1β-FAT-KO male littermates housed at thermoneutrality and fed chow diet that have been subjected to vehicle or CL-316,234 treatment for 10 days. Gene expression was determined by real-time quantitative PCR. Results are expressed as means ± SEM (n=5-7 animals/group). # indicates statistical significance of the comparison between vehicle- and CL-316,234-treated groups. # P≤ 0.05; ## P≤ 0.01.

RESULTS

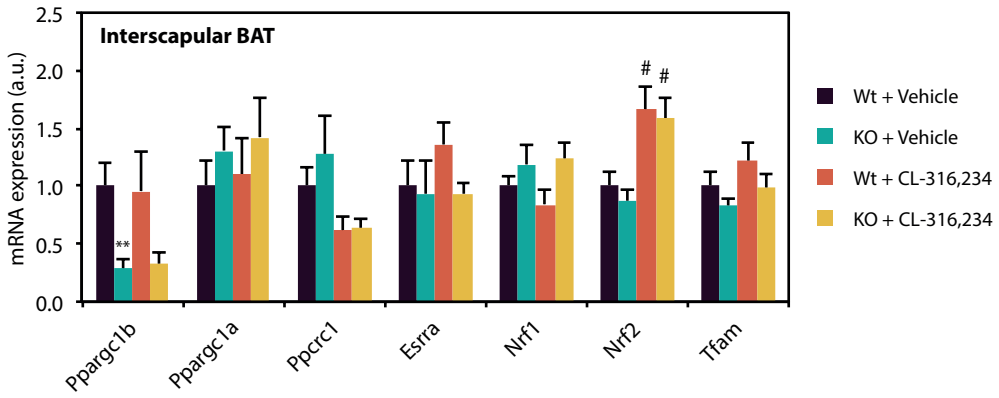

Figure 67. Expression of well-established regulators of mitochondrial gene expression in interscapular BAT from wild type and PGC1β-FAT-KO male littermates housed at thermoneutrality and fed chow diet that have been subjected to vehicle or CL-316,234 treatment for 10 days. Gene expression was determined by real-time quantitative PCR. Results are expressed as means ± SEM (n=5-7 animals/group. * indicates statistical significance of the comparison between wild type and PGC1β-FAT-KO mice. # indicates statistical significance of the comparison between vehicle- and CL-316,234-treated groups. *# P≤ 0.05; **## P≤ 0.01.

RESULTS

5.DISCUSSION

5.1. Analysis of the pathways regulated by PGC-1□ in WAT

5.2. Role of PGC-1β in white adipocyte physiology

5.3. Role of PGC-1β in the regulation of mitochondrial biogenesis induced by rosiglitazone in WAT

5.4. Role of PGC-1β in the function of BAT

5.5. Role of PGC-1β in the function of BAT in the recruitment of brite adipocytes in WAT

5.5. Effect of mitochondrial dysfunction on insulin resistance

5.6. Contribution of PGC-1β to rosiglitazone-dependent oxidative capacity in WAT

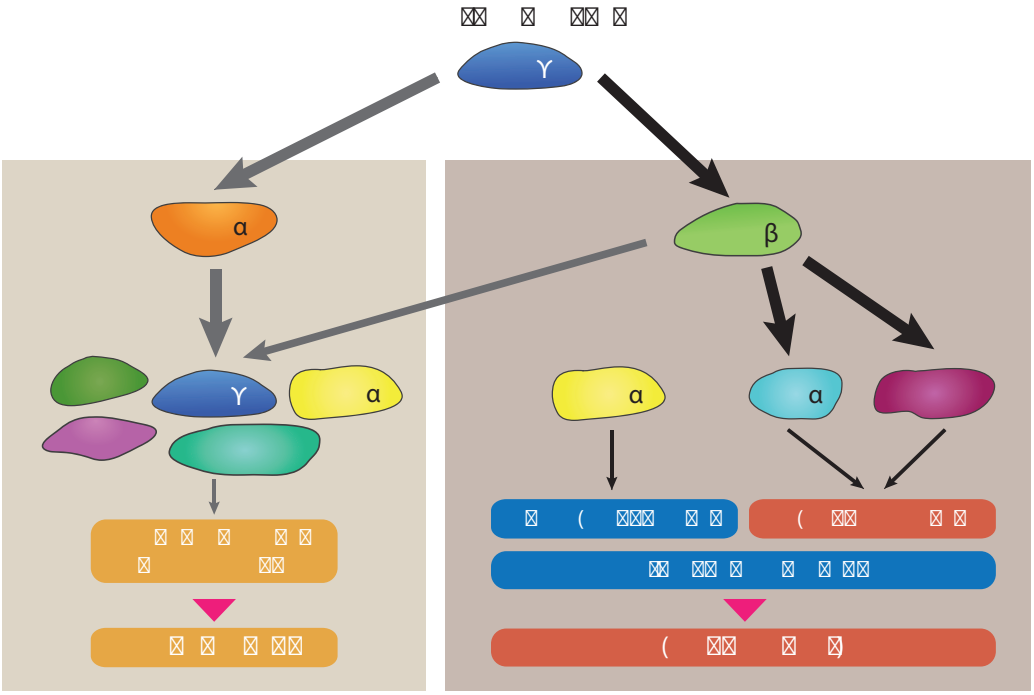

Figure 1. Schematic overview of the effects of thiazolidinediones on the activity of PGC-1α and PGC-1β in WAT. While the activity of PGC-1α seems to be restricted to the transcriptional regulation of the thermogenic gene program in WAT, PGC-1β regulates the expression of OxPhos and TCA genes as well as some genes involved in thermogenesis, although to at a lower extent than PGC-1α.

6.CONCLUSIONS

7.REFERENCES

1. Federation, I.D., *IDF Diabetes Atlas*. 6th ed. 2013, Brussels, Belgium.
2. Soriguer, F., et al., *Prevalence of diabetes mellitus and impaired glucose regulation in Spain: the Di@bet.es Study.* Diabetologia, 2012. **55**(1): p. 88-93.
3. Struijs, J.N., et al., *Comorbidity in patients with diabetes mellitus: impact on medical health care utilization.* BMC Health Serv Res, 2006. **6**: p. 84.
4. Reaven, G.M., et al., *Measurement of plasma glucose, free fatty acid, lactate, and insulin for 24 h in patients with NIDDM.* Diabetes, 1988. **37**(8): p. 1020-4.
5. DeFronzo, R.A., R.C. Bonadonna, and E. Ferrannini, *Pathogenesis of NIDDM. A balanced overview.* Diabetes Care, 1992. **15**(3): p. 318-68.
6. Lillioja, S., et al., *Insulin resistance and insulin secretory dysfunction as precursors of non-insulin-dependent diabetes mellitus. Prospective studies of Pima Indians.* N Engl J Med, 1993. **329**(27): p. 1988-92.
7. Vauhkonen, I., et al., *Defects in insulin secretion and insulin action in non-insulin-dependent diabetes mellitus are inherited. Metabolic studies on offspring of diabetic probands.* J Clin Invest, 1998. **101**(1): p. 86-96.
8. Watanabe, R.M., *The genetics of insulin resistance: Where's Waldo?* Curr Diab Rep, 2010. **10**(6): p. 476-84.
9. Manson, J.E., et al., *Physical activity and incidence of non-insulin-dependent diabetes mellitus in women.* Lancet, 1991. **338**(8770): p. 774-8.
10. Lonnroth, P. and U. Smith, *Aging enhances the insulin resistance in obesity through both receptor and postreceptor alterations.* J Clin Endocrinol Metab, 1986. **62**(2): p. 433-7.
11. Finkelstein, E.A., et al., *Obesity and severe obesity forecasts through 2030.* Am J Prev Med, 2012. **42**(6): p. 563-70.
12. Kershaw, E.E. and J.S. Flier, *Adipose tissue as an endocrine organ.* J Clin Endocrinol Metab, 2004. **89**(6): p. 2548-56.
13. Abbasi, F., et al., *Relationship between obesity, insulin resistance, and coronary heart disease risk.* J Am Coll Cardiol, 2002. **40**(5): p. 937-43.
14. Poitout, V., *Glucolipotoxicity of the pancreatic beta-cell: myth or reality?* Biochem Soc Trans, 2008. **36**(Pt 5): p. 901-4.
15. Sovik, O., et al., *Studies of insulin resistance in congenital generalized lipodystrophy.* Acta Paediatr Suppl, 1996. **413**: p. 29-37.
16. Moitra, J., et al., *Life without white fat: a transgenic mouse.* Genes Dev, 1998. **12**(20): p. 3168-81.
17. Gregoire, F., et al., *The stroma-vascular fraction of rat inguinal and epididymal adipose tissue and the adipoconversion of fat cell precursors in primary culture.* Biol Cell, 1990. **69**(3): p. 215-22.
18. Gesta, S. and C.R. Kahn, *White Adipose Tissue*, in *Adipose Tissue Biology*, M.E. Symonds, Editor. 2012, Springer.
19. Cinti, S., *The adipose organ.* Prostaglandins Leukot Essent Fatty Acids, 2005. **73**(1): p. 9-15.
20. James, D.E., et al., *Insulin-regulatable tissues express a unique insulin-sensitive glucose transport protein.* Nature, 1988. **333**(6169): p. 183-5.
21. Macaulay, S.L. and L. Jarett, *Insulin mediator causes dephosphorylation of the alpha subunit of pyruvate dehydrogenase by stimulating phosphatase activity.* Arch Biochem Biophys, 1985. **237**(1): p. 142-50.
22. Foufelle, F., et al., *Glucose stimulation of lipogenic enzyme gene expression in cultured white adipose tissue. A role for glucose 6-phosphate.* J Biol Chem, 1992. **267**(29): p. 20543-6.
23. Sul, H.S., et al., *Regulation of the fatty acid synthase promoter by insulin.* J Nutr, 2000. **130**(2S Suppl): p. 315S-320S.
24. Seo, T., et al., *Lipoprotein lipase-mediated selective uptake from low density lipoprotein requires cell surface proteoglycans and is independent of scavenger receptor class B type 1.* J Biol Chem, 2000. **275**(39): p. 30355-62.
25. Goldberg, I.J., R.H. Eckel, and N.A. Abumrad, *Regulation of fatty acid uptake into tissues: lipoprotein lipase- and CD36-mediated pathways.* J Lipid Res, 2009. **50 Suppl**: p. S86-90.
26. Fain, J.N., et al., *Comparison of the release of adipokines by adipose tissue, adipose tissue matrix, and adipocytes from visceral and subcutaneous abdominal adipose tissues of obese humans.* Endocrinology, 2004. **145**(5): p. 2273-82.
27. Rosen, E.D. and B.M. Spiegelman, *Adipocytes as regulators of energy balance and glucose homeostasis.* Nature, 2006. **444**(7121): p. 847-53.
28. Day, C. and C.J. Bailey, *Obesity in the pathogenesis of type 2 diabetes.* The British Journal of Diabetes & Vascular Disease, 2011. **11**(2): p. 55-61.
29. Considine, R.V., et al., *Serum immunoreactive-leptin concentrations in normal-weight and obese humans.* N Engl J Med, 1996. **334**(5): p. 292-5.
30. Coleman, D.L., *Obese and diabetes: two mutant genes causing diabetes-obesity syndromes in mice.* Diabetologia, 1978. **14**(3): p. 141-8.
31. Farooqi, S., et al., *ob gene mutations and human obesity.* Proc Nutr Soc, 1998. **57**(3): p. 471-5.
32. Huang, W., et al., *Liver triglyceride secretion and lipid oxidative metabolism are rapidly altered by leptin in vivo.* Endocrinology, 2006. **147**(3): p. 1480-7.

33. Scherer, P.E., et al., *A novel serum protein similar to C1q, produced exclusively in adipocytes.* J Biol Chem, 1995. **270**(45): p. 26746-9.
34. Pajvani, U.B., et al., *Structure-function studies of the adipocyte-secreted hormone Acrp30/adiponectin. Implications fpr metabolic regulation and bioactivity.* J Biol Chem, 2003. **278**(11): p. 9073-85.
35. Fruebis, J., et al., *Proteolytic cleavage product of 30-kDa adipocyte complement-related protein increases fatty acid oxidation in muscle and causes weight loss in mice.* Proc Natl Acad Sci U S A, 2001. **98**(4): p. 2005-10.
36. Yamauchi, T., et al., *The fat-derived hormone adiponectin reverses insulin resistance associated with both lipoatrophy and obesity.* Nat Med, 2001. **7**(8): p. 941-6.
37. Kadowaki, T. and T. Yamauchi, *Adiponectin and adiponectin receptors.* Endocr Rev, 2005. **26**(3): p. 439-51.
38. Tsigos, C., et al., *Dose-dependent effects of recombinant human interleukin-6 on glucose regulation.* J Clin Endocrinol Metab, 1997. **82**(12): p. 4167-70.
39. Hotamisligil, G.S., et al., *Increased adipose tissue expression of tumor necrosis factor-alpha in human obesity and insulin resistance.* J Clin Invest, 1995. **95**(5): p. 2409-15.
40. Hotamisligil, G.S., *The role of TNFalpha and TNF receptors in obesity and insulin resistance.* J Intern Med, 1999. **245**(6): p. 621-5.
41. Prins, J.B., et al., *Tumor necrosis factor-alpha induces apoptosis of human adipose cells.* Diabetes, 1997. **46**(12): p. 1939-44.
42. Qian, H., et al., *TNFalpha induces and insulin inhibits caspase 3-dependent adipocyte apoptosis.* Biochem Biophys Res Commun, 2001. **284**(5): p. 1176-83.
43. Himms-Hagen, J., *Thermogenesis in brown adipose tissue as an energy buffer. Implications for obesity.* N Engl J Med, 1984. **311**(24): p. 1549-58.
44. Cinti, S., *The Adipose Organ*, in *Adipose Tissue and Adipokines in Health and Disease*, G. Fantuzzi and T. Mazzone, Editors. 2007, Humana Press. p. pp 3-19.
45. Cypess, A.M., et al., *Identification and importance of brown adipose tissue in adult humans.* N Engl J Med, 2009. **360**(15): p. 1509-17.
46. Virtanen, K.A., et al., *Functional brown adipose tissue in healthy adults.* N Engl J Med, 2009. **360**(15): p. 1518-25.
47. van Marken Lichtenbelt, W.D., et al., *Cold-activated brown adipose tissue in healthy men.* N Engl J Med, 2009. **360**(15): p. 1500-8.
48. Villena, J.A., *Brown Adipose Tissue and Control of Body Weight: A New Potential Target for the Treatment of Obesity*, in *Obesity Epidemic*, i.P. Ltd., Editor. 2014, iConcept Press Ltd.
49. Nicholls, D.G. and R.M. Locke, *Thermogenic mechanisms in brown fat.* Physiol Rev, 1984. **64**(1): p. 1-64.
50. Klingenberg, M., *Nucleotide binding to uncoupling protein. Mechanism of control by protonation.* Biochemistry, 1988. **27**(2): p. 781-91.
51. Locke, R.M., E. Rial, and D.G. Nicholls, *The acute regulation of mitochondrial proton conductance in cells and mitochondria from the brown fat of cold-adapted and warm-adapted guinea pigs.* Eur J Biochem, 1982. **129**(2): p. 381-7.
52. Divakaruni, A.S., D.M. Humphrey, and M.D. Brand, *Fatty acids change the conformation of uncoupling protein 1 (UCP1).* J Biol Chem, 2012. **287**(44): p. 36845-53.
53. Timmons, J.A., et al., *Myogenic gene expression signature establishes that brown and white adipocytes originate from distinct cell lineages.* Proc Natl Acad Sci U S A, 2007. **104**(11): p. 4401-6.
54. Wu, J., et al., *Beige adipocytes are a distinct type of thermogenic fat cell in mouse and human.* Cell, 2012. **150**(2): p. 366-76.
55. Petrovic, N., et al., *Chronic peroxisome proliferator-activated receptor gamma (PPARgamma) activation of epididymally derived white adipocyte cultures reveals a population of thermogenically competent, UCP1-containing adipocytes molecularly distinct from classic brown adipocytes.* J Biol Chem, 2010. **285**(10): p. 7153-64.
56. Harms, M. and P. Seale, *Brown and beige fat: development, function and therapeutic potential.* Nat Med, 2013. **19**(10): p. 1252-63.
57. Wu, J., P. Cohen, and B.M. Spiegelman, *Adaptive thermogenesis in adipocytes: is beige the new brown?* Genes Dev, 2013. **27**(3): p. 234-50.
58. Bloom, J.D., et al., *Disodium (R,R)-5-[2-[[2-(3-chlorophenyl)-2-hydroxyethyl]-amino] propyl]-1,3-benzodioxole-2,2-dicarboxylate (CL 316,243). A potent beta-adrenergic agonist virtually specific for beta 3 receptors. A promising antidiabetic and antiobesity agent.* J Med Chem, 1992. **35**(16): p. 3081-4.
59. Kato, H., et al., *Mechanism of amelioration of insulin resistance by beta3-adrenoceptor agonist AJ-9677 in the KK-Ay/Ta diabetic obese mouse model.* Diabetes, 2001. **50**(1): p. 113-22.
60. Umekawa, T., et al., *Anti-obesity and anti-diabetic effects of CL316,243, a highly specific beta 3-adrenoceptor agonist, in Otsuka Long-Evans Tokushima Fatty rats: induction of uncoupling protein and activation of glucose transporter 4 in white fat.* Eur J Endo-

crinol, 1997. **136**(4): p. 429-37.
61. Cypess, A.M., et al., *Cold but not sympathomimetics activates human brown adipose tissue in vivo.* Proc Natl Acad Sci U S A, 2012. **109**(25): p. 10001-5.
62. Carmona, M.C., et al., *S 26948: a new specific peroxisome proliferator activated receptor gamma modulator with potent antidiabetes and antiatherogenic effects.* Diabetes, 2007. **56**(11): p. 2797-808.
63. Sell, H., et al., *Peroxisome proliferator-activated receptor gamma agonism increases the capacity for sympathetically mediated thermogenesis in lean and ob/ob mice.* Endocrinology, 2004. **145**(8): p. 3925-34.
64. Prins, J.B. and S. O'Rahilly, *Regulation of adipose cell number in man.* Clin Sci (Lond), 1997. **92**(1): p. 3-11.
65. Paolisso, G., et al., *A high concentration of fasting plasma non-esterified fatty acids is a risk factor for the development of NIDDM.* Diabetologia, 1995. **38**(10): p. 1213-7.
66. Weyer, C., et al., *Subcutaneous abdominal adipocyte size, a predictor of type 2 diabetes, is linked to chromosome 1q21--q23 and is associated with a common polymorphism in LMNA in Pima Indians.* Mol Genet Metab, 2001. **72**(3): p. 231-8.
67. Rosen, E.D. and B.M. Spiegelman, *Molecular regulation of adipogenesis.* Annu Rev Cell Dev Biol, 2000. **16**: p. 145-71.
68. Gregoire, F.M., *Adipocyte differentiation: from fibroblast to endocrine cell.* Exp Biol Med (Maywood), 2001. **226**(11): p. 997-1002.
69. Green, H. and O. Kehinde, *An established preadipose cell line and its differentiation in culture. II. Factors affecting the adipose conversion.* Cell, 1975. **5**(1): p. 19-27.
70. Green, H. and O. Kehinde, *Spontaneous heritable changes leading to increased adipose conversion in 3T3 cells.* Cell, 1976. **7**(1): p. 105-13.
71. Fajas, L., *Adipogenesis: a cross-talk between cell proliferation and cell differentiation.* Ann Med, 2003. **35**(2): p. 79-85.
72. Farmer, S.R., *Transcriptional control of adipocyte formation.* Cell Metab, 2006. **4**(4): p. 263-73.
73. Girard, J., et al., *Regulation of lipogenic enzyme gene expression by nutrients and hormones.* FASEB J, 1994. **8**(1): p. 36-42.
74. Smith, P.J., et al., *Insulin-like growth factor-I is an essential regulator of the differentiation of 3T3-L1 adipocytes.* J Biol Chem, 1988. **263**(19): p. 9402-8.
75. Suryawan, A., L.V. Swanson, and C.Y. Hu, *Insulin and hydrocortisone, but not triiodothyronine, are required for the differentiation of pig preadipocytes in primary culture.* J Anim Sci, 1997. **75**(1): p. 105-11.
76. Rosivatz, E., et al., *A small molecule inhibitor for phosphatase and tensin homologue deleted on chromosome 10 (PTEN).* ACS Chem Biol, 2006. **1**(12): p. 780-90.
77. Wu, Z., N.L. Bucher, and S.R. Farmer, *Induction of peroxisome proliferator-activated receptor gamma during the conversion of 3T3 fibroblasts into adipocytes is mediated by C/EBPbeta, C/EBPdelta, and glucocorticoids.* Mol Cell Biol, 1996. **16**(8): p. 4128-36.
78. Smas, C.M., et al., *Transcriptional repression of pref-1 by glucocorticoids promotes 3T3-L1 adipocyte differentiation.* J Biol Chem, 1999. **274**(18): p. 12632-41.
79. Cao, Z., R.M. Umek, and S.L. McKnight, *Regulated expression of three C/EBP isoforms during adipose conversion of 3T3-L1 cells.* Genes Dev, 1991. **5**(9): p. 1538-52.
80. Wabitsch, M., et al., *The role of growth hormone/insulin-like growth factors in adipocyte differentiation.* Metabolism, 1995. **44**(10 Suppl 4): p. 45-9.
81. Gharbi-Chihi, J., et al., *Triiodothyronine and adipose conversion of OB17 preadipocytes : binding to high affinity sites and effects on fatty acid synthetizing and esterifying enzymes.* J Recept Res, 1981. **2**(2): p. 153-73.
82. Safonova, I., et al., *Retinoids are positive effectors of adipose cell differentiation.* Mol Cell Endocrinol, 1994. **104**(2): p. 201-11.
83. Negrel, R., D. Gaillard, and G. Ailhaud, *Prostacyclin as a potent effector of adipose-cell differentiation.* Biochem J, 1989. **257**(2): p. 399-405.
84. Reginato, M.J., et al., *Prostaglandins promote and block adipogenesis through opposing effects on peroxisome proliferator-activated receptor gamma.* J Biol Chem, 1998. **273**(4): p. 1855-8.
85. Fajas, L., et al., *The organization, promoter analysis, and expression of the human PPARgamma gene.* J Biol Chem, 1997. **272**(30): p. 18779-89.
86. Smas, C.M. and H.S. Sul, *Pref-1, a protein containing EGF-like repeats, inhibits adipocyte differentiation.* Cell, 1993. **73**(4): p. 725-34.
87. Wang, Y., et al., *Pref-1, a preadipocyte secreted factor that inhibits adipogenesis.* J Nutr, 2006. **136**(12): p. 2953-6.
88. Rosen, E.D., et al., *PPAR gamma is required for the differentiation of adipose tissue in vivo and in vitro.* Mol Cell, 1999. **4**(4): p. 611-7.
89. Tontonoz, P., E. Hu, and B.M. Spiegelman, *Stimulation of adipogenesis in fibroblasts by PPAR gamma 2, a lipid-activated*

transcription factor. Cell, 1994. **79**(7): p. 1147-56.
90. Tamori, Y., et al., *Role of peroxisome proliferator-activated receptor-gamma in maintenance of the characteristics of mature 3T3-L1 adipocytes.* Diabetes, 2002. **51**(7): p. 2045-55.
91. Rosen, E.D. and B.M. Spiegelman, *PPARgamma : a nuclear regulator of metabolism, differentiation, and cell growth.* J Biol Chem, 2001. **276**(41): p. 37731-4.
92. Iwaki, M., et al., *Induction of adiponectin, a fat-derived antidiabetic and antiatherogenic factor, by nuclear receptors.* Diabetes, 2003. **52**(7): p. 1655-63.
93. Tomaru, T., et al., *Adipocyte-specific expression of murine resistin is mediated by synergism between peroxisome proliferator-activated receptor gamma and CCAAT/enhancer-binding proteins.* J Biol Chem, 2009. **284**(10): p. 6116-25.
94. Hollenberg, A.N., et al., *Functional antagonism between CCAAT/Enhancer binding protein-alpha and peroxisome proliferator-activated receptor-gamma on the leptin promoter.* J Biol Chem, 1997. **272**(8): p. 5283-90.
95. Hofmann, C., et al., *Altered gene expression for tumor necrosis factor-alpha and its receptors during drug and dietary modulation of insulin resistance.* Endocrinology, 1994. **134**(1): p. 264-70.
96. Forman, B.M., et al., *15-Deoxy-delta 12, 14-prostaglandin J2 is a ligand for the adipocyte determination factor PPAR gamma.* Cell, 1995. **83**(5): p. 803-12.
97. Forman, B.M., J. Chen, and R.M. Evans, *Hypolipidemic drugs, polyunsaturated fatty acids, and eicosanoids are ligands for peroxisome proliferator-activated receptors alpha and delta.* Proc Natl Acad Sci U S A, 1997. **94**(9): p. 4312-7.
98. Lehmann, J.M., et al., *An antidiabetic thiazolidinedione is a high affinity ligand for peroxisome proliferator-activated receptor gamma (PPAR gamma).* J Biol Chem, 1995. **270**(22): p. 12953-6.
99. Wilson-Fritch, L., et al., *Mitochondrial remodeling in adipose tissue associated with obesity and treatment with rosiglitazone.* J Clin Invest, 2004. **114**(9): p. 1281-9.
100. Bogacka, I., et al., *Pioglitazone induces mitochondrial biogenesis in human subcutaneous adipose tissue in vivo.* Diabetes, 2005. **54**(5): p. 1392-9.
101. Rong, J.X., et al., *Adipose mitochondrial biogenesis is suppressed in db/db and high-fat diet-fed mice and improved by rosiglitazone.* Diabetes, 2007. **56**(7): p. 1751-60.
102. Laplante, M., et al., *Mechanisms of the depot specificity of peroxisome proliferator-activated receptor gamma action on adipose tissue metabolism.* Diabetes, 2006. **55**(10): p. 2771-8.
103. Miinea, C.P., et al., *AS160, the Akt substrate regulating GLUT4 translocation, has a functional Rab GTPase-activating protein domain.* Biochem J, 2005. **391**(Pt 1): p. 87-93.
104. May, O., *Diabetes and Insulin Signaling: A New Strategy to Promote Pancreatic b Cell Survival.* Cayman Chemical Library, 2008.
105. Zamora, M. and J.A. Villena, *Targeting Mitochondrial Biogenesis to Treat Insulin Resistance.* Curr Pharm Des, 2014.
106. Boden, G., et al., *Effects of fat on insulin-stimulated carbohydrate metabolism in normal men.* J Clin Invest, 1991. **88**(3): p. 960-6.
107. Roden, M., et al., *Mechanism of free fatty acid-induced insulin resistance in humans.* J Clin Invest, 1996. **97**(12): p. 2859-65.
108. Krssak, M., et al., *Intramyocellular lipid concentrations are correlated with insulin sensitivity in humans: a 1H NMR spectroscopy study.* Diabetologia, 1999. **42**(1): p. 113-6.
109. Samuel, V.T. and G.I. Shulman, *Mechanisms for insulin resistance: common threads and missing links.* Cell, 2012. **148**(5): p. 852-71.
110. Dresner, A., et al., *Effects of free fatty acids on glucose transport and IRS-1-associated phosphatidylinositol 3-kinase activity.* J Clin Invest, 1999. **103**(2): p. 253-9.
111. Kim, J.K., et al., *PKC-theta knockout mice are protected from fat-induced insulin resistance.* J Clin Invest, 2004. **114**(6): p. 823-7.
112. Yu, C., et al., *Mechanism by which fatty acids inhibit insulin activation of insulin receptor substrate-1 (IRS-1)-associated phosphatidylinositol 3-kinase activity in muscle.* J Biol Chem, 2002. **277**(52): p. 50230-6.
113. Griffin, M.E., et al., *Free fatty acid-induced insulin resistance is associated with activation of protein kinase C theta and alterations in the insulin signaling cascade.* Diabetes, 1999. **48**(6): p. 1270-4.
114. Powell, D.J., et al., *Ceramide disables 3-phosphoinositide binding to the pleckstrin homology domain of protein kinase B (PKB)/Akt by a PKCzeta-dependent mechanism.* Mol Cell Biol, 2003. **23**(21): p. 7794-808.
115. Shi, H., et al., *TLR4 links innate immunity and fatty acid-induced insulin resistance.* J Clin Invest, 2006. **116**(11): p. 3015-25.
116. Guilherme, A., et al., *Adipocyte dysfunctions linking obesity to insulin resistance and type 2 diabetes.* Nat Rev Mol Cell Biol, 2008. **9**(5): p. 367-77.
117. Balistreri, C.R., C. Caruso, and G. Candore, *The role of adipose tissue and adipokines in obesity-related inflammatory*

diseases. Mediators Inflamm, 2010. **2010**: p. 802078.
118. Cancello, R., et al., *Reduction of macrophage infiltration and chemoattractant gene expression changes in white adipose tissue of morbidly obese subjects after surgery-induced weight loss.* Diabetes, 2005. **54**(8): p. 2277-86.
119. Weisberg, S.P., et al., *Obesity is associated with macrophage accumulation in adipose tissue.* J Clin Invest, 2003. **112**(12): p. 1796-808.
120. Zeyda, M. and T.M. Stulnig, *Adipose tissue macrophages.* Immunol Lett, 2007. **112**(2): p. 61-7.
121. Xu, H., et al., *Chronic inflammation in fat plays a crucial role in the development of obesity-related insulin resistance.* J Clin Invest, 2003. **112**(12): p. 1821-30.
122. Petruschke, T. and H. Hauner, *Tumor necrosis factor-alpha prevents the differentiation of human adipocyte precursor cells and causes delipidation of newly developed fat cells.* J Clin Endocrinol Metab, 1993. **76**(3): p. 742-7.
123. Xing, H., et al., *TNF alpha-mediated inhibition and reversal of adipocyte differentiation is accompanied by suppressed expression of PPARgamma without effects on Pref-1 expression.* Endocrinology, 1997. **138**(7): p. 2776-83.
124. Sopasakis, V.R., et al., *High local concentrations and effects on differentiation implicate interleukin-6 as a paracrine regulator.* Obes Res, 2004. **12**(3): p. 454-60.
125. Hauner, H., et al., *Effects of tumour necrosis factor alpha (TNF alpha) on glucose transport and lipid metabolism of newly-differentiated human fat cells in cell culture.* Diabetologia, 1995. **38**(7): p. 764-71.
126. van Hall, G., et al., *Interleukin-6 stimulates lipolysis and fat oxidation in humans.* J Clin Endocrinol Metab, 2003. **88**(7): p. 3005-10.
127. Zick, Y., *Role of Ser/Thr kinases in the uncoupling of insulin signaling.* Int J Obes Relat Metab Disord, 2003. **27 Suppl 3**: p. S56-60.
128. Stephens, J.M. and P.H. Pekala, *Transcriptional repression of the C/EBP-alpha and GLUT4 genes in 3T3-L1 adipocytes by tumor necrosis factor-alpha. Regulations is coordinate and independent of protein synthesis.* J Biol Chem, 1992. **267**(19): p. 13580-4.
129. Holland, W.L., et al., *Lipid-induced insulin resistance mediated by the proinflammatory receptor TLR4 requires saturated fatty acid-induced ceramide biosynthesis in mice.* J Clin Invest, 2011. **121**(5): p. 1858-70.
130. Hotamisligil, G.S., *Endoplasmic reticulum stress and the inflammatory basis of metabolic disease.* Cell, 2010. **140**(6): p. 900-17.
131. Ron, D. and P. Walter, *Signal integration in the endoplasmic reticulum unfolded protein response.* Nat Rev Mol Cell Biol, 2007. **8**(7): p. 519-29.
132. Ozcan, U., et al., *Endoplasmic reticulum stress links obesity, insulin action, and type 2 diabetes.* Science, 2004. **306**(5695): p. 457-61.
133. Ozcan, U., et al., *Chemical chaperones reduce ER stress and restore glucose homeostasis in a mouse model of type 2 diabetes.* Science, 2006. **313**(5790): p. 1137-40.
134. Deng, J., et al., *Translational repression mediates activation of nuclear factor kappa B by phosphorylated translation initiation factor 2.* Mol Cell Biol, 2004. **24**(23): p. 10161-8.
135. Urano, F., et al., *Coupling of stress in the ER to activation of JNK protein kinases by transmembrane protein kinase IRE1.* Science, 2000. **287**(5453): p. 664-6.
136. Petersen, K.F., et al., *Mitochondrial dysfunction in the elderly: possible role in insulin resistance.* Science, 2003. **300**(5622): p. 1140-2.
137. Petersen, K.F., et al., *Impaired mitochondrial activity in the insulin-resistant offspring of patients with type 2 diabetes.* N Engl J Med, 2004. **350**(7): p. 664-71.
138. Bonnard, C., et al., *Mitochondrial dysfunction results from oxidative stress in the skeletal muscle of diet-induced insulin-resistant mice.* J Clin Invest, 2008. **118**(2): p. 789-800.
139. Sparks, L.M., et al., *A high-fat diet coordinately downregulates genes required for mitochondrial oxidative phosphorylation in skeletal muscle.* Diabetes, 2005. **54**(7): p. 1926-33.
140. Rector, R.S., et al., *Mitochondrial dysfunction precedes insulin resistance and hepatic steatosis and contributes to the natural history of non-alcoholic fatty liver disease in an obese rodent model.* J Hepatol, 2010. **52**(5): p. 727-36.
141. Raffaella, C., et al., *Alterations in hepatic mitochondrial compartment in a model of obesity and insulin resistance.* Obesity (Silver Spring), 2008. **16**(5): p. 958-64.
142. Szendroedi, J., et al., *Muscle mitochondrial ATP synthesis and glucose transport/phosphorylation in type 2 diabetes.* PLoS Med, 2007. **4**(5): p. e154.
143. Perez-Carreras, M., et al., *Defective hepatic mitochondrial respiratory chain in patients with nonalcoholic steatohepatitis.* Hepatology, 2003. **38**(4): p. 999-1007.
144. Wilson-Fritch, L., et al., *Mitochondrial biogenesis and remodeling during adipogenesis and in response to the insulin sensitizer rosiglitazone.* Mol Cell Biol, 2003. **23**(3): p. 1085-94.

145. Tormos, K.V., et al., *Mitochondrial complex III ROS regulate adipocyte differentiation.* Cell Metab, 2011. **14**(4): p. 537-44.
146. Lu, R.H., et al., *Mitochondrial development and the influence of its dysfunction during rat adipocyte differentiation.* Mol Biol Rep, 2010. **37**(5): p. 2173-82.
147. Koh, E.H., et al., *Essential role of mitochondrial function in adiponectin synthesis in adipocytes.* Diabetes, 2007. **56**(12): p. 2973-81.
148. Gao, C.L., et al., *Mitochondrial dysfunction is induced by high levels of glucose and free fatty acids in 3T3-L1 adipocytes.* Mol Cell Endocrinol, 2010. **320**(1-2): p. 25-33.
149. Krishnan, J., et al., *Dietary obesity-associated Hif1alpha activation in adipocytes restricts fatty acid oxidation and energy expenditure via suppression of the Sirt2-NAD+ system.* Genes Dev, 2012. **26**(3): p. 259-70.
150. Bogacka, I., et al., *Structural and functional consequences of mitochondrial biogenesis in human adipocytes in vitro.* J Clin Endocrinol Metab, 2005. **90**(12): p. 6650-6.
151. Mustelin, L., et al., *Acquired obesity and poor physical fitness impair expression of genes of mitochondrial oxidative phosphorylation in monozygotic twins discordant for obesity.* Am J Physiol Endocrinol Metab, 2008. **295**(1): p. E148-54.
152. Choo, H.J., et al., *Mitochondria are impaired in the adipocytes of type 2 diabetic mice.* Diabetologia, 2006. **49**(4): p. 784-91.
153. Turner, N., *Mitochondrial Metabolism and Insulin Action*, in *Type 2 Diabetes*, K. Masuo, Editor. 2013, InTech.
154. Mootha, V.K., et al., *Integrated analysis of protein composition, tissue diversity, and gene regulation in mouse mitochondria.* Cell, 2003. **115**(5): p. 629-40.
155. Pagliarini, D.J., et al., *A mitochondrial protein compendium elucidates complex I disease biology.* Cell, 2008. **134**(1): p. 112-23.
156. Hock, M.B. and A. Kralli, *Transcriptional control of mitochondrial biogenesis and function.* Annu Rev Physiol, 2009. **71**: p. 177-203.
157. Larsson, N.G., et al., *Mitochondrial transcription factor A is necessary for mtDNA maintenance and embryogenesis in mice.* Nat Genet, 1998. **18**(3): p. 231-6.
158. Falkenberg, M., et al., *Mitochondrial transcription factors B1 and B2 activate transcription of human mtDNA.* Nat Genet, 2002. **31**(3): p. 289-94.
159. McCulloch, V., B.L. Seidel-Rogol, and G.S. Shadel, *A human mitochondrial transcription factor is related to RNA adenine methyltransferases and binds S-adenosylmethionine.* Mol Cell Biol, 2002. **22**(4): p. 1116-25.
160. Metodiev, M.D., et al., *Methylation of 12S rRNA is necessary for in vivo stability of the small subunit of the mammalian mitochondrial ribosome.* Cell Metab, 2009. **9**(4): p. 386-97.
161. Virbasius, J.V. and R.C. Scarpulla, *Transcriptional activation through ETS domain binding sites in the cytochrome c oxidase subunit IV gene.* Mol Cell Biol, 1991. **11**(11): p. 5631-8.
162. Evans, M.J. and R.C. Scarpulla, *Interaction of nuclear factors with multiple sites in the somatic cytochrome c promoter. Characterization of upstream NRF-1, ATF, and intron Sp1 recognition sequences.* J Biol Chem, 1989. **264**(24): p. 14361-8.
163. Scarpulla, R.C., *Transcriptional paradigms in mammalian mitochondrial biogenesis and function.* Physiol Rev, 2008. **88**(2): p. 611-38.
164. Huo, L. and R.C. Scarpulla, *Mitochondrial DNA instability and peri-implantation lethality associated with targeted disruption of nuclear respiratory factor 1 in mice.* Mol Cell Biol, 2001. **21**(2): p. 644-54.
165. Cam, H., et al., *A common set of gene regulatory networks links metabolism and growth inhibition.* Mol Cell, 2004. **16**(3): p. 399-411.
166. Wu, Z., et al., *Mechanisms controlling mitochondrial biogenesis and respiration through the thermogenic coactivator PGC-1.* Cell, 1999. **98**(1): p. 115-24.
167. Andersson, U. and R.C. Scarpulla, *Pgc-1-related coactivator, a novel, serum-inducible coactivator of nuclear respiratory factor 1-dependent transcription in mammalian cells.* Mol Cell Biol, 2001. **21**(11): p. 3738-49.
168. Lin, J., et al., *Peroxisome proliferator-activated receptor gamma coactivator 1beta (PGC-1beta), a novel PGC-1-related transcription coactivator associated with host cell factor.* J Biol Chem, 2002. **277**(3): p. 1645-8.
169. Wang, C., et al., *Cyclin D1 repression of nuclear respiratory factor 1 integrates nuclear DNA synthesis and mitochondrial function.* Proc Natl Acad Sci U S A, 2006. **103**(31): p. 11567-72.
170. Ristevski, S., et al., *The ETS transcription factor GABPalpha is essential for early embryogenesis.* Mol Cell Biol, 2004. **24**(13): p. 5844-9.
171. Villena, J.A., et al., *Mitochondrial biogenesis in brown adipose tissue is associated with differential expression of transcription regulatory factors.* Cell Mol Life Sci, 2002. **59**(11): p. 1934-44.
172. Ojuka, E.O., et al., *Raising Ca2+ in L6 myotubes mimics effects of exercise on mitochondrial biogenesis in muscle.* FASEB J, 2003. **17**(6): p. 675-81.

173. Baar, K., et al., *Adaptations of skeletal muscle to exercise: rapid increase in the transcriptional coactivator PGC-1.* FASEB J, 2002. **16**(14): p. 1879-86.
174. Cartoni, R., et al., *Mitofusins 1/2 and ERRalpha expression are increased in human skeletal muscle after physical exercise.* J Physiol, 2005. **567**(Pt 1): p. 349-58.
175. Yang, Z.F., S. Mott, and A.G. Rosmarin, *The Ets transcription factor GABP is required for cell-cycle progression.* Nat Cell Biol, 2007. **9**(3): p. 339-46.
176. Evans, R.M., G.D. Barish, and Y.X. Wang, *PPARs and the complex journey to obesity.* Nat Med, 2004. **10**(4): p. 355-61.
177. Burkart, E.M., et al., *Nuclear receptors PPARbeta/delta and PPARalpha direct distinct metabolic regulatory programs in the mouse heart.* J Clin Invest, 2007. **117**(12): p. 3930-9.
178. Reilly, S.M. and C.H. Lee, *PPAR delta as a therapeutic target in metabolic disease.* FEBS Lett, 2008. **582**(1): p. 26-31.
179. Wang, Y.X., et al., *Regulation of muscle fiber type and running endurance by PPARdelta.* PLoS Biol, 2004. **2**(10): p. e294.
180. Puigserver, P., et al., *A cold-inducible coactivator of nuclear receptors linked to adaptive thermogenesis.* Cell, 1998. **92**(6): p. 829-39.
181. Hondares, E., et al., *Thiazolidinediones and rexinoids induce peroxisome proliferator-activated receptor-coactivator (PGC)-1alpha gene transcription: an autoregulatory loop controls PGC-1alpha expression in adipocytes via peroxisome proliferator-activated receptor-gamma coactivation.* Endocrinology, 2006. **147**(6): p. 2829-38.
182. Pardo, R., et al., *Rosiglitazone-induced mitochondrial biogenesis in white adipose tissue is independent of peroxisome proliferator-activated receptor gamma coactivator-1alpha.* PLoS One, 2011. **6**(11): p. e26989.
183. Greschik, H., et al., *Structural and functional evidence for ligand-independent transcriptional activation by the estrogen-related receptor 3.* Mol Cell, 2002. **9**(2): p. 303-13.
184. Kallen, J., et al., *Evidence for ligand-independent transcriptional activation of the human estrogen-related receptor alpha (ERRalpha): crystal structure of ERRalpha ligand binding domain in complex with peroxisome proliferator-activated receptor coactivator-1alpha.* J Biol Chem, 2004. **279**(47): p. 49330-7.
185. Giguere, V., *Transcriptional control of energy homeostasis by the estrogen-related receptors.* Endocr Rev, 2008. **29**(6): p. 677-96.
186. Villena, J.A. and A. Kralli, *ERRalpha: a metabolic function for the oldest orphan.* Trends Endocrinol Metab, 2008. **19**(8): p. 269-76.
187. Dufour, C.R., et al., *Genome-wide orchestration of cardiac functions by the orphan nuclear receptors ERRalpha and gamma.* Cell Metab, 2007. **5**(5): p. 345-56.
188. Schreiber, S.N., et al., *The transcriptional coactivator PGC-1 regulates the expression and activity of the orphan nuclear receptor estrogen-related receptor alpha (ERRalpha).* J Biol Chem, 2003. **278**(11): p. 9013-8.
189. Sonoda, J., et al., *PGC-1beta controls mitochondrial metabolism to modulate circadian activity, adaptive thermogenesis, and hepatic steatosis.* Proc Natl Acad Sci U S A, 2007. **104**(12): p. 5223-8.
190. Villena, J.A., et al., *Orphan nuclear receptor estrogen-related receptor alpha is essential for adaptive thermogenesis.* Proc Natl Acad Sci U S A, 2007. **104**(4): p. 1418-23.
191. Huss, J.M., R.P. Kopp, and D.P. Kelly, *Peroxisome proliferator-activated receptor coactivator-1alpha (PGC-1alpha) coactivates the cardiac-enriched nuclear receptors estrogen-related receptor-alpha and -gamma. Identification of novel leucine-rich interaction motif within PGC-1alpha.* J Biol Chem, 2002. **277**(43): p. 40265-74.
192. Mootha, V.K., et al., *Erralpha and Gabpa/b specify PGC-1alpha-dependent oxidative phosphorylation gene expression that is altered in diabetic muscle.* Proc Natl Acad Sci U S A, 2004. **101**(17): p. 6570-5.
193. Laganiere, J., et al., *A polymorphic autoregulatory hormone response element in the human estrogen-related receptor alpha (ERRalpha) promoter dictates peroxisome proliferator-activated receptor gamma coactivator-1alpha control of ERRalpha expression.* J Biol Chem, 2004. **279**(18): p. 18504-10.
194. Ichida, M., S. Nemoto, and T. Finkel, *Identification of a specific molecular repressor of the peroxisome proliferator-activated receptor gamma Coactivator-1 alpha (PGC-1alpha).* J Biol Chem, 2002. **277**(52): p. 50991-5.
195. Huss, J.M., et al., *The nuclear receptor ERRalpha is required for the bioenergetic and functional adaptation to cardiac pressure overload.* Cell Metab, 2007. **6**(1): p. 25-37.
196. Lin, J., C. Handschin, and B.M. Spiegelman, *Metabolic control through the PGC-1 family of transcription coactivators.* Cell Metab, 2005. **1**(6): p. 361-70.
197. Powelka, A.M., et al., *Suppression of oxidative metabolism and mitochondrial biogenesis by the transcriptional corepressor RIP140 in mouse adipocytes.* J Clin Invest, 2006. **116**(1): p. 125-36.
198. Lin, J., et al., *Transcriptional co-activator PGC-1 alpha drives the formation of slow-twitch muscle fibres.* Nature, 2002. **418**(6899): p. 797-801.
199. Seth, A., et al., *The transcriptional corepressor RIP140 regulates oxidative metabolism in skeletal muscle.* Cell Metab, 2007.

6(3): p. 236-45.
200. Christian, M., R. White, and M.G. Parker, *Metabolic regulation by the nuclear receptor corepressor RIP140.* Trends Endocrinol Metab, 2006. **17**(6): p. 243-50.
201. Kressler, D., et al., *The PGC-1-related protein PERC is a selective coactivator of estrogen receptor alpha.* J Biol Chem, 2002. **277**(16): p. 13918-25.
202. Puigserver, P., et al., *Activation of PPARgamma coactivator-1 through transcription factor docking.* Science, 1999. **286**(5443): p. 1368-71.
203. Monsalve, M., et al., *Direct coupling of transcription and mRNA processing through the thermogenic coactivator PGC-1.* Mol Cell, 2000. **6**(2): p. 307-16.
204. Chang, J.S., et al., *NT-PGC-1alpha protein is sufficient to link beta3-adrenergic receptor activation to transcriptional and physiological components of adaptive thermogenesis.* J Biol Chem, 2012. **287**(12): p. 9100-11.
205. He, X., et al., *Peri-implantation lethality in mice lacking the PGC-1-related coactivator protein.* Dev Dyn, 2012. **241**(5): p. 975-83.
206. Fernandez-Marcos, P.J. and J. Auwerx, *Regulation of PGC-1alpha, a nodal regulator of mitochondrial biogenesis.* Am J Clin Nutr, 2011. **93**(4): p. 884S-90.
207. Lin, J., et al., *Defects in adaptive energy metabolism with CNS-linked hyperactivity in PGC-1alpha null mice.* Cell, 2004. **119**(1): p. 121-35.
208. St-Pierre, J., et al., *Suppression of reactive oxygen species and neurodegeneration by the PGC-1 transcriptional coactivators.* Cell, 2006. **127**(2): p. 397-408.
209. Leone, T.C., et al., *PGC-1alpha deficiency causes multi-system energy metabolic derangements: muscle dysfunction, abnormal weight control and hepatic steatosis.* PLoS Biol, 2005. **3**(4): p. e101.
210. Lelliott, C.J., et al., *Ablation of PGC-1beta results in defective mitochondrial activity, thermogenesis, hepatic function, and cardiac performance.* PLoS Biol, 2006. **4**(11): p. e369.
211. Arany, Z., et al., *Transcriptional coactivator PGC-1 alpha controls the energy state and contractile function of cardiac muscle.* Cell Metab, 2005. **1**(4): p. 259-71.
212. Lehman, J.J., et al., *The transcriptional coactivator PGC-1alpha is essential for maximal and efficient cardiac mitochondrial fatty acid oxidation and lipid homeostasis.* Am J Physiol Heart Circ Physiol, 2008. **295**(1): p. H185-96.
213. Lai, L., et al., *Transcriptional coactivators PGC-1alpha and PGC-lbeta control overlapping programs required for perinatal maturation of the heart.* Genes Dev, 2008. **22**(14): p. 1948-61.
214. Martin, O.J., et al., *A role for peroxisome proliferator-activated receptor gamma coactivator-1 in the control of mitochondrial dynamics during postnatal cardiac growth.* Circ Res, 2014. **114**(4): p. 626-36.
215. Garnier, A., et al., *Control by circulating factors of mitochondrial function and transcription cascade in heart failure: a role for endothelin-1 and angiotensin II.* Circ Heart Fail, 2009. **2**(4): p. 342-50.
216. Sebastiani, M., et al., *Induction of mitochondrial biogenesis is a maladaptive mechanism in mitochondrial cardiomyopathies.* J Am Coll Cardiol, 2007. **50**(14): p. 1362-9.
217. Sihag, S., et al., *PGC-1alpha and ERRalpha target gene downregulation is a signature of the failing human heart.* J Mol Cell Cardiol, 2009. **46**(2): p. 201-12.
218. Karamanlidis, G., et al., *Defective DNA replication impairs mitochondrial biogenesis in human failing hearts.* Circ Res, 2010. **106**(9): p. 1541-8.
219. Lin, J., et al., *PGC-1beta in the regulation of hepatic glucose and energy metabolism.* J Biol Chem, 2003. **278**(33): p. 30843-8.
220. Herzig, S., et al., *CREB regulates hepatic gluconeogenesis through the coactivator PGC-1.* Nature, 2001. **413**(6852): p. 179-83.
221. Yoon, J.C., et al., *Control of hepatic gluconeogenesis through the transcriptional coactivator PGC-1.* Nature, 2001. **413**(6852): p. 131-8.
222. Lustig, Y., et al., *Separation of the gluconeogenic and mitochondrial functions of PGC-1{alpha} through S6 kinase.* Genes Dev, 2011. **25**(12): p. 1232-44.
223. Rodgers, J.T., et al., *Nutrient control of glucose homeostasis through a complex of PGC-1alpha and SIRT1.* Nature, 2005. **434**(7029): p. 113-8.
224. Lin, J., et al., *Hyperlipidemic effects of dietary saturated fats mediated through PGC-1beta coactivation of SREBP.* Cell, 2005. **120**(2): p. 261-73.
225. Wolfrum, C. and M. Stoffel, *Coactivation of Foxa2 through Pgc-1beta promotes liver fatty acid oxidation and triglyceride/VLDL secretion.* Cell Metab, 2006. **3**(2): p. 99-110.
226. Vianna, C.R., et al., *Hypomorphic mutation of PGC-1beta causes mitochondrial dysfunction and liver insulin resistance.* Cell Metab, 2006. **4**(6): p. 453-64.

227. St-Pierre, J., et al., *Bioenergetic analysis of peroxisome proliferator-activated receptor gamma coactivators 1alpha and 1beta (PGC-1alpha and PGC-1beta) in muscle cells.* J Biol Chem, 2003. **278**(29): p. 26597-603.
228. Arany, Z., et al., *HIF-independent regulation of VEGF and angiogenesis by the transcriptional coactivator PGC-1alpha.* Nature, 2008. **451**(7181): p. 1008-12.
229. Handschin, C., et al., *PGC-1alpha regulates the neuromuscular junction program and ameliorates Duchenne muscular dystrophy.* Genes Dev, 2007. **21**(7): p. 770-83.
230. Leick, L., et al., *PGC-1alpha is not mandatory for exercise- and training-induced adaptive gene responses in mouse skeletal muscle.* Am J Physiol Endocrinol Metab, 2008. **294**(2): p. E463-74.
231. Rowe, G.C., et al., *PGC-1alpha is dispensable for exercise-induced mitochondrial biogenesis in skeletal muscle.* PLoS One, 2012. **7**(7): p. e41817.
232. Arany, Z., et al., *The transcriptional coactivator PGC-1beta drives the formation of oxidative type IIX fibers in skeletal muscle.* Cell Metab, 2007. **5**(1): p. 35-46.
233. Kamei, Y., et al., *PPARgamma coactivator 1beta/ERR ligand 1 is an ERR protein ligand, whose expression induces a high-energy expenditure and antagonizes obesity.* Proc Natl Acad Sci U S A, 2003. **100**(21): p. 12378-83.
234. Cen, B., A. Selvaraj, and R. Prywes, *Myocardin/MKL family of SRF coactivators: key regulators of immediate early and muscle specific gene expression.* J Cell Biochem, 2004. **93**(1): p. 74-82.
235. Vercauteren, K., et al., *PGC-1-related coactivator: immediate early expression and characterization of a CREB/NRF-1 binding domain associated with cytochrome c promoter occupancy and respiratory growth.* Mol Cell Biol, 2006. **26**(20): p. 7409-19.
236. Mootha, V.K., et al., *PGC-1alpha-responsive genes involved in oxidative phosphorylation are coordinately downregulated in human diabetes.* Nat Genet, 2003. **34**(3): p. 267-73.
237. Patti, M.E., et al., *Coordinated reduction of genes of oxidative metabolism in humans with insulin resistance and diabetes: Potential role of PGC1 and NRF1.* Proc Natl Acad Sci U S A, 2003. **100**(14): p. 8466-71.
238. Ek, J., et al., *Mutation analysis of peroxisome proliferator-activated receptor-gamma coactivator-1 (PGC-1) and relationships of identified amino acid polymorphisms to Type II diabetes mellitus.* Diabetologia, 2001. **44**(12): p. 2220-6.
239. Hara, K., et al., *A genetic variation in the PGC-1 gene could confer insulin resistance and susceptibility to Type II diabetes.* Diabetologia, 2002. **45**(5): p. 740-3.
240. Barres, R., et al., *Non-CpG methylation of the PGC-1alpha promoter through DNMT3B controls mitochondrial density.* Cell Metab, 2009. **10**(3): p. 189-98.
241. Rim, J.S. and L.P. Kozak, *Regulatory motifs for CREB-binding protein and Nfe2l2 transcription factors in the upstream enhancer of the mitochondrial uncoupling protein 1 gene.* J Biol Chem, 2002. **277**(37): p. 34589-600.
242. Kleiner, S., et al., *Development of insulin resistance in mice lacking PGC-1alpha in adipose tissues.* Proc Natl Acad Sci U S A, 2012. **109**(24): p. 9635-40.
243. Uldry, M., et al., *Complementary action of the PGC-1 coactivators in mitochondrial biogenesis and brown fat differentiation.* Cell Metab, 2006. **3**(5): p. 333-41.
244. Barlow, C., et al., *Targeted expression of Cre recombinase to adipose tissue of transgenic mice directs adipose-specific excision of loxP-flanked gene segments.* Nucleic Acids Res, 1997. **25**(12): p. 2543-5.
245. Black, B.L., et al., *Differential effects of fat and sucrose on body composition in A/J and C57BL/6 mice.* Metabolism, 1998. **47**(11): p. 1354-9.
246. He, W., et al., *Adipose-specific peroxisome proliferator-activated receptor gamma knockout causes insulin resistance in fat and liver but not in muscle.* Proc Natl Acad Sci U S A, 2003. **100**(26): p. 15712-7.
247. Paigen, B., et al., *Physiological effects of housing density on C57BL/6J mice over a 9-month period.* J Anim Sci, 2012. **90**(13): p. 5182-92.
248. Park, S.Y., et al., *Unraveling the temporal pattern of diet-induced insulin resistance in individual organs and cardiac dysfunction in C57BL/6 mice.* Diabetes, 2005. **54**(12): p. 3530-40.
249. Livak, K.J. and T.D. Schmittgen, *Analysis of relative gene expression data using real-time quantitative PCR and the 2(-Delta Delta C(T)) Method.* Methods, 2001. **25**(4): p. 402-8.
250. Srere, P.A., in *Methods in Enzymology*. 1969. p. 3-11.
251. M., D., *Assessing Functional Integrity of Mitochondria in Vitro and in Vivo*, in *Mitochondria*, P.L.A.a.S. E.A., Editor. 2001. p. 75-95.
252. Hannon, G.J. and J.J. Rossi, *Unlocking the potential of the human genome with RNA interference.* Nature, 2004. **431**(7006): p. 371-8.
253. Kilroy, G., D.H. Burk, and Z.E. Floyd, *High efficiency lipid-based siRNA transfection of adipocytes in suspension.* PLoS One, 2009. **4**(9): p. e6940.
254. Gnaiger, E., *Polarographic oxygen sensors, the oxygraph, and high-resolution respirometry to assess mitochondrial function*, in *Drug-Induced Mitochondrial Dysfunction*, J. Dykens and Y. Will, Editors. 2008, John Wiley & Sons, Inc. p. 327–

352.
255. Villena, J.A., et al., *Desnutrin, an adipocyte gene encoding a novel patatin domain-containing protein, is induced by fasting and glucocorticoids: ectopic expression of desnutrin increases triglyceride hydrolysis.* J Biol Chem, 2004. **279**(45): p. 47066-75.
256. Martens, K., A. Bottelbergs, and M. Baes, *Ectopic recombination in the central and peripheral nervous system by aP2/FABP4-Cre mice: implications for metabolism research.* FEBS Lett, 2010. **584**(5): p. 1054-8.
257. Fu, Y., et al., *The adipocyte lipid binding protein (ALBP/aP2) gene facilitates foam cell formation in human THP-1 macrophages.* Atherosclerosis, 2002. **165**(2): p. 259-69.
258. Shimomura, I., et al., *Insulin resistance and diabetes mellitus in transgenic mice expressing nuclear SREBP-1c in adipose tissue: model for congenital generalized lipodystrophy.* Genes Dev, 1998. **12**(20): p. 3182-94.
259. Wang, H., et al., *Relationships between muscle mitochondrial DNA content, mitochondrial enzyme activity and oxidative capacity in man: alterations with disease.* Eur J Appl Physiol Occup Physiol, 1999. **80**(1): p. 22-7.
260. Boden, G., et al., *Thiazolidinediones upregulate fatty acid uptake and oxidation in adipose tissue of diabetic patients.* Diabetes, 2005. **54**(3): p. 880-5.
261. Deng, T., et al., *A peroxisome proliferator-activated receptor gamma (PPARgamma)/PPARgamma coactivator 1beta autoregulatory loop in adipocyte mitochondrial function.* J Biol Chem, 2011. **286**(35): p. 30723-31.
262. Nye, C., et al., *Reassessing triglyceride synthesis in adipose tissue.* Trends Endocrinol Metab, 2008. **19**(10): p. 356-61.
263. Vega, R.B., J.M. Huss, and D.P. Kelly, *The coactivator PGC-1 cooperates with peroxisome proliferator-activated receptor alpha in transcriptional control of nuclear genes encoding mitochondrial fatty acid oxidation enzymes.* Mol Cell Biol, 2000. **20**(5): p. 1868-76.
264. Rieusset, J., J. Auwerx, and H. Vidal, *Regulation of gene expression by activation of the peroxisome proliferator-activated receptor gamma with rosiglitazone (BRL 49653) in human adipocytes.* Biochem Biophys Res Commun, 1999. **265**(1): p. 265-71.
265. Fukui, H. and C.T. Moraes, *The mitochondrial impairment, oxidative stress and neurodegeneration connection: reality or just an attractive hypothesis?* Trends Neurosci, 2008. **31**(5): p. 251-6.
266. Juurinen, L., et al., *Rosiglitazone reduces liver fat and insulin requirements and improves hepatic insulin sensitivity and glycemic control in patients with type 2 diabetes requiring high insulin doses.* J Clin Endocrinol Metab, 2008. **93**(1): p. 118-24.
267. Tiikkainen, M., et al., *Effects of rosiglitazone and metformin on liver fat content, hepatic insulin resistance, insulin clearance, and gene expression in adipose tissue in patients with type 2 diabetes.* Diabetes, 2004. **53**(8): p. 2169-76.
268. Akiyama, T., et al., *High-fat hypercaloric diet induces obesity, glucose intolerance and hyperlipidemia in normal adult male Wistar rat.* Diabetes Res Clin Pract, 1996. **31**(1-3): p. 27-35.
269. Inokuma, K., et al., *Indispensable role of mitochondrial UCP1 for antiobesity effect of beta3-adrenergic stimulation.* Am J Physiol Endocrinol Metab, 2006. **290**(5): p. E1014-21.
270. Himms-Hagen, J., et al., *Multilocular fat cells in WAT of CL-316243-treated rats derive directly from white adipocytes.* Am J Physiol Cell Physiol, 2000. **279**(3): p. C670-81.
271. Gao, C.L., et al., *Overexpression of PGC-1beta improves insulin sensitivity and mitochondrial function in 3T3-L1 adipocytes.* Mol Cell Biochem, 2011. **353**(1-2): p. 215-23.
272. Shao, D., et al., *PGC-1 beta-regulated mitochondrial biogenesis and function in myotubes is mediated by NRF-1 and ERR alpha.* Mitochondrion, 2010. **10**(5): p. 516-27.
273. Finkel, T. and N.J. Holbrook, *Oxidants, oxidative stress and the biology of ageing.* Nature, 2000. **408**(6809): p. 239-47.
274. Ji, H., et al., *PGC-1beta modulates the expression of genes involved in mitochondrial function and adipogenesis during preadipocyte differentiation.* Reprod Domest Anim, 2012. **47**(3): p. 419-27.
275. Espinoza, D.O., et al., *Dual modulation of both lipid oxidation and synthesis by peroxisome proliferator-activated receptor-gamma coactivator-1alpha and -1beta in cultured myotubes.* FASEB J, 2010. **24**(4): p. 1003-14.
276. Vercauteren, K., N. Gleyzer, and R.C. Scarpulla, *Short hairpin RNA-mediated silencing of PRC (PGC-1-related coactivator) results in a severe respiratory chain deficiency associated with the proliferation of aberrant mitochondria.* J Biol Chem, 2009. **284**(4): p. 2307-19.
277. Meirhaeghe, A., et al., *Characterization of the human, mouse and rat PGC1 beta (peroxisome-proliferator-activated receptor-gamma co-activator 1 beta) gene in vitro and in vivo.* Biochem J, 2003. **373**(Pt 1): p. 155-65.
278. Wang, P., et al., *Absence of an adipogenic effect of rosiglitazone on mature 3T3-L1 adipocytes: increase of lipid catabolism and reduction of adipokine expression.* Diabetologia, 2007. **50**(3): p. 654-65.
279. Wei, W., et al., *PGC1beta mediates PPARgamma activation of osteoclastogenesis and rosiglitazone-induced bone loss.* Cell Metab, 2010. **11**(6): p. 503-16.
280. Cohen, P., et al., *Ablation of PRDM16 and beige adipose causes metabolic dysfunction and a subcutaneous to visceral fat switch.*

Cell, 2014. **156**(1-2): p. 304-16.
281. Kontani, Y., et al., *UCP1 deficiency increases susceptibility to diet-induced obesity with age.* Aging Cell, 2005. **4**(3): p. 147-55.
282. Feldmann, H.M., et al., *UCP1 ablation induces obesity and abolishes diet-induced thermogenesis in mice exempt from thermal stress by living at thermoneutrality.* Cell Metab, 2009. **9**(2): p. 203-9.
283. Jimenez, M., et al., *Beta(1)/beta(2)/beta(3)-adrenoceptor knockout mice are obese and cold-sensitive but have normal lipolytic responses to fasting.* FEBS Lett, 2002. **530**(1-3): p. 37-40.
284. Castillo, M., et al., *Disruption of thyroid hormone activation in type 2 deiodinase knockout mice causes obesity with glucose intolerance and liver steatosis only at thermoneutrality.* Diabetes, 2011. **60**(4): p. 1082-9.
285. Marsili, A., et al., *Mice with a targeted deletion of the type 2 deiodinase are insulin resistant and susceptible to diet induced obesity.* PLoS One, 2011. **6**(6): p. e20832.
286. Debevec, D., et al., *Receptor interacting protein 140 regulates expression of uncoupling protein 1 in adipocytes through specific peroxisome proliferator activated receptor isoforms and estrogen-related receptor alpha.* Mol Endocrinol, 2007. **21**(7): p. 1581-92.
287. Ohno, H., et al., *PPARgamma agonists induce a white-to-brown fat conversion through stabilization of PRDM16 protein.* Cell Metab, 2012. **15**(3): p. 395-404.
288. Jimenez, M., et al., *Beta 3-adrenoceptor knockout in C57BL/6J mice depresses the occurrence of brown adipocytes in white fat.* Eur J Biochem, 2003. **270**(4): p. 699-705.
289. Kopecky, J., et al., *Expression of the mitochondrial uncoupling protein gene from the aP2 gene promoter prevents genetic obesity.* J Clin Invest, 1995. **96**(6): p. 2914-23.
290. Kopecky, J., et al., *Reduction of dietary obesity in aP2-Ucp transgenic mice: physiology and adipose tissue distribution.* Am J Physiol, 1996. **270**(5 Pt 1): p. E768-75.
291. Kelley, D.E., et al., *Dysfunction of mitochondria in human skeletal muscle in type 2 diabetes.* Diabetes, 2002. **51**(10): p. 2944-50.
292. Kusminski, C.M. and P.E. Scherer, *Mitochondrial dysfunction in white adipose tissue.* Trends Endocrinol Metab, 2012. **23**(9): p. 435-43.
293. Befroy, D.E., et al., *Impaired mitochondrial substrate oxidation in muscle of insulin-resistant offspring of type 2 diabetic patients.* Diabetes, 2007. **56**(5): p. 1376-81.
294. Lee, K.Y., et al., *Lessons on conditional gene targeting in mouse adipose tissue.* Diabetes, 2013. **62**(3): p. 864-74.
295. Holloszy, J.O., *"Deficiency" of mitochondria in muscle does not cause insulin resistance.* Diabetes, 2013. **62**(4): p. 1036-40.
296. Wredenberg, A., et al., *Respiratory chain dysfunction in skeletal muscle does not cause insulin resistance.* Biochem Biophys Res Commun, 2006. **350**(1): p. 202-7.
297. Vernochet, C., et al., *Adipose-specific deletion of TFAM increases mitochondrial oxidation and protects mice against obesity and insulin resistance.* Cell Metab, 2012. **16**(6): p. 765-76.
298. Pospisilik, J.A., et al., *Targeted deletion of AIF decreases mitochondrial oxidative phosphorylation and protects from obesity and diabetes.* Cell, 2007. **131**(3): p. 476-91.
299. Zechner, C., et al., *Total skeletal muscle PGC-1 deficiency uncouples mitochondrial derangements from fiber type determination and insulin sensitivity.* Cell Metab, 2010. **12**(6): p. 633-42.

8.ANNEX

Annex

Table 1. List of up-regulated genes in PGC1β-FAT-KO mice

Entrez ID	Symbol	Gene Name	logFC	P.Value
26938	St6galnac5	ST6 (alpha-N-acetyl-neuraminyl-2,3-beta-galac-tosyl-1,3)-N-acetylgalactosaminide alpha-2,6-sialyltrans-ferase 5	0.992	2.43E-03
18979	Pon1	paraoxonase 1	0.867	3.17E-03
13107	Cyp2f2	cytochrome P450, family 2, subfamily f, polypeptide 2	0.856	2.16E-02
12053	Bcl6	B-cell leukemia/lymphoma 6	0.797	1.49E-03
19416	Rasd1	RAS, dexamethasone-induced 1	0.781	5.06E-04
237175	Gpr64	G protein-coupled receptor 64	0.761	2.35E-02
20860	Sult1e1	sulfotransferase family 1E, member 1	0.719	1.36E-03
320974	Lrrn4	leucine rich repeat neuronal 4	0.696	5.29E-04
22414	Wnt2b	wingless related MMTV integration site 2b	0.656	3.69E-04
100647	Upk3b	uroplakin 3B	0.637	8.33E-04
19872	Rny1	RNA, Y3 small cytoplasmic (associated with Ro protein); RNA, Y1 small cytoplasmic, Ro-associated	0.630	3.34E-04
17528	Mpz	myelin protein zero	0.599	3.53E-02
234267	Gpm6a	glycoprotein m6a	0.590	6.56E-03
22223	Uchl1	ubiquitin carboxy-terminal hydrolase L1	0.589	2.89E-02
21743	Inmt	indolethylamine N-methyltransferase	0.550	9.62E-05
192190	Pkhd1l1	polycystic kidney and hepatic disease 1-like 1	0.548	1.30E-02
70676	Gulp1	GULP, engulfment adaptor PTB domain containing 1	0.540	2.72E-02
17933	Myt1l	myelin transcription factor 1-like	0.532	2.43E-04
14264	Fmod	fibromodulin	0.504	7.17E-03
55987	Cpxm2	carboxypeptidase X 2 (M14 family)	0.500	3.95E-03
235281	Scn3b	sodium channel, voltage-gated, type III, beta	0.499	1.36E-02
79362	Bhlhe41	basic helix-loop-helix family, member e41	0.498	6.59E-03
319229	Sctr	secretin receptor; similar to Sctr protein	0.482	3.41E-02
13170	Dbp	D site albumin promoter binding protein	0.469	1.56E-02
18619	Penk	preproenkephalin	0.461	9.31E-03
192199	Rspo1	R-spondin homolog (Xenopus laevis)	0.459	1.98E-03
230157	Tmeff1	transmembrane protein with EGF-like and two follista-tin-like domains 1	0.458	4.65E-02
12797	Cnn1	calponin 1	0.449	2.20E-02
15483	Hsd11b1	hydroxysteroid 11-beta dehydrogenase 1	0.449	1.61E-02
14734	Gpc3	glypican 3	0.445	9.60E-03
330695	Ctxn1	cortexin 1	0.444	8.62E-03
12737	Cldn1	claudin 1	0.440	1.39E-02
18823	Plp1	proteolipid protein (myelin) 1	0.438	3.65E-02
11568	Aebp1	AE binding protein 1	0.437	3.68E-03
56332	Amotl2	angiomotin-like 2	0.435	7.74E-03
13731	Emp2	epithelial membrane protein 2	0.430	2.20E-02

380967	Tmem106c	transmembrane protein 106C	0.421	1.57E-03
94214	Spock2	sparc/osteonectin, cwcv and kazal-like domains proteo-glycan 2	0.416	1.10E-03
399558	Flrt2	fibronectin leucine rich transmembrane protein 2	0.408	2.99E-03
23967	Osr1	odd-skipped related 1 (Drosophila)	0.400	1.03E-02
21345	Tagln	transgelin	0.400	2.69E-02
58804	Cdc42ep5	CDC42 effector protein (Rho GTPase binding) 5	0.400	2.58E-02
13497	Drp2	dystrophin related protein 2	0.391	4.97E-02
269037	Ctif	CBP80/20-dependent translation initiation factor	0.391	2.46E-02
217166	Nr1d1	nuclear receptor subfamily 1, group D, member 1	0.390	1.27E-02
100217418	Snora44	small nucleolar RNA, H/ACA box 44	0.387	3.00E-02
269831	Tspan12	tetraspanin 12	0.386	3.06E-02
19871	Rnu73b	U73B small nuclear RNA; U73A small nuclear RNA	0.385	3.17E-02
272428	Acsm5	acyl-CoA synthetase medium-chain family member 5	0.383	3.43E-02
14546	Gdap10	ganglioside-induced differentiation-associated-protein 10	0.382	1.17E-02
226049	Dmrt2	doublesex and mab-3 related transcription factor 2	0.380	4.37E-02
66637	Tsen15	tRNA splicing endonuclease 15 homolog (S. cerevisiae)	0.380	1.64E-02
56543	Kcnd3	potassium voltage-gated channel, Shal-related family, member 3	0.380	1.23E-02
11737	Anp32a	acidic (leucine-rich) nuclear phosphoprotein 32 family, member A	0.379	4.04E-02
17268	Meis1	Meis homeobox 1	0.377	1.12E-02
19116	Prlr	prolactin receptor	0.376	3.20E-02
83453	Chrdl1	chordin-like 1	0.373	3.61E-02
74116	Pi16	peptidase inhibitor 16	0.370	3.14E-02
67272	Cmtm5	CKLF-like MARVEL transmembrane domain containing 5	0.370	2.98E-02
12263	C2	complement component 2 (within H-2S)	0.370	4.25E-02
224836	Usp49	ubiquitin specific peptidase 49	0.370	1.91E-02
77976	Nuak1	NUAK family, SNF1-like kinase, 1	0.366	2.85E-02
15360	Hmgcs2	3-hydroxy-3-methylglutaryl-Coenzyme A synthase 2	0.364	2.52E-02
14190	Fgl2	fibrinogen-like protein 2	0.364	3.00E-02
18295	Ogn	osteoglycin	0.362	1.34E-02
17965	Nbl1	neuroblastoma, suppression of tumorigenicity 1	0.362	2.17E-03
338521	Fa2h	fatty acid 2-hydroxylase	0.361	4.28E-02
73102	Slc22a23	solute carrier family 22, member 23	0.360	3.10E-02
14465	Gata6	GATA binding protein 6	0.358	9.64E-03
665033	Col6a5	collagen, type VI, alpha 5	0.357	3.63E-02
15400	Hoxa3	homeo box A3	0.355	3.36E-02
74134	Cyp2s1	cytochrome P450, family 2, subfamily s, polypeptide 1	0.354	5.26E-03
211660	Cspp1	centrosome and spindle pole associated protein 1	0.349	3.63E-02
102614	Rpp25	ribonuclease P 25 subunit (human)	0.349	2.08E-02
22418	Wnt5a	wingless-related MMTV integration site 5A	0.349	2.60E-02

74533	Gzf1	GDNF-inducible zinc finger protein 1	0.345	2.87E-02
233107	Kctd15	potassium channel tetramerisation domain containing 15	0.340	2.91E-02
19882	Mst1r	macrophage stimulating 1 receptor (c-met-related tyrosine kinase)	0.339	3.89E-02
66193	Pithd1	PITH (C-terminal proteasome-interacting domain of thioredoxin-like) domain containing 1	0.339	4.51E-02
66999	Med28	mediator of RNA polymerase II transcription, subunit 28 homolog (yeast)	0.337	1.65E-02
104369	Snora69	small nucleolar RNA, H/ACA box 69	0.337	1.40E-02
270106	Rpl13	ribosomal protein L13	0.336	4.82E-03
58237	Nkain4	Na+/K+ transporting ATPase interacting 4	0.336	8.16E-03
15289	Hmgb1	high mobility group box 1	0.336	1.99E-02
24059	Slco2a1	solute carrier organic anion transporter family, member 2a1	0.333	1.30E-02
260299	Cadm4	cell adhesion molecule 4	0.330	8.83E-03
237052	Tceal1	transcription elongation factor A (SII)-like 1	0.328	2.68E-02
16369	Irs3	insulin receptor substrate 3	0.328	4.32E-02
330096	Shisa3	shisa homolog 3 (Xenopus laevis)	0.328	1.84E-02
14447	Gapdhs	glyceraldehyde-3-phosphate dehydrogenase, sperma-togenic	0.327	2.87E-02
18626	Per1	period homolog 1 (Drosophila)	0.325	1.97E-02
71724	Aox3	aldehyde oxidase 3	0.324	1.75E-02
69938	Scrn1	secernin 1	0.324	4.79E-02
243277	Gpr133	G protein-coupled receptor 133	0.320	1.43E-02
27210	Snord34	small nucleolar RNA, C/D box 34	0.320	3.27E-02
72543	Fam125b	family with sequence similarity 125, member B; similar to RIKEN cDNA 2610528K11 gene	0.319	1.33E-02
72865	Cxx1c	CAAX box 1 homolog C (human)	0.318	1.55E-02
102693	Phldb1	pleckstrin homology-like domain, family B, member 1	0.317	4.17E-02
74199	Vit	vitrin	0.313	2.08E-02
56047	Msln	mesothelin	0.313	1.56E-02
19655	Rbmx	RNA binding motif protein, X chromosome	0.312	2.79E-02
20475	Six5	sine oculis-related homeobox 5 homolog (Drosophila)	0.311	4.01E-02
74194	Rnd3	Rho family GTPase 3	0.311	1.95E-02
55983	Pdzrn3	PDZ domain containing RING finger 3	0.310	2.93E-02
277154	Nynrin	cDNA sequence BC030046	0.308	3.80E-02
77739	Adamtsl1	ADAMTS-like 1	0.308	2.15E-02
15402	Hoxa5	homeo box A5	0.305	4.92E-02
18708	Pik3r1	phosphatidylinositol 3-kinase, regulatory subunit, polypeptide 1 (p85 alpha)	0.305	2.62E-02
105859	Csdc2	cold shock domain containing C2, RNA binding	0.304	3.34E-02
19017	Ppargc1a	peroxisome proliferative activated receptor, gamma, coactivator 1 alpha	0.303	4.46E-02
18645	Pfn2	profilin 2	0.301	3.34E-02

12953	Cry2	similar to mKIAA0658 protein; cryptochrome 2 (photol-yase-like)	0.301	4.30E-02
78287	Zfyve20	zinc finger, FYVE domain containing 20	0.300	3.33E-02
231803	Mepce	methylphosphate capping enzyme	0.299	9.31E-03
18606	Enpp2	ectonucleotide pyrophosphatase/phosphodiesterase 2	0.298	1.60E-02
11535	Adm	adrenomedullin	0.294	2.07E-02
75677	Cldn22	claudin 22	0.294	3.52E-02
21685	Tef	thyrotroph embryonic factor	0.293	4.06E-02
71508	Zfp935	zinc finger protein 935	0.290	3.53E-02
227700	Sh3glb2	SH3-domain GRB2-like endophilin B2	0.289	4.11E-02
14234	Foxc2	forkhead box C2	0.289	3.61E-02
106014	Fam19a5	family with sequence similarity 19, member A5	0.287	3.34E-02
20200	S100a6	S100 calcium binding protein A6 (calcyclin)	0.284	4.09E-02
242669	Adc	arginine decarboxylase	0.283	2.25E-02
236733	Usp11	ubiquitin specific peptidase 11	0.280	2.47E-02
26561	Mmp23	matrix metallopeptidase 23	0.275	1.82E-02
18007	Neo1	neogenin	0.274	2.75E-02
71145	Scara5	scavenger receptor class A, member 5 (putative)	0.272	3.60E-02
20856	Stc2	stanniocalcin 2	0.272	4.25E-02
68655	Fndc1	fibronectin type III domain containing 1	0.271	2.89E-02
17131	Smad7	MAD homolog 7 (Drosophila)	0.270	2.89E-02
407821	Znrf3	zinc and ring finger 3	0.270	3.97E-02
387314	Tmtc1	transmembrane and tetratricopeptide repeat containing 1	0.270	1.75E-02
80290	Gpr146	G protein-coupled receptor 146	0.269	2.60E-02
56506	Cib2	calcium and integrin binding family member 2	0.269	3.04E-02
15425	Hoxc6	homeo box C6	0.269	4.65E-02
22658	Pcgf2	polycomb group ring finger 2	0.269	2.26E-02
15413	Hoxb5	homeo box B5	0.268	1.22E-02
19223	Ptgis	prostaglandin I2 (prostacyclin) synthase	0.268	3.44E-02
20595	Smn1	survival motor neuron 1	0.267	4.37E-02
22183	Zrsr1	zinc finger (CCCH type), RNA binding motif and serine/arginine rich 1	0.266	4.03E-02
57170	Dolpp1	dolichyl pyrophosphate phosphatase 1	0.265	2.96E-02
211586	Tfdp2	transcription factor Dp 2	0.264	3.64E-02
78651	Lsm6	LSM6 homolog, U6 small nuclear RNA associated (S. cerevisiae)	0.262	4.32E-02
208146	Yeats2	YEATS domain containing 2	0.262	2.62E-02
170745	Xpnpep2	X-prolyl aminopeptidase (aminopeptidase P) 2, membra-ne-bound	0.262	2.38E-02
20516	Slc20a2	hypothetical protein LOC100045882; solute carrier family 20, member 2	0.262	4.48E-02

232337	Zfp637	zinc finger protein 637	0.260	3.62E-02
208211	Alg1	asparagine-linked glycosylation 1 homolog (yeast, beta-1,4-mannosyltransferase)	0.260	3.86E-02
71962	Gatsl3	GATS protein-like 3	0.260	3.30E-02
77134	Hnrnpa0	heterogeneous nuclear ribonucleoprotein A0	0.259	1.96E-02
110751	Adam33	a disintegrin and metallopeptidase domain 33	0.259	1.98E-02
20471	Six1	sine oculis-related homeobox 1 homolog (Drosophila)	0.257	4.20E-02
67039	Rbm25	RNA binding motif protein 25	0.257	3.03E-02
13853	Epm2a	epilepsy, progressive myoclonic epilepsy, type 2 gene alpha	0.256	2.67E-02
100039795	Ildr2	immunoglobulin-like domain containing receptor 2	0.254	2.20E-02
12628	Cfh	complement component factor h	0.254	3.69E-02
192170	Eif4a3	eukaryotic translation initiation factor 4A3	0.253	4.21E-02
242509	Bnc2	basonuclin 2	0.252	4.51E-02
59289	Ccbp2	chemokine binding protein 2	0.251	2.01E-02
207165	Bptf	bromodomain PHD finger transcription factor	0.249	3.37E-02
67623	Tm7sf3	transmembrane 7 superfamily member 3	0.249	1.66E-02
227619	Man1b1	mannosidase, alpha, class 1B, member 1	0.247	3.28E-02
17300	Foxc1	forkhead box C1	0.246	1.90E-02
192198	Lrrc4	leucine rich repeat containing 4	0.246	3.70E-02
65960	Twsg1	twisted gastrulation homolog 1 (Drosophila)	0.245	3.05E-02
50909	C1rb	complement component 1, r subcomponent; predicted gene 8551	0.243	3.95E-02
271005	Klhdc1	kelch domain containing 1	0.241	4.77E-02
66404	Rtfdc1	replication termination factor 2 domain containing 1	0.241	2.41E-02
12395	Runx1t1	runt-related transcription factor 1; translocated to, 1 (cyclin D-related)	0.241	4.61E-02
72567	Bclaf1	BCL2-associated transcription factor 1	0.241	2.62E-02
67917	Zcchc3	zinc finger, CCHC domain containing 3	0.241	4.08E-02
20665	Sox10	SRY-box containing gene 10	0.238	2.58E-02
15423	Hoxc4	homeo box C4	0.236	1.95E-02
17754	Mtap1a	microtubule-associated protein 1 A	0.233	4.72E-02
74737	Pcf11	cleavage and polyadenylation factor subunit homolog (S. cerevisiae)	0.232	3.44E-02
102774	Bbs4	Bardet-Biedl syndrome 4 (human)	0.232	3.69E-02
18671	Abcb1a	ATP-binding cassette, sub-family B (MDR/TAP), member 1A	0.231	2.19E-02
20044	Rps14	ribosomal protein S14	0.231	3.11E-02
72931	Swi5	SWI5 recombination repair homolog (yeast)	0.228	3.60E-02
404634	H2afy2	H2A histone family, member Y2	0.228	3.70E-02
53861	Zranb2	zinc finger, RAN-binding domain containing 2	0.226	4.60E-02
17184	Matr3	matrin 3; similar to Matrin 3	0.225	2.98E-02

328110	Prpf39	PRP39 pre-mRNA processing factor 39 homolog (yeast)	0.224	2.38E-02
100047183	Ahnak2	AHNAK nucleoprotein 2;	0.224	3.89E-02
56395	Tmem115	transmembrane protein 115	0.224	4.37E-02
230584	Yipf1	Yip1 domain family, member 1	0.223	4.89E-02
23897	Hax1	HCLS1 associated X-1; silica-induced gene 111	0.223	2.59E-02
108058	Camk2d	calcium/calmodulin-dependent protein kinase II, delta	0.222	3.56E-02
320538	Ubn2	ubinuclein 2	0.221	2.81E-02
23837	Cfdp1	craniofacial development protein 1	0.221	2.56E-02
21652	Phf1	PHD finger protein 1	0.220	5.00E-02
231474	Paqr3	progestin and adipoQ receptor family member III	0.220	4.62E-02
22380	Wbp4	WW domain binding protein 4	0.220	4.06E-02
12512	Cd63	CD63 antigen	0.218	3.33E-02
27055	Fkbp9	FK506 binding protein 9	0.217	3.17E-02
237943	Gpatch8	G patch domain containing 8	0.216	3.13E-02
107242	AI837181	expressed sequence AI837181	0.216	3.81E-02
241308	Ralgps1	Ral GEF with PH domain and SH3 binding motif 1	0.216	4.20E-02
67785	Zmym4	zinc finger, MYM-type 4	0.214	4.30E-02
12808	Cobl	cordon-bleu	0.213	4.89E-02
13007	Csrp1	cysteine and glycine-rich protein 1	0.211	3.95E-02
66854	Trim35	tripartite motif-containing 35	0.211	4.87E-02
108160	Fam50a	family with sequence similarity 50, member A	0.210	3.88E-02
75686	Nudt16	nudix (nucleoside diphosphate linked moiety X)-type motif 16	0.207	4.75E-02
68961	Phkg2	phosphorylase kinase, gamma 2 (testis)	0.206	4.81E-02
320299	Iqcb1	IQ calmodulin-binding motif containing 1	0.204	4.20E-02
68099	Fam92a	family with sequence similarity 92, member A	0.203	4.68E-02

Table 2. List of down-regulated genes in PGC1β-FAT-KO mice. Mitochondrial genes are highlighted in turquoise.

Entrez ID	Symbol	Gene Name	logFC	P.Value
14077	Fabp3	acid binding protein 3, muscle and heart	-1.351	2.7E-04
12895	Cpt1b	carnitine palmitoyltransferase 1b, muscle	-1.277	9.6E-05
12683	Cidea	cell death-inducing DNA fragmentation factor, alpha subunit-like effector A	-1.261	2.7E-04
12865	Cox7a1	cytochrome c oxidase, subunit VIIa 1	-1.252	6.1E-05
12700	Cish	cytokine inducible SH2-containing protein	-0.974	1.3E-02
620807	Mup6	major urinary protein 6	-0.937	3.3E-02
12869	Cox8b	cytochrome c oxidase, subunit VIIIb	-0.895	1.9E-04
103172	Chchd10	coiled-coil-helix-coiled-coil-helix domain containing 10	-0.866	6.0E-04
12684	Cideb	cell death-inducing DNA fragmentation factor, alpha subunit-like effector B	-0.802	4.7E-02
67426	Cabc1	aarF domain containing kinase 3	-0.801	7.7E-04
18775	Prl3d1	prolactin family 3, subfamily d, member 1	-0.779	2.8E-02
15484	Hsd11b2	hydroxysteroid 11-beta dehydrogenase 2	-0.774	3.6E-02
63993	Slc5a7	solute carrier family 5 (choline transporter), member 7	-0.754	2.0E-02
27273	Pdk4	pyruvate dehydrogenase kinase, isoenzyme 4	-0.720	3.2E-03
385643	Kng2	kininogen 2	-0.711	1.4E-02
232493	Gys2	glycogen synthase 2	-0.588	4.4E-02
18406	Orm2	orosomucoid 2	-0.565	2.2E-02
75552	Paqr9	progestin and adipoQ receptor family member IX	-0.537	1.9E-02
26970	Pla2g2e	phospholipase A2, group IIE	-0.523	3.5E-02
73656	Ms4a6c	membrane-spanning 4-domains, subfamily A, member 6C	-0.512	4.7E-02
19013	Ppara	peroxisome proliferator activated receptor alpha	-0.499	2.8E-02
17294	Mest	mesoderm specific transcript	-0.494	1.3E-02
229791	D3Bwg0562e	DNA segment, Chr 3, Brigham & Women's Genetics 0562 expressed	-0.482	8.0E-03
246728	Oas2	2'-5' oligoadenylate synthetase 2	-0.482	4.4E-03
77219	Ptgr2	prostaglandin reductase 2	-0.473	5.0E-03
11429	Aco2	aconitase 2, mitochondrial	-0.462	8.0E-04
20510	Slc1a1	solute carrier family 1 (neuronal/epithelial high affinity glutamate transporter, system Xag), member 1	-0.457	4.5E-02
13063	Cycs	cytochrome c, somatic	-0.452	6.8E-03
75735	Pank1	pantothenate kinase 1	-0.437	4.7E-03
18430	Oxtr	oxytocin receptor	-0.433	4.5E-02
170718	Idh3b	isocitrate dehydrogenase 3 (NAD+) beta	-0.428	6.9E-04
11555	Adrb2	adrenergic receptor, beta 2	-0.426	6.1E-03
66925	Sdhd	succinate dehydrogenase complex, subunit D, integral membrane protein	-0.423	9.3E-04
21906	Otop1	otopetrin 1	-0.422	7.7E-03

435804	Olfr1335	olfactory receptor 1335	-0.413	2.6E-02
67775	Rtp4	receptor transporter protein 4	-0.409	7.8E-03
99899	Ifi44	interferon-induced protein 44	-0.396	1.1E-02
170439	Elovl6	ELOVL family member 6, elongation of long chain fatty acids (yeast)	-0.395	3.4E-02
105675	Ppif	peptidylprolyl isomerase F (cyclophilin F)	-0.394	1.0E-02
16832	Ldhb	lactate dehydrogenase B	-0.394	4.6E-03
23960	Oas1g	2'-5' oligoadenylate synthetase 1G	-0.392	7.8E-03
18655	Pgk1	phosphoglycerate kinase 1	-0.391	2.2E-03
216783	Olfr320	olfactory receptor 320	-0.384	7.4E-03
64136	Sdf2l1	stromal cell-derived factor 2-like 1	-0.372	1.4E-02
66218	Ndufb9	NADH dehydrogenase (ubiquinone) 1 beta subcomplex, 9	-0.364	3.1E-03
12858	Cox5a	cytochrome c oxidase, subunit Va	-0.361	4.4E-03
13004	Ncan	neurocan	-0.356	4.0E-02
20916	Sucla2	succinate-Coenzyme A ligase, ADP-forming, beta subunit	-0.354	1.8E-03
666907	Ms4a4a	membrane-spanning 4-domains, subfamily A, member 4A	-0.348	3.5E-02
21877	Tk1	thymidine kinase 1	-0.346	1.7E-02
22273	Uqcrc1	ubiquinol-cytochrome c reductase core protein 1	-0.342	4.0E-03
258220	Olfr1148	olfactory receptor 1148	-0.342	3.5E-02
66445	Cyc1	cytochrome c-1	-0.341	1.4E-02
68738	Acss1	acyl-CoA synthetase short-chain family member 1	-0.340	6.7E-03
66576	Uqcrh	ubiquinol-cytochrome c reductase hinge protein	-0.337	4.1E-03
20135	Rrm2	ribonucleotide reductase M2	-0.337	1.7E-02
67680	Sdhb	succinate dehydrogenase complex, subunit B, iron sulfur (Ip)	-0.337	1.0E-02
230075	Ndufb6	NADH dehydrogenase (ubiquinone) 1 beta subcomplex, 6	-0.333	4.0E-03
66052	Sdhc	succinate dehydrogenase complex, subunit C, integral membrane protein	-0.333	4.0E-03
15957	Ifit1	interferon-induced protein with tetratricopeptide repeats 1	-0.329	2.3E-02
28080	Atp5o	ATP synthase, H+ transporting, mitochondrial F1 complex, O subunit	-0.328	4.1E-03
14194	Fh1	fumarate hydratase 1	-0.327	3.2E-03
227197	Ndufs1	NADH dehydrogenase (ubiquinone) Fe-S protein 1	-0.327	4.3E-03
52538	Acaa2	acetyl-Coenzyme A acyltransferase 2 (mitochondrial 3-oxoacyl-Coenzyme A thiolase)	-0.319	3.3E-02
12859	Cox5b	cytochrome c oxidase, subunit Vb	-0.318	4.4E-03
66075	Chchd3	coiled-coil-helix-coiled-coil-helix domain containing 3	-0.318	2.7E-03
67834	Idh3a	isocitrate dehydrogenase 3 (NAD+) alpha	-0.312	8.5E-03
170826	Ppargc1b	peroxisome proliferative activated receptor, gamma, coactivator 1 beta	-0.312	1.5E-02

20321	Frrs1	ferric-chelate reductase 1	-0.312	3.1E-02
70316	Ndufab1	NADH dehydrogenase (ubiquinone) 1, alpha/beta subcomplex, 1	-0.312	1.4E-02
17995	Ndufv1	NADH dehydrogenase (ubiquinone) flavoprotein 1	-0.311	8.5E-03
11853	Rhoc	ras homolog gene family, member C	-0.310	2.7E-02
26381	Esrrg	estrogen-related receptor gamma	-0.308	2.3E-02
12850	Coq7	demethyl-Q 7	-0.308	3.7E-03
11946	Atp5a1	ATP synthase, H+ transporting, mitochondrial F1 complex, alpha subunit 1	-0.306	3.7E-03
20128	Trim30	tripartite motif-containing 30A	-0.302	4.4E-02
11950	Atp5f1	ATP synthase, H+ transporting, mitochondrial F0 complex, subunit B1	-0.301	3.2E-03
11958	Atp5k	ATP synthase, H+ transporting, mitochondrial F1F0 complex, subunit e	-0.299	2.3E-02
110323	Cox6b1	cytochrome c oxidase, subunit VIb polypeptide 1	-0.299	9.3E-03
246730	Oas1a	2'-5' oligoadenylate synthetase 1A	-0.296	3.6E-02
218772	Rarb	retinoic acid receptor, beta	-0.288	2.6E-02
19139	Prps1	phosphoribosyl pyrophosphate synthetase 1	-0.287	3.2E-02
66107	1100001G20Rik	RIKEN cDNA 1100001G20 gene	-0.282	1.6E-02
66477	Usmg5	upregulated during skeletal muscle growth 5	-0.278	1.8E-02
320720	Fastkd1	FAST kinase domains 1	-0.276	3.0E-02
19272	Ptprk	protein tyrosine phosphatase, receptor type, K	-0.276	9.7E-03
66046	Ndufb5	NADH dehydrogenase (ubiquinone) 1 beta subcomplex, 5	-0.274	7.5E-03
75406	Ndufs7	NADH dehydrogenase (ubiquinone) Fe-S protein 7	-0.267	2.0E-02
16190	Il4ra	interleukin 4 receptor, alpha	-0.264	2.7E-02
71878	Fam83d	family with sequence similarity 83, member D	-0.264	3.2E-02
29815	Bcar3	breast cancer anti-estrogen resistance 3	-0.263	4.0E-02
94065	Mrpl34	mitochondrial ribosomal protein L34	-0.257	9.4E-03
17448	Mdh2	malate dehydrogenase 2, NAD	-0.255	1.2E-02
20656	Sod2	superoxide dismutase 2, mitochondrial	-0.254	1.4E-02
17449	Mdh1	malate dehydrogenase 1, NAD (soluble)	-0.254	3.8E-02
56451	Suclg1	succinate-CoA ligase, GDP-forming, alpha subunit	-0.253	2.0E-02
18648	Pgam1	phosphoglycerate mutase 1	-0.253	1.7E-02
68203	Diras2	DIRAS family, GTP-binding RAS-like 2	-0.250	2.7E-02
17992	Ndufa4	NADH dehydrogenase (ubiquinone) 1 alpha subcomplex, 4	-0.248	2.7E-02
280635	Emilin3	elastin microfibril interfacer 3	-0.245	3.7E-02
23962	Oasl2	2'-5' oligoadenylate synthetase-like 2	-0.243	4.8E-02
235582	Glyctk	glycerate kinase	-0.240	2.5E-02
68493	Ndufaf4	NADH dehydrogenase (ubiquinone) 1 alpha subcomplex, assembly factor 4	-0.239	2.9E-02
214254	Nudt15	nudix (nucleoside diphosphate linked moiety X)-type motif 15	-0.239	1.9E-02

22272	Uqcrq	ubiquinol-cytochrome c reductase, complex III subunit VII	-0.238	3.0E-02
67003	Uqcrc2	ubiquinol cytochrome c reductase core protein 2	-0.235	1.5E-02
235339	Dlat	dihydrolipoamide S-acetyltransferase	-0.233	3.6E-02
231655	Oasl1	2'-5' oligoadenylate synthetase-like 1	-0.230	3.4E-02
546546	Serpina3h	serine (or cysteine) peptidase inhibitor, clade A, member 3H	-0.227	2.6E-02
72900	Ndufv2	NADH dehydrogenase (ubiquinone) flavoprotein 2	-0.222	2.3E-02
56046	Uqcc	ubiquinol-cytochrome c reductase complex chaperone, CBP3 homolog (yeast)	-0.221	4.9E-02
67264	Ndufb8	NADH dehydrogenase (ubiquinone) 1 beta subcomplex 8	-0.220	3.0E-02
68349	Ndufs3	NADH dehydrogenase (ubiquinone) Fe-S protein 3	-0.218	3.6E-02
67273	Ndufa10	NADH dehydrogenase (ubiquinone) 1 alpha subcomplex 10	-0.215	3.3E-02
21991	Tpi1	triosephosphate isomerase 1	-0.215	4.5E-02
66377	Ndufc1	NADH dehydrogenase (ubiquinone) 1, subcomplex unknown, 1	-0.212	3.7E-02
68611	Mrpl28	mitochondrial ribosomal protein L28	-0.209	3.6E-02
72416	Lrpprc	leucine-rich PPR-motif containing	-0.203	4.2E-02
66841	Etfdh	electron transferring flavoprotein, dehydrogenase	-0.201	4.6E-02
94045	P2rx5	purinergic receptor P2X, ligand-gated ion channel, 5	-0.197	5.0E-02